AN ABSTRACT OF THE DISSERTATION OF

Timothy W. Rhoads for the degree of Doctor of Philosophy in Biochemistry & Biophysics presented on July 6, 2012.

Title: Measuring Protein Metal Binding via Mass Spectrometry: Copper, Zinc Superoxide Dismutase and Amyotrophic Lateral Sclerosis.

Abstract approved:_____

Joseph S. Beckman

Amyotrophic lateral sclerosis (ALS) is a devastating disease characterized by the progressive degeneration of motor neurons. Dominantly-inherited mutations to the antioxidant enzyme Cu,Zn superoxide dismutase (SOD1) cause 3-6% of all ALS cases. The complete mechanism behind the toxicity of mutant SOD1 remains unclear, although significant evidence points to aberrant or incomplete metal-binding having a role in a toxic gain-of-function. However, the relevance of the metal-binding of SOD1 to mutant-SOD1-linked ALS remains controversial. Direct assessments of protein metal-binding from transgenic, SOD1-overexpressing rodent models of the disease are difficult to acquire due to the non-covalent nature of the interaction. The relatively small amount of disease-afflicted spinal cord tissue in which the motor neurons reside compounds the difficulty of measuring the protein metal binding of SOD1 from transgenic mice. This dissertation addresses the metals bound to SOD1 throughout the disease course in transgenic mice using a novel mass spectrometry assay. The methodology developed here offers the first detailed examination of partially unfolded intermediates of SOD1 present in the spinal cord of pre-symptomatic, symptomatic, and end-stage transgenic mice overexpressing the ALS-associated SOD1 mutation G93A (glycine mutated to alanine at position 93). These results were compared to age-

matched transgenic mice expressing wild-type SOD1 that do not develop ALS symptoms.

To extract SOD1 from relevant spinal cord tissue, a 300 μm necropsy punch was used to remove a small piece of tissue from the ventral or dorsal gray matter of a 1 mm-thick slice of spinal cord. Physiological salts that interfere with electrospray mass spectrometry were removed by binding the proteins to a C4 Ziptip®, a pipette tip containing hydrophobic, reversed-phase packing material. Washing the Ziptip-bound proteins with water eliminated interfering salts. Bound proteins could then be eluted into a mass spectrometer with low concentrations of acetonitrile plus formic acid. Electrospray ionization conditions were determined that could keep both copper and zinc bound to SOD1. Using a high-resolution Fourier transform-ion cyclotron resonance mass spectrometer, we used the assay to collect isotopically-resolved protein mass data. Theoretical protein isotope distributions were calculated from the empirical formulas of SOD1 and matched to the experimental data with a least squares fitting algorithm to determine the multiple intermediates of SOD1 present.

Spinal cord tissue, wild-type in particular, was notable for containing significantly more one-metal SOD1 than any other tissue, despite having 3-fold less SOD1 than liver. We quantitatively compared the levels of soluble, partially unfolded intermediates of SOD1 from wild-type and G93A SOD1 spinal cords. Wild-type mouse spinal cord contained significantly more of all of the partially unfolded intermediates copper-deficient SOD1, disulfide reduced SOD1, and apo SOD1. The amount of zinc-containing SOD1 was exceptionally high in wild-type mice, comprising 60% of the total SOD1 in wild-type spinal cord. The larger amounts of these SOD1 intermediates in wild-type transgenic mice indicate that they are not directly responsible for toxicity in vivo. However, copper-containing, zinc-deficient SOD1 was the one species found in higher concentrations in G93A SOD1 spinal cord. The concentration

was on average 0.6-0.8 μM in G93A spinal cord, compared to 0.1-0.3 μM zinc-deficient SOD1 found in the wild-type mouse spinal cord. A concentration above 0.5 μM zinc-deficient SOD1 was sufficient to induce motor neuron death *in vitro*. These results suggest that copper-containing, zinc-deficient SOD1 could be the toxic species responsible for motor neuron death in ALS.

Measuring Protein Metal Binding via Mass Spectrometry: Copper, Zinc Superoxide Dismutase and Amyotrophic Lateral Sclerosis

by

Timothy W. Rhoads

A DISSERTATION

submitted to

Oregon State University

in partial fulfillment of

the requirements for the

degree of

Doctor of Philosophy

Presented July 6, 2012

Commencement June 2013

Doctor of Philosophy dissertation of Timothy W. Rhoads presented on July 6, 2012.

APPROVED:

Major Professor, representing Biochemistry & Biophysics

Head of the Department of Biochemistry & Biophysics

Dean of the Graduate School

I understand that my dissertation will become part of the permanent collection of Oregon State University libraries. My signature below authorizes release of my dissertation to any reader upon request.

Timothy W. Rhoads, Author

ACKNOWLEDGEMENTS

I owe a great debt of gratitude to many people for their contributions to this work over the last five years. I must first thank my advisor, Dr. Joseph Beckman, for the opportunity to do this research in the first place. Your guidance and humor the past five years have helped me grow as a person and a scientist. I continue to be amazed by your dedication to and passion for the research.

I also thank my undergraduate thesis advisor, Dr. Stephen Warren, for his patience in teaching a clueless undergraduate how to do research. Without his guidance I never would have started down this path.

I owe many thanks to our lab manager, Nathan Lopez, without whom I truly believe the lab would cease to function. I cannot express enough gratitude for your scientific insights, ability to fix ANYTHING, and willingness to listen to me rant.

Many, many thanks to Jeff Morré, resident guru of the mass spec lab. Your help, humor, and insight the past few years has been invaluable. Plus that Ziptip idea was kind of handy.

I also owe many thanks to Jim Gibson for helping me to keep the FT-MS in a functioning state and for teaching me much about the functional details of the instrument. My dissertation would not have been possible without it.

I thank members of the Beckman lab, past and present, for the welcoming atmosphere of the lab: Blaine Roberts, Dan Zollinger, Mark Levy, Mandi Gandelman, Derek Drechsel, Joe Mendoza, Keith Nylin, Vlad and Irina Ermilov, Kari Trumbull, and Jongtae Yang.

I must thank the amazing friends I've met along the way: Jason and Megan Hirko, Rick and Stacy Cooley, Camden Driggers, Galen Miller, Sherry Farley, Katie Lebold, Jared and Katharine Williams, Kate and Matt Cleveland,

Russell Carpenter, Kathy Morrow, Carly Dougher, Robert Ingle, Matt Housley, Lauren Atwell, Mark Levy, Mandi Gandelman, Scott Leonard, and Cameron Long. I can't thank you enough for your friendship and support. Also to all of the members of soccer teams I have played on the last five years, I can't say how much I have enjoyed the experience. I definitely wouldn't have kept my sanity without it!

I thank my committee members Jeff Greenwood, Andy Karplus, Gary Merrill, and Janine Trempy. I would not have succeeded without your help and guidance, and I am extremely grateful to each of you for helping me to develop as a scientist. I also owe a great deal of thanks to Ron Adams, who stepped in to serve as my graduate representative for my defense somewhat at the last minute due to conflicts with scheduling, for which I am extremely grateful.

I would like to acknowledge grant support from the National Institute for Neurological Disorders and Strokes (# R01NS058628A), the National Center for Complementary and Alternative Medicine (# P01AT002034), and the National Institute for Environmental Health Sciences (# P30ES000210).

Finally I have to thank my parents, John and Sharon, and my siblings, Mike and Emily, for their love and support. I do not have the words to express their contribution.

CONTRIBUTION OF AUTHORS

Linda DeNoyer (SpectrumSquare Associates) provided the analysis programs used for the mass spectrometry data in Chapter 2. Daniel Zollinger provided the recombinant protein used in Chapter 2. Claudia Maier provided help with experimental design and editing of the final manuscript for Chapter 2. Sam Bradford provided the laser capture microdissection data for Chapter 3. Brian Arbogast and Jeff Morré provided instrumentation support and advice for the mass spectrometers used in Chapters 2, 3, and 4, and J.M. was involved in the initial design of the Ziptip assay that forms the basis for those chapters. Jared Williams was involved in the experimental design, analysis and writing of Chapters 3 and 4. Nathan Lopez was involved in the experimental design, analysis, and writing of Chapters 2, 3, and 4. Joseph Beckman was involved in the design, analysis, and writing of all experiments and chapters.

TABLE OF CONTENTS

TABLE OF CONTENTS (Continued)

TABLE OF CONTENTS (Continued)

LIST OF FIGURES

LIST OF FIGURES (Continued)

LIST OF TABLES

Measuring Protein Metal Binding via Mass Spectrometry: Copper,Zinc Superoxide Dismutase and Amyotrophic Lateral Sclerosis

Chapter 1

Introduction and Thesis Overview

1.1 Amyotrophic Lateral Sclerosis

Amyotrophic lateral sclerosis (ALS) is a devastating neurodegenerative disorder characterized by tremors, muscle weakness, and muscle wasting leading to general paralysis and death [1]. It is better known in the United States as Lou Gehrig's disease, after the Yankees first baseman who was stricken with the disease during the latter part of his playing career. Lou Gehrig is still considered to be the greatest first baseman to ever play baseball, and one of the most prolific hitters of his generation [2]. However, in 1938 at the age of 35, he complained of being tired by mid-season, and by 1939, he could barely run around the bases [3]. He retired from baseball that season and was referred to the Mayo clinic, where he was diagnosed with ALS. He died two years later, just shy of 38 years old [3]. Despite more than 70 years passing since, there is still no effective treatment for the disease.

ALS is a disease of motor neurons, the cells in the body responsible for controlling muscle movement [4]. Motor neurons serve as the mediator of signals between the brain and the muscles and fall into two broad categories: upper motor neurons and lower motor neurons. Upper motor neurons originate in the brain motor cortex or the brain stem and carry signals down the spinal cord to lower motor neurons, but do not directly enervate the muscles. Lower motor neurons are found in the ventral horn of the spinal cord and pass out axons up to a meter in length to enervate and control muscles. ALS is due to the progressive death of both upper and lower motor neurons, leading to an inability to control voluntary muscle movement [5]. The disease is uniformly fatal, and patients typically die within 2-5 years, usually from respiratory failure due to an inability to control the diaphragm [6]. Jean-Martin Charcot, a preeminent French neurologist, is generally credited with the first detailed description of the disease in 1874 [7]. He painstakingly laid out the symptoms

and correlated them with anatomical observations at autopsy, arriving at a remarkably complete clinical picture of the disease:

> "I do not think that elsewhere in medicine, in pulmonary or cardiac pathology, greater precision can be achieved. The diagnosis as well as the anatomy and physiology of the condition 'amyotrophic lateral sclerosis' is one of the most completely understood conditions in the realm of clinical neurology."

The clinical picture of the disease has changed little since this statement [8]. Yet while the description of the disease may have been understood, it would be well over 100 years before insights into a mechanism for the disease could be found [9].

ALS strikes approximately 5 out of 100,000 individuals, with most cases (80-90%) referred to as 'sporadic' ALS (sALS) because of a lack of a family history of the disease [6]. The remaining 10-20% of ALS cases show a genetic inheritance pattern and are termed 'familial' (fALS). These cases also lack a reason for symptom onset other than a family history of the disease. It was not until 1993 that the first gene linked to ALS was identified. In 1991, Siddique *et al*. described localizing a genetic defect linked to the disease in 23 families to the long arm of chromosome 21 [10]. Two years later, Rosen *et al*. identified the gene locus as superoxide dismutase 1 (SOD1) and revealed 11 different point mutations associated with the disease [11]. The mutations account for approximately 3-6% of all ALS cases (20% of fALS and 1-2% of sALS) and for the first time provided a distinct molecular target for researching the disease [12,13].

1.2 Superoxide Dismutase 1

The fact that single amino acid changes to SOD1 can lead to ALS highlights the need to understand the structure of the protein and how it might be altered by mutation. SOD1 is a 32-kD, homodimeric antioxidant enzyme primarily responsible for scavenging superoxide radicals in the cell. Each subunit binds a copper and a zinc ion that are essential to its function. The bulk of the polypeptide is folded into an 8-stranded Greek-key β-barrel structure (Figure 1.1) [14,15].

Two loops also form significant parts of the structure of the enzyme: Loop IV, also called the zinc-binding loop, and Loop VI, also called the electrostatic loop. Three histidines (H46, H48, H120) from the β-barrel and one from Loop IV (H63) comprise the copper binding site, situated on the front-middle area of the β-barrel. The histidine from Loop IV is also a ligand for the adjacent zinc ion, with two additional histidines (H71, H80) and an aspartate (D83) comprising the rest of the four zinc binding ligands.

Zinc is a key structural feature, acting as one of the pins for Loop IV, which forms much of the dimer interface. A second pin, in the form of an intrasubunit disulfide bond between C46 (Loop IV) and C157 (β-barrel), tethers the other end of the loop to the main structure of the protein. This disulfide linkage is unusual due to the fact that the protein maintains the bond in the oxidized state even in the highly reducing environment of the cytosol. The unique structural features of SOD1 convey an extremely high level of stability to the protein. SOD1 remains active even in 10 M urea, and has a melting temperature above 70 °C [16,17].

The copper ion is the central part of the active site of the protein. It is mostly occluded from solvent by Loop VI, which sits over the top of the metal-binding region, with the exception of a small channel, the mouth of which is guarded by the positively charged arginine 143. Such an arrangement seems

to increase the efficiency of the enzyme, as the positively-charged arginine can electrostatically guide superoxide anions to the copper [18]. Mutation of the arginine to amino acids other than lysine causes at least a 10-fold drop in protein activity [19]. The normal activity consists of the copper ion cycling between the +2 and +1 oxidation states to dismutate superoxide radicals into oxygen and hydrogen peroxide:

$$(1) \quad O_2^{\cdot -} + Cu^{2+} \rightarrow O_2 + Cu^{1+}$$

$$(2) \quad O_2^{\cdot -} + 2H^{+} + Cu^{1+} \rightarrow H_2O_2 + Cu^{2+}$$

The enzyme is one of the most efficient known, with a rate constant of 2-3x10^9 $M^{-1}s^{-1}$ for both reactions [20].

Interruption of the normal activity of SOD1 as a result of mutation was an early hypothesis for the cause of ALS; however toxicity as a result of the loss of SOD1 activity was discounted due to several pieces of evidence. First, many ALS-causing mutant proteins, including G93A, retain the same level of activity as the wild-type protein [21]. Second, an SOD1 knockout mouse was developed that failed to show any symptoms of the disease over its normal lifespan [22]. Finally, a mouse model of ALS was developed in which mutant SOD1 was grossly overexpressed, leading to a recapitulation of many features of the human disease [23]. The overall dismutation activity in the mouse model animals is approximately 4-fold higher than in non-transgenic mice. Mutations to SOD1 clearly cause it to gain an aberrant, toxic property that is responsible for the disease presentation. The creation of the animal model enables the toxic gain-of-function to be studied in detail.

1.3 Transgenic Animal Model

In 1994, Gurney et al. found that overexpression of mutant SOD1 in a mouse yielded an ALS model that recapitulated many features of the human disease [23]. Expression of SOD1 with a glycine mutated to alanine at position

93 caused mice to develop motor neuron pathology, ataxia and muscle wasting, leading to paralysis and death. The transgene used to make this mouse was a 12.1-kb fragment of genomic DNA containing the entire SOD1 gene, including the native upstream region and promoter [24]. This resulted in the incorporation of variable copy numbers of the gene into the mouse genome. A key point is that higher gene copy number was correlated with more aggressive disease progression. In the most aggressive line, B6SJL-Tg(SOD1-G93A)1Gur/J, symptoms start at around 100-110 days of age and are terminal by 120-130 days of age. This line carries around 25 copies of the G93A human SOD1 gene [25]. The control animals for these mice are B6SJL-Tg(SOD1)2Gur/J, which were made in a similar fashion but overexpress the wild-type SOD1 protein. These animals display no characteristic ALS symptoms and live a normal lifespan. However, the wild-type SOD1 animals only carry about 7 copies of the gene and the mRNA levels are about half that of the G93A mice [23].

The SOD1 overexpressing mice are some of the most successful models of neurodegenerative disease [26]. Many of the SOD1 mutants expressed in mice result in at least some of the classic disease symptoms [27,28], providing a wealth of knowledge about the disease progression. Several key modifiers of the disease, out of the many that have been studied, have dramatic effects on the onset and progression. The copper chaperone for SOD1 (CCS) has been of great interest because it is responsible for conferring the copper ion that is central to SOD1 activity to the protein [29]. G93A mice that have been bred to have the endogenous mouse CCS knocked out (CCS null G93A) show no differences in disease onset or progression, despite radioactive ^{64}Cu incorporation experiments that demonstrated lower copper-loading [30]. The authors drew the conclusion that the copper cofactor could not play a role in the disease despite the fact that the SOD1 retained almost 20% of normal activity. Furthermore, the tissues were homogenized in 1%

detergent with 1 mM metal chelator present, suggesting that the measurements may represent a significant underestimate of the copper bound to the protein [31]. CCS overexpression in the context of the G93A SOD1 mouse line has almost the opposite effect of the knockout [32]. Mice overexpressing both G93A and CCS die 80% faster from ALS symptoms than those that have just the G93A SOD1 transgene alone, consistent with copper toxicity having a role in the disease. However, the precise effect of CCS overexpression on the metals bound to SOD1 is not known.

Small-molecule antioxidants such as glutathione may also play a role in the disease. The knock out of the modulatory subunit of γ-glutamylcysteine ligase (GCLM) in concert with G93A SOD1-overexpression produces animals that die from ALS 50% faster than the G93A transgene by itself [33]. The knockout of GCLM leads to glutathione levels that are 80% lower than wild-type animals, suggesting that glutathione may play a protective role, which has been demonstrated in cell culture [34]. Induction of Nrf2, an activator of glutathione synthesis, is also protective [35]. Glutathione is a potent reducing agent and is capable of reducing the disulfide bond of SOD1, but is also an excellent copper chelator and may impact the metal-binding of SOD1 [36].

Clearly the various mouse models provide an excellent source of information about the progression of ALS. The role that SOD1 plays in the disease progression, however, is still nebulous. Exactly how do single-amino acid changes to a 16-kDa protein lead to a neurodegenerative phenotype? Almost two decades of research since the discovery of mutations to SOD1 have not revealed a clear answer. Linking all of the mutations to a common disease mechanism has been exceedingly difficult due to the diversity of the mutations to SOD1 that have been linked to ALS. At the most recent count, there are 165 mutations that lead to the development of disease (Figure 1.2) [37].

These mutations can occur in all five exons and are therefore spread along a wide array of environments in the structure of the protein. Most of the mutations are dominantly inherited, single amino acid substitutions. However, the D90A mutation is recessive in some populations [38,39], and several truncation and insertion mutations have also been described [38]. These features have made a common toxic characteristic difficult to discern.

Several hypotheses concerning the toxic function have been proposed. Much of the research has focused on the level of destabilization imparted to the protein by mutation. SOD1 is a highly stable enzyme that has an unfolding half-life of 70 days at 37 °C [40]. However, mutations lessen that stability to varying degrees and in many cases the level of destabilization imparted by the mutation correlates with the pace of disease progression [41]. This has led to the hypothesis that destabilization leading to aggregation of the protein is responsible for the toxicity of the mutant protein [42]. The aggregates are insoluble proteinaceous inclusions that can be observed both in the human disease and in the mouse model [43,44]. These aggregates are presumed to be toxic by interfering with the proteasome, sequestering other crucial cellular components, or perhaps disrupting axonal transport [45,46]. Direct toxicity of aggregates has been difficult to demonstrate, however, and it is not clear that propensity to aggregate can fully explain the toxicity of mutant SOD1 [47,48]. Many of the lower expressing SOD1 ALS models demonstrate little to no aggregation. Indeed, SOD1 aggregates may simply be a symptom of the disease [49,50].

1.4 Copper, Zinc, and SOD1

Although destabilization of the protein leading to aggregation may not explain the toxicity of mutant SOD1, the stability of the protein may be related to the disease in another fashion. The presence of soluble yet partially-

unfolded forms of SOD1 in mouse models has increasingly been documented, along with biophysical folding studies of the protein suggesting that such species represent stable intermediates in the unfolding pathway [51,52]. Much of the research has focused on the intermediate states of the apo protein as the precursor of aggregate species serving as the toxic molecule [53]. Often overlooked is the fact that the metal ion cofactors are intrinsically involved in the folding, stability, and function of the protein [54,55]. Alterations to the normal metal-binding of the protein can dramatically change how SOD1 folds, interacts with chaperones, and how effectively it scavenges superoxide [56,57]. The copper ion in particular is capable of oxidative chemistry beyond scavenging of superoxide. For instance, it can carry out the back reaction that results in the production of superoxide instead of the dismutation:

$$(3) \quad \mathrm{Cu^{1+}} + \mathrm{O_2} \rightarrow \mathrm{Cu^{2+}} + \mathrm{O_2^{\cdot -}}$$

Superoxide by itself is a relatively weak reductant and not highly toxic [58]; however, superoxide has another fate that may play a role in ALS progression. The radical-radical recombination of superoxide with nitric oxide produces the peroxynitrite anion, a highly toxic species [59]. Nitric oxide is capable of out-competing SOD1 for reaction with superoxide, with a rate constant of 1×10^{10} $M^{-1}s^{-1}$ for the formation of peroxynitrite [60].

$$(4) \quad \mathrm{NO^{\cdot}} + \mathrm{O_2^{\cdot -}} \longrightarrow \mathrm{ONOO^{-}}$$

Peroxynitrite is a potent oxidant that can lead to protein nitration *in vivo* [61,62]. Such nitration can fundamentally alter the function of the protein, leading to cellular damage and death [63-65]. Motor neurons in particular seem to be sensitive to this, as trophic factor withdrawal leads to motor neuron death via peroxynitrite [66,67].

Alvaro Estévez has begun to describe a more specific consequence of peroxynitrite: the downstream toxicity of the nitration of a single protein, HSP90. In an attempt to determine if nitrotyrosine played an active role in peroxynitrite-mediated cell death, PC12 cells were treated with peroxynitrite

and the homogenates subjected to mass spectrometry analysis to identify any nitrated targets. HSP90 treated with peroxynitrite and delivered back to cells was able to initiate a Fas-dependent cellular death cascade. Nitration at tyrosine 33 or 56, but not mutation to phenylalanine, was sufficient to initiate the cascade even if present on only 1% of the HSP90. Using an antibody to nitrated HSP90 revealed intense staining in motor neurons of ALS-model mice, suggesting this pathway may be relevant for ALS.

How might SOD1 participate in peroxynitrite-mediated toxicity? The loss of zinc from SOD1 yields a protein that binds only copper. Blaine Roberts, a former member of the Beckman lab, and colleagues showed that zinc loss opens up of parts of the protein [68], more readily enabling the chemistry described by reaction (3). Furthermore, zinc-deficient SOD1 is actually capable of catalyzing protein nitration [57]. Zinc-deficient SOD1 has been shown to be toxic to motor neurons in cell culture through a peroxynitrite-mediated mechanism involving tyrosine nitration [69-71]. The zinc-deficient protein was toxic regardless of whether or not it contained an ALS-associated mutation; that is, even wild-type SOD1 can be toxic if it loses its zinc ion. The structural zinc ion is bound significantly less tightly than the copper cofactor and mutant SOD1s are susceptible to losing zinc [55,57,72]. However, a number of groups have found evidence that zinc-deficient SOD1, and by extension the idea of copper-mediated toxicity, is not relevant to disease progression. The previously mentioned CCS null G93A SOD1 mice were used as evidence that CCS-dependent copper-loading had no impact on the disease progression, thus suggesting copper was not playing a role in the disease [30]. The high levels of metal chelators used in that study, however, suggest that the experiments were not accurate measures of either copper or zinc bound to SOD1 [31].

Further evidence cited against the zinc-deficient SOD1 hypothesis was the generation of a transgenic mouse expressing SOD1 with mutations to the

four copper-liganding histidines (H46R, H48Q, H63G, H120G), yielding a protein (Quad SOD1) that has diminished capacity to bind copper [73]. Although the mouse does demonstrate an ALS-like phenotype, copper is known to be capable of binding to the zinc site, and the metal-binding of the Quad SOD1 in vivo is not known [74]. Wang *et al*. measured copper incorporation of the Quad protein using radioactive ^{64}Cu, and demonstrated no copper incorporation into the protein. However, as with the CCS null G93A mice, high levels of detergent (2% SDS, 0.5% Nonidet P40) were used in preparation for gel electrophoresis, likely impacting the degree of metal binding to the protein. Recently, Prudencio *et al*. generated a SOD1 protein that lacks all metal-binding and free cysteine residues, and mice expressing this SOD1 do not develop disease [75]. The authors suggest this is because a lack of cysteines at positions 6 and 111 confers a dramatically lowered propensity to aggregate relative to other ALS mutants that have those thiols present. Nevertheless, the lack of both primary and secondary metal binding sites leading to a protein that does not lead to disease symptoms is strongly suggestive of the involvement of metal-binding in pathology.

The perturbations of SOD1 mouse models used to argue against the potential role of zinc-deficient SOD1 in ALS, the knowledge that zinc-deficient SOD1 is toxic to motor neurons in cell culture via a peroxynitrite-mediated mechanism, and the elucidation of a downstream pathway tying nitrated HSP90 to cell death all highlight a knowledge gap in determining if this represents the pathway of ALS progression: is zinc-deficient SOD1 present in a disease relevant context? The SOD1 metal-binding *in vivo* is not known for the Quad SOD1, the CCS null G93A, the normal G93A SOD1, or even the wild-type SOD1 mice. Indirect measures of metal-binding, such as activity assays, are used as evidence for the amount of copper binding, but they do not provide an accurate picture of how the metal is distributed at the subunit-level, information that is crucial for determining if aberrantly metal-bound

populations of SOD1 are involved in ALS. Addressing this question and determining the metal-binding of SOD1 in disease-relevant tissue throughout the progression of disease in an animal model has been the primary goal of my dissertation.

1.5 Contents of the Dissertation

The remainder of my dissertation is comprised of 4 chapters focused on the development of methods to look at the metal-binding distribution of SOD1 throughout the course of ALS in disease model-animals. Chapters 2-4 are full research articles, of which Chapter 2 is published, and Chapter 3 will be submitted in the near future. Chapter 5 draws together the insights gained from the research, places the work in the context of the field, and describes the possibilities for future research.

Chapter 2: "Measuring copper and zinc superoxide dismutase from spinal cord tissue using electrospray mass spectrometry" Timothy W. Rhoads, Nathan I. Lopez, Daniel R. Zollinger, Jeffrey T. Morré, Brian L. Arbogast, Claudia S. Maier, Linda DeNoyer, Joseph S. Beckman. *Analytical Biochemistry*, 2011, **415** (1), 52-58.

This manuscript presents the development of a mass spectrometry-based assay to measure SOD1 from the spinal cords of transgenic rats and mice. Utilizing a C_4 Ziptip® and a custom interface to a time-of-flight mass spectrometer, we were able to detect human SOD1 from 200 µg or less of regiospecific areas of transgenic rat spinal cord tissue. We demonstrated that electrospray ionization conditions could be made sufficiently gentle to keep native metals bound, and that three distinct metal-binding populations of SOD1 were observed: apo (no-metals), one-metal, and two-metals bound.

This represented the first look at the specific metal binding distribution of SOD1 in ALS-affected tissue. However, the resolution of the time-of-flight mass spectrometer used for the study was not sufficient to distinguish between copper- and zinc-bound SOD1, necessitating further work.

Chapter 3: “Theoretical protein isotopic distributions as a means to parse small-mass-difference post-translational interactions via mass spectrometry” Timothy W. Rhoads, Jared R. Williams, Nathan I. Lopez, Jeffrey T. Morré, Joseph S. Beckman. Manuscript submitted to *Journal of the American Society for Mass Spectrometry*.

Due to the small mass difference between zinc and copper, we needed some additional tools to be able to distinguish between the two in the context of SOD1 from transgenic spinal cord tissue. We present in this chapter the transfer of our Ziptip methodology to a Fourier transform ion cyclotron resonance mass spectrometer, an instrument capable of acquiring high resolution mass data. For an intact protein, the mass peak was resolved into individual isotopic species. This data required improvements to our methods of data analysis. As such, we developed a suite of custom-written programs to fit combinations of theoretical isotope distributions to the experimental distributions, arriving at a best-fit that represents the relative proportions of each metal. We also developed a simple and rapid assay for assessing the oxidation status of the disulfide bond, setting the stage for being able to measure the metal-distribution of SOD1 in a larger number of animals.

Chapter 4: “Assessing the impact of metal-binding and disulfide status of superoxide dismutase on amyotrophic lateral sclerosis” Timothy W. Rhoads, Jared R. Williams, Nathan I. Lopez, Joseph S. Beckman. Manuscript in preparation.

This chapter presents a larger scale examination of the metal-binding of SOD1 in tissues from ALS model mice and controls (G93A and wild-type). We assessed the metal-binding of SOD1 in the spinal cords and brains of 40 mice of varying ages and disease progression, finding that wild-type SOD1 overexpressing mice contained more of all forms of partially-unfolded intermediates of SOD1 except for copper-containing, zinc-deficient SOD1, which was higher in G93A mice. We discovered that a small molecule present in the spinal cords of these animals prevented us from measuring copper-containing, zinc-deficient SOD1 unless we included the thiol-oxidant diamide in the tissue buffer. The necessity of diamide to measure zinc-deficient SOD1 suggests other molecules that may be involved in the disease, which will be addressed in Chapter 5. We found that with the inclusion of diamide, we could measure 800 nM zinc-deficient SOD1 in the spinal cords of G93A transgenic mice and that the level in wild-type SOD1 mice was 200 nM, significantly lower. Experiments performed by Alvaro Estévez's lab indicated that the level in G93A animals is enough to be toxic while that in wild-type animals is below the toxic threshold.

Chapter 5 describes the conclusions that can be drawn from the work and the direction of the research going forward. We have developed a method that allows us to look closely at SOD from relevant tissue in a simple, rapid manner and have our first look at the specific metal-binding status of the protein as the disease progresses. These studies set the stage for further research into the role that metal-binding plays in ALS.

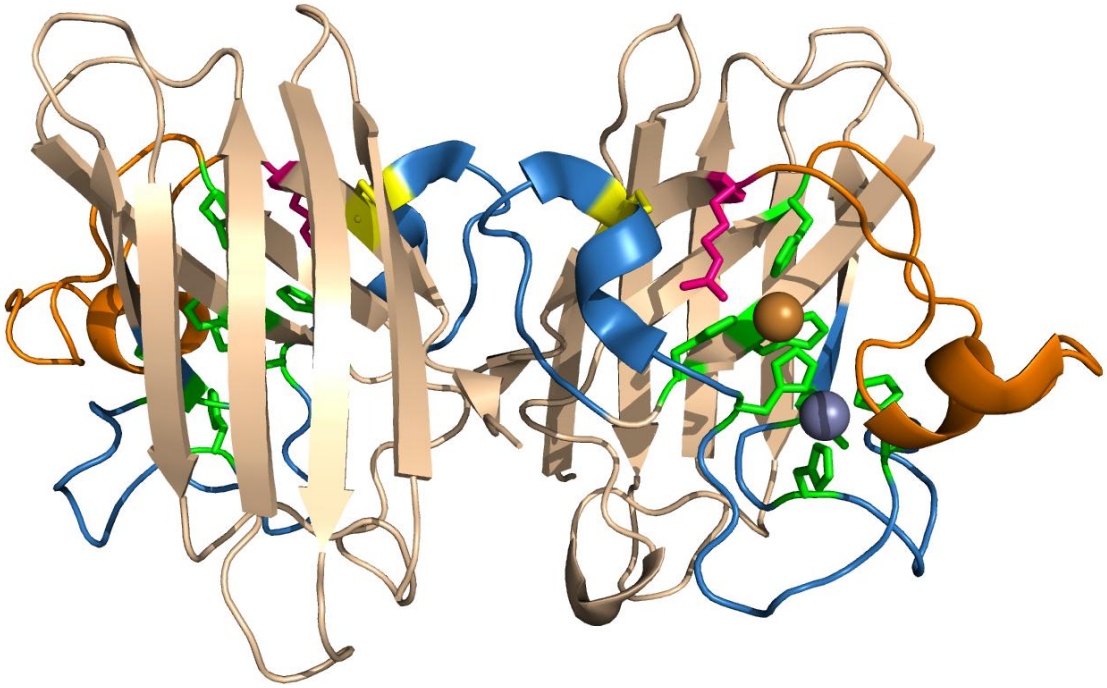

Figure 1.1 Superoxide Dismutase 1 dimer. Superoxide dismutase 1 cartoon depiction (pdb code 2c9v). Features of the protein highlighted: Copper (burnt orange), zinc (grey), metal ligands (green), Loop IV (blue), disulfide bond (yellow), Loop VI (orange), Arg143 (pink).

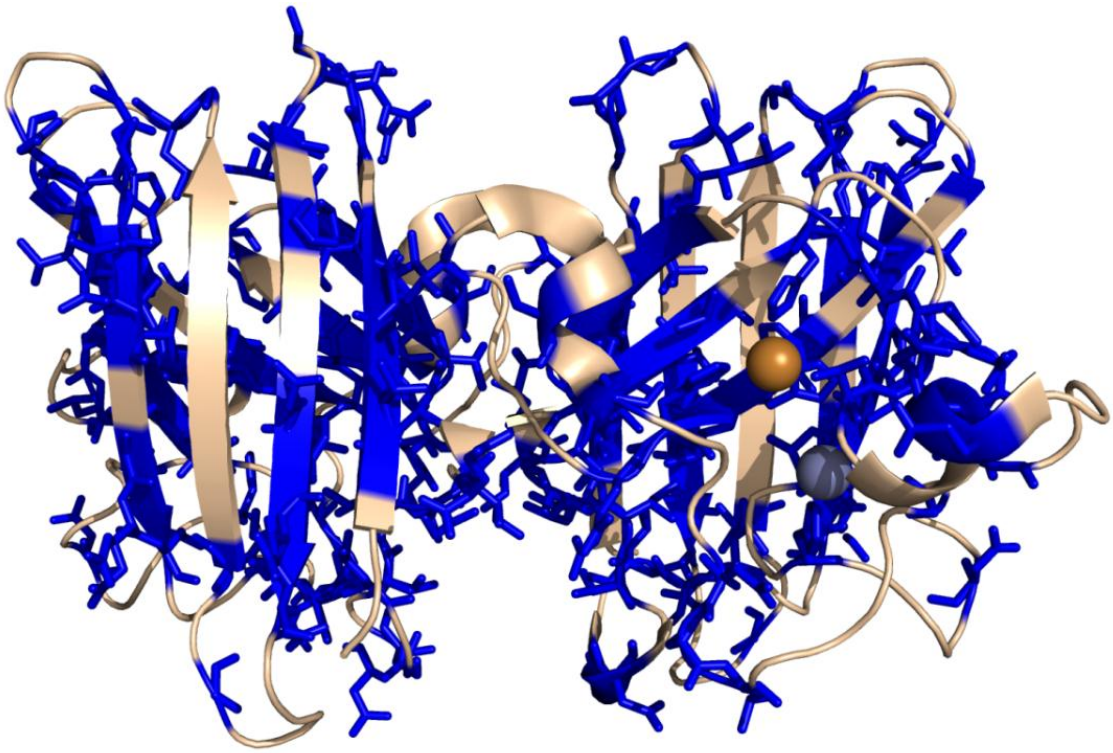

Figure 1.2 ALS-linked Mutations to SOD1. Human Cu,Zn superoxide dismutase (Pdb code 2c9v) with the ALS-causing mutations highlighted in blue. The list of mutations is available at http://alsod.iop.kcl.ac.uk/.

Chapter 2

Measuring copper and zinc superoxide dismutase from spinal cord tissue using electrospray mass spectrometry

Timothy W. Rhoads, Nathan I. Lopez, Daniel R. Zollinger, Jeffrey T. Morré, Brian L. Arbogast, Claudia S. Maier, Linda DeNoyer, Joseph S. Beckman

Published in *Analytical Biochemistry* (2011), 415(1), 52-58.

2.1 Abstract

Metals are key cofactors for many proteins, yet quantifying the metals bound to specific proteins is a persistent challenge in vivo. We have developed a rapid and sensitive method using electrospray ionization mass spectrometry to measure Cu,Zn superoxide dismutase (SOD1) directly from the spinal cord of SOD1-overexpressing transgenic rats. Metal dyshomeostasis has been implicated in motor neuron death in amyotrophic lateral sclerosis (ALS). Using the assay, SOD1 was directly measured from 100 μg of spinal cord, allowing for anatomical quantitation of apo, metal-deficient, and holo SOD1. SOD1 was bound on a C_4 ZipTip® that served as a disposable column, removing interference by physiological salts and lipids. SOD1 was eluted with 30% acetonitrile, plus 100 μM formic acid to provide sufficient hydrogen ions to ionize the protein without dislodging metals. SOD1 was quantified by including bovine SOD1 as an internal standard. SOD1 could be measured in subpicomole amounts and resolved to within two Daltons of the predicted parent mass. The methods can be adapted to quantify modifications to other proteins in vivo that can be resolved by mass spectrometry.

2.2 Introduction

Approximately one-third of all proteins are predicted to require a metal cofactor for activity [76] and as many as half of all the structures deposited in the Protein Data Bank contain a metal ion [77]. Metal ion binding to proteins is critically important for many biological processes [78], but characterizing the metal ions bound to a protein in a biological context is difficult. Spectroscopic techniques, such as atomic absorption, electron paramagnetic resonance, and Mössbauer reveal metal coordination by proteins, but are insensitive and require purified protein in high concentrations [79]. Inductively-coupled plasma mass spectrometry and assays utilizing colorimetric chelators inform on the total metal content in the sample, thus conveying only average metal ion stoichiometry [80,81]. Electrospray ionization mass spectrometry (ESI-MS) is a well-established technique used in the study of non-covalent modifications and interactions of proteins such as metal binding [82-85]. Once the ionization parameters are properly optimized, metal ions such as zinc and copper remain tightly associated with proteins during electrospray ionization and ESI-MS has been used to compare both relative and absolute metal ion affinities of many proteins [86,87].

The activity of Cu,Zn superoxide dismutase (SOD1) is vitally dependent upon its copper and zinc cofactors [88]. The redox-active copper is the center of the protein's activity. SOD1 also contains a structural zinc atom closely coordinated to the copper that is essential for the proper folding of the protein [55]. Evaluating the metals bound to SOD1 is also important because mutations to the protein cause a toxic-gain-of-function that is responsible for 2-7% of all cases of amyotrophic lateral sclerosis (ALS) [9,12]. ALS is a fatal neurodegenerative disorder characterized by the progressive death of motor neurons. However, the mechanism of the toxic function in vivo is still controversial. Most of the mutant SOD1 proteins bind one copper and one zinc

ion per subunit and many retain almost the same level of enzymatic activity as the wild-type protein [89-91]. However, the mutant SOD1 proteins seem to be more susceptible to the loss of the zinc ion than the wild-type SOD1 protein in vitro [57,92,93]. We have previously shown that purified zinc-deficient SOD1 delivered to cultured motor neurons is toxic [94]. Furthermore, expression of mutant SOD1 in motor neurons isolated from SOD1-transgenic animals kills by the same mechanism [95]. Consequently, the ability to assess the amounts of copper and zinc bound to SOD1 in the specific spinal cord regions affected by ALS may provide clues as to the nature of the toxic function in vivo.

Here we introduce a sensitive ESI-MS based method that allows the quantification of SOD1 directly from spinal cord tissue of transgenic ALS-model rats and concurrently reports on the zinc and copper ion content of the protein. We demonstrate the efficacy of the method for SOD1 from transgenic spinal cord tissue, although it can be applied to other proteins in complex mixtures.

2.3 Materials and Methods

2.3.1 Reagents and Equipment

Lyophilized bovine SOD1 (EC1.15.1.1, Sigma-Aldrich, St. Louis, MO, USA) was rehydrated with Milli-Q water (reverse-osmosis system), and the concentration was determined spectrophotometrically at 259 nm (ε= 5150 $M^{-1}cm^{-1}$ for the Cu,Zn containing monomer) [88].

Two types of human SOD1 were used in the development of this assay. The first type was recombinant SOD1 expressed in *Escherichia coli* (recombinant SOD1) with coexpression of the copper chaperone for SOD1 (CCS). The protein was purified as described in Hayward *et al.* [96]. Ammonium sulfate was used in high concentrations for hydrophobic interaction chromatography, causing a sulfate adduct (+98 Da) to be often present in mass spectrometry samples. The concentration was determined spectrophotometrically at 265 nm (ε= 9200 $M^{-1}cm^{-1}$ for the Cu,Zn containing monomer) [88]. Recombinant SOD1 was found to have the amino-terminal methionine cleaved and was not acetylated [97]. The second type was SOD1 from tissue samples of mutant G93A SOD1-overexpressing transgenic rats (referred to as tissue SOD1). These rats develop fatal motor neuron disease and die around 120 days old [98]. In eukaryotic sources, SOD1 is acetylated on the amino-terminus, increasing the protein mass by 42.1 Da.

The solvent used for the mass spectrometric experiments was 30% acetonitrile, 70% water and 100 μM formic acid, delivered at a flow rate of 30 μL/min from a single isocratic pump (Shimadzu, Kyoto, Japan). The solvent was degassed for 10 minutes with helium and was changed each week. HPLC-grade solvents were used for all mass spectrometer experiments. Water was obtained from Burdick and Jackson (Muskegon, MI, USA) and 10% formic acid from Michrom Bioresources (Auburn, CA, USA). Universal grade acetonitrile was obtained from VWR (West Chester, PA, USA).

SOD1 was introduced into the mass spectrometer via one of two methods: by direct injection of SOD1 in low ionic strength aqueous buffers, or by binding to a C_4 reversed phase Ziptip® for tissue samples or higher ionic strength solutions as described below. For direct injection, solvent was pumped from the HPLC pump through PEEK® tubing with an interior diameter of 0.005 inches to a 2-way, 6-port Rheodyne injection port. The SOD1 was introduced into the sample loop of the injector via a 50 μL Hamilton syringe with a blunt tip. Solvent was then pumped through the loop and across a 1 μm inline stainless steel microfilter (Upchurch Scientific, Oak Harbor, WA, USA) to prevent clogging. The 0.005 inch inner diameter PEEK® tubing led from the microfilter into the mass spectrometer inlet.

2.3.2 Ziptip Method

A C_4 Ziptip (Millipore, Billerica, MA, USA) was used as a disposable desalting column while binding SOD1. The Ziptip is a P10 pipette tip with 0.6 μL of reversed phase C_4 packing material that is typically used to remove salts from peptide samples in preparation for mass spectrometry detection. For the assay, a Ziptip was prepared by rinsing three times (10 μL each) with acetonitrile, followed by four washes with water. The washes were accomplished by using a P10 pipette to repeatedly draw 10 μL of fresh solvent up through the Ziptip, and then to expel the solvent. The SOD1 sample was then bound to the Ziptip by pipetting the protein solution three times, followed by rinsing six times with water to remove salts. The Ziptip was then inserted between the injection port and the microfilter (Figure 2.1).

2.3.3 Tissue Measurements

Fresh spinal cord tissues from transgenic G93A-SOD1$^{+/-}$ overexpressing rats housed in Institutional Animal Care and Use Committee-approved facilities were extracted via dissection of euthanized animals and

frozen at -80 °C until use. The tissue was too brittle to section immediately at this temperature, and was placed on an insulating plastic plate on top of dry ice and allowed to warm to approximately -20 °C. Punches were taken from 1 mm thick transverse sections of tissue using a 500 micron biopsy punch (Figure 2.1). An air-filled syringe was attached to the rear of the punch to expel the tissue (Zivic Instruments, Pittsburgh, PA, USA). The punches were weighed on a Cahn 25 Automatic Electrobalance with a sensitivity of 0.1 μg (Cerritos, CA, USA). SOD1 was released from the tissue punch by thawing the tissue in 5 μL of 10 mM ammonium acetate, adjusted with acetic acid to pH 5.1, that included 200 nM bovine SOD1 (punch thawing buffer). The pH was chosen to reduce adventitious metal binding and because interfering lipoproteins from central nervous system tissues precipitated, thereby preventing clogging of the tubing [99]. The thawed tissue was vortexed at maximum speed for 30 seconds then centrifuged for two minutes at 16,000 rcf. The supernatant was adsorbed onto the Ziptip, eluted and analyzed in the mass spectrometer.

The amount of SOD1 released from tissue was verified by western blot analysis. The supernatants from three punches were combined to provide enough sample per lane for the western blot. The punches were thawed in 15 μL of 10 mM ammonium acetate at pH 5.1, vortexed and centrifuged as above. The tissue supernatant and pellet fractions were separated, the volume of each was adjusted to 30 μL with Laemmli buffer [100], and the samples were heated for five min at 95 °C. Samples were then run on a 10% SDS-PAGE at 150V for 60 min in a Bio-Rad Mini Protean II system. Gels were transferred to a polyvinylidene fluoride membrane (Bio-Rad product # 162-0177) for 60 min at 100V. SOD1 was detected using rabbit polyclonal antibodies raised in the laboratory against human SOD1 (1:10,000). Affinity-purified antibodies retained cross reactivity with mouse and rat SOD1. The

secondary antibody was goat anti-rabbit IgG heavy plus light chain-horse radish peroxidase conjugate (Bio-Rad #170-6515).

2.3.4 Data Analysis

Proteins were detected using a LCT Premier Time-of-Flight mass spectrometer (Waters, Milford, MA, USA) with an electrospray ionization (ESI) interface in positive ion mode with capillary and sample cone voltages set to 3000 and 60 V, respectively. Nitrogen was used as a desolvation gas (400 L/hr), with a desolvation temperature of 120 °C. The scan range was set from 820 to 2450 m/z, which allowed for all SOD1 peaks to be recorded.

Data were collected using MassLynx software (Waters, v. 4.1) and mass spectrum deconvolution and integration was performed using the program MOP™ (Multiple Overlaying Pictures, Spectrum Square Associates, Inc.) described below. Custom code written in Matlab™ (The MathWorks, Inc., Natick, MA, USA) was used to transfer the data from MassLynx to MOP™ and perform the peak integration. Deconvolution of electrospray m/z data to yield the zero charge parent mass spectrum was accomplished with the Bayesian/maximum entropy algorithm MOP™. The program makes no assumptions about the types of proteins present in the spectrum. The only information provided to the program is 1) that hydrogen ions are the source of charge, and 2) the resolution of the mass spectrometer. The program assumes that noise is distributed according to a Poisson distribution and incorporates a mass-dependent point-spread function for a time-of-flight mass analyzer to account for instrumental blurring. The program uses an algorithm based on Bayes theorem to calculate the most probable parent mass distribution that would result in the observed multiply charged experimental spectrum with experimental noise. It incorporates a multinomial Bayesian prior and thus becomes the standard maximum entropy approach. The algorithm preserves the observed number of ion counts in the original spectrum and thus

the output peak areas remain proportional to the concentration of the species present. SOD1 concentrations were determined by the use of bovine SOD1 as an internal standard. A comparison of the total integration of the human SOD1 peaks with the integration of the bovine SOD1 peak at a known concentration generated a ratio that allowed us to determine the human SOD1 concentration in the original solution. Bovine SOD1 was chosen because it behaves similarly to human SOD1 and binds the same metals, and therefore serves as an internal protein control in addition to a standard.

Molecular weights and theoretical isotope distributions were calculated from the empirical formula of SOD1 using the program *iMass* [101,102]. Identical results were obtained using the isotopicdist function in the Bioinformatics Toolbox of Matlab™. To account for the two positive charges of each of the copper and zinc ions, two hydrogen atoms were subtracted for each metal ion bound so that SOD1 remained electrically neutral. In addition, two hydrogen atoms were subtracted for the internal disulfide bond in SOD1.

2.4 Results

Copper and zinc remained associated with SOD1 during electrospray ionization in a aqueous solution containing 100 µM formic acid and 30% acetonitrile as shown by the mass spectrum of recombinant SOD1 ALS-mutant G93A (Figure 2.2A). Recombinant SOD1 protein was used to develop the assay before using tissue samples. The mass spectrometer displayed six prominent peaks corresponding to the 13th through 8th charge states, with the most intense being the 10th-12th charge states. Deconvolution using the Bayesian maximum-entropy method generated the parent mass spectrum (Figure 2.2B). The main peak was centered at 15941 Da, which agreed well with the average mass of 15941.7 calculated for the Cu,Zn G93A SOD1 monomer ($C_{680}H_{1081}N_{203}O_{224}S_4CuZn$). The width of the observed SOD1 peak corresponds to the broadening predicted from the natural isotope distribution using the empirical formula for Cu,Zn G93A SOD1 (Figure 2.2C).

Physiological concentrations of sodium chloride caused the mass spectrum to be unrecognizable as recombinant SOD1 and could not be deconvoluted (Figure 2.3A). A Ziptip used as a rapid and disposable desalting column reversed the effects of the salt (Figure 2.3B). The Ziptip contained C_4 reverse-phase packing material upon which the SOD1 could be adsorbed and rinsed with water to remove salts. An internal standard of bovine SOD1 was included in each sample to quantify the levels of SOD1 and control for any sample loss. Bovine SOD1 is shorter by two amino acids than human SOD1 and thus is well resolved from the three potential metal ion-containing forms of human SOD1. The charge state distribution for Cu,Zn G93A SOD1 in the presence of high salt could be deconvoluted after use of the Ziptip to give a mass of 15941 Da, identical to the spectrum of SOD1 with no salt present.

The chromatogram from a sample of bovine and recombinant G93A SOD1 showed that less than three minutes was needed for SOD1 to

isocratically elute from the Ziptip into the mass spectrometer (Figure 2.4A). The concentration of acetonitrile in the running solvent (30%) was optimized to be at the lowest level possible while still rapidly releasing SOD1 from the Ziptip. Dilute formic acid (100 µM) included in the running solvent substantially improved ionization of the protein. Although acidic conditions are known to cause metal ion release from SOD1, the formic acid concentration was optimized to provide sufficient hydrogen ions for ionization while allowing copper and zinc to remain stably bound to SOD1 [16]. Metal ions were retained under the acid conditions over the period necessary to acquire the data, as shown by the deconvoluted mass spectrum of recombinant SOD1 incubated in water versus running solvent (30% acetonitrile/water with 100 µM formic acid) for 5 minutes at room temperature (Figure 2.4B,C). Without the rinse step that accompanies the use of a Ziptip, the sulfate adduct peak 98 mass units higher than the mass of the recombinant SOD1 monomer was more prominent.

Tissue G93A SOD1 could easily be picked out from the other abundant background proteins as it was significantly overexpressed in the spinal cord of G93A-SOD1 overexpressing transgenic rats (Figure 2.5A). The SOD1 could be quantified by use of the Ziptip and the inclusion of bovine SOD1 as an internal standard. To generate a standard curve, bovine SOD1 was kept at 800 nM, while the concentration of recombinant G93A SOD1 was varied over a range of 200 nM-1.2 µM (Figure 2.5D). The relationship was linear over the concentration range tested with a slope of approximately 1.3 (R^2=0.995). Representative spectra from the dorsal and ventral (Figure 2.5B) grey matter of the spinal cord of an ALS-model rat showed three distinct metal-bound species: a Cu,Zn SOD1 peak, a one-metal SOD1 peak, and a small apoSOD1 peak. The one-metal peak was approximately 2-fold larger in the disease-affected ventral spinal cord as compared to that from the dorsal spinal cord. Thawing of frozen tissue punches was sufficient to release SOD1 and other

soluble proteins from the punch into solution; this was verified via Western blots that showed less than 2% of SOD1 in the remaining pellet compared to the supernatant fraction (Figure 2.5C).

2.5 Discussion

Analysis of proteins in complex mixtures on a Ziptip via mass spectrometry provides a rapid, quantitative means to assay noncovalent modifications directly from tissues that is comparable and possibly more sensitive than western blotting. The remarkable sensitivity of the method allows for anatomical microdissection of the tissue. ALS affects motor neurons, which are localized in the ventral spinal cord (Figure 2.1). This assay allows SOD1 to be directly measured from the disease-affected regions, and is able to distinguish between one-, two-, and no-metal bound states; the one-metal bound species is significantly larger in the ventral compared to the dorsal spinal cord. This difference is lost if the entire spinal cord is used, as several previous methods have done [50,103,104].

Three main issues needed to be addressed in developing the assay. The first was to maintain metal binding to the protein while providing sufficient acidity to permit efficient electrospray ionization [105,106]. We found that 0.1% formic acid, commonly used in ESI-MS coupled liquid chromatography, was too strong and could cause SOD1 to lose metals during the assay [16]. Hayward *et al*, used 0.1% formic acid to look at apo mutant SOD1 proteins [96]. Leaving out formic acid resulted in poor ionization because the solvent could not provide enough hydrogen ions in solution to effectively ionize SOD1. The largest amounts of human Cu,Zn SOD1 eluting from the Ziptip were in the range of 1-10 pmol in a volume of a few microliters, resulting in a concentration of 1-10 μM. Because the charge states of SOD1 typically ranged from 8 to 13, the concentration of hydrogen ions needed to be 8-13 μM (Figure 2.2A). We found that solvent containing 100 μM formic acid delivered at a flow rate of 30 μL/min provided enough protons for efficient ionization. The 100 μM formic acid concentration is approximately 200-fold more dilute than the standard 0.1% concentration, and was able to efficiently ionize SOD1

without altering metal binding after five minutes, twice the time needed to run the assay (Figure 2.4B,C).

The second issue to overcome was how to efficiently remove salts from the protein solution that would otherwise interfere with electrospray ionization. Salts suppress ionization of proteins, interfering with the deconvolution of raw m/z data (Figure 2.3A). Sodium ions in particular can associate strongly with an ionizing protein and sodium chloride is approximately 100 mM in the central nervous system, thereby presenting a significant potential interference to ionizing proteins directly from tissue. We used a C_4 Ziptip to desalt the samples. The Ziptip is a P10 pipette tip with a small amount of HPLC reversed-phase packing material. As tissue lysate is drawn over it, soluble proteins bind to the packing material. Once bound, the proteins could be rinsed multiple times with water, washing off salts and other small hydrophilic molecules while leaving the proteins bound to the packing material. The bound proteins could be eluted in the mass spectrometer with the minimal concentration of acetonitrile needed to elute SOD1 (30%) (Figure 2.4A).

The third issue was to quantify the amount of human SOD1 released from the tissue. This was accomplished by including an internal standard, bovine SOD1, at a known concentration in the punch thawing buffer. Comparing the integration of the peak areas from MOP™ of the bovine and human SOD1 allowed us to calculate the amount of human SOD1 in the punch supernatant, which could be used to estimate the concentration of human SOD1 in the tissue. SOD1 was found to be 16 pmol/mg tissue in the dorsal spinal cord and 26 pmol/mg tissue in the ventral spinal cord. These amounts roughly translate to 16 and 26 μM in the cells, respectively. A standard curve of recombinant human SOD1 compared to bovine SOD1 was used to determine if the ionization of the human and bovine proteins differed (Figure 2.5D). The slope of 1.3 on the standard curve suggests that human SOD1 may ionize more efficiently than bovine SOD1 due to the higher number

of basic amino acid residues present in the human SOD1 sequence. This can also be seen in the differing charge state distributions of human and bovine SOD1, in which the human protein picks up two more positive charges on average than bovine SOD1 (Figure 2.3B).

One of the primary advantages of our method is the ability to monitor the metal-binding of SOD1 at the monomer level in complex mixtures, in contrast to other approaches that can determine the metal-binding of the population of SOD1 as a whole solution, thus giving only average stoichiometry [104]. This is an important distinction in being able to determine if metal-deficient SOD1 species are involved in ALS. An SOD1 dimer has 9 different metal-binding combinations distinguishable by mass. The intrasubunit disulfide bond further complicates matters, as it can be in an oxidized or reduced state, altering the mass of the protein by two Da. Indeed several groups have reported that as much as 20-30% of the SOD1 in the ALS model animals is reduced [107]. Combining these two phenomena, the SOD1 dimer has 27 distinct combinations of metal-binding and disulfide states, which would yield a complex and hard-to-interpret spectrum. An advantage of the described method is that the dimer dissociates in the course of the assay and only monomer is detected (Figure 2.2B). The SOD1 monomer has only eight distinct metal-binding/disulfide states, with the resulting spectrum being significantly easier to interpret, facilitating analysis of the metal-binding status of individual subunit populations.

A second advantage is that the method is highly adaptable, allowing monitoring of other proteins and post-translational modifications. We have used the method to measure recombinant proteins in solution such as CCS, hemoglobin, and di-iron mono-oxygenases. Other proteins were also observed when measuring SOD1 from tissue, such as ubiquitin and acyl-CoA-binding protein which were tentatively identified by their mass (Figure 2.5A). The endogenous rat SOD1 was also identified, although in a significantly lower

amount that the human SOD1 (Figure 2.5B). Taking advantage of other materials available for ZipTips (C18, etc.) could further extend the method to additional proteins. Modifying the solvent composition and the ionization parameters, such as the ionization voltage and capillary temperature, allows the method to be optimized for other proteins and post-translational modifications, possibly including small-molecule binding, nitration, metals, and phosphorylation. Furthermore, these modifications can be monitored in a dynamic fashion, as both modified and unmodified populations of a protein are observed at the same time.

The main limitation to our assay is the inability to distinguish between copper-containing, zinc-deficient SOD1 and zinc-containing, copper deficient SOD1. The isotopically broad mass spectrometer signature of a protein is wider than the mass difference between zinc and copper, and thus we cannot differentiate between the two (Figure 2.2C). However, we find a significant one-metal SOD1 peak that is substantially larger in the ventral gray matter, which provides additional evidence that non-natively metal-bound SOD1 species are involved in the progression of the disease (Figure 2.5B). Further work that is now ongoing will be needed to determine the composition of the one metal peak and elucidate whether either species has a role in the disease.

2.6 Acknowledgements

We thank Keith Nylin for his early work in this area, and Dr. Mark Levy and Jared Williams for critical reading of the manuscript. This work was supported by the National Institute for Environmental and Health Sciences (NIEHS P30ES000210), the National Institutes of Neurological Disorders and Stroke (NINDS R01NS058628A) and the National Center for Complementary and Alternative Medicine (NCCAM P01AT002034), as well as the Amyotrophic Lateral Sclerosis Association.

2.7 Abbreviations

ESI-MS, electrospray ionization mass spectrometry; SOD1, Cu,Zn superoxide dismutase; ALS, amyotrophic lateral sclerosis; CCS, copper chaperone for superoxide dismutase; MOP, multiple overlaying pictures.

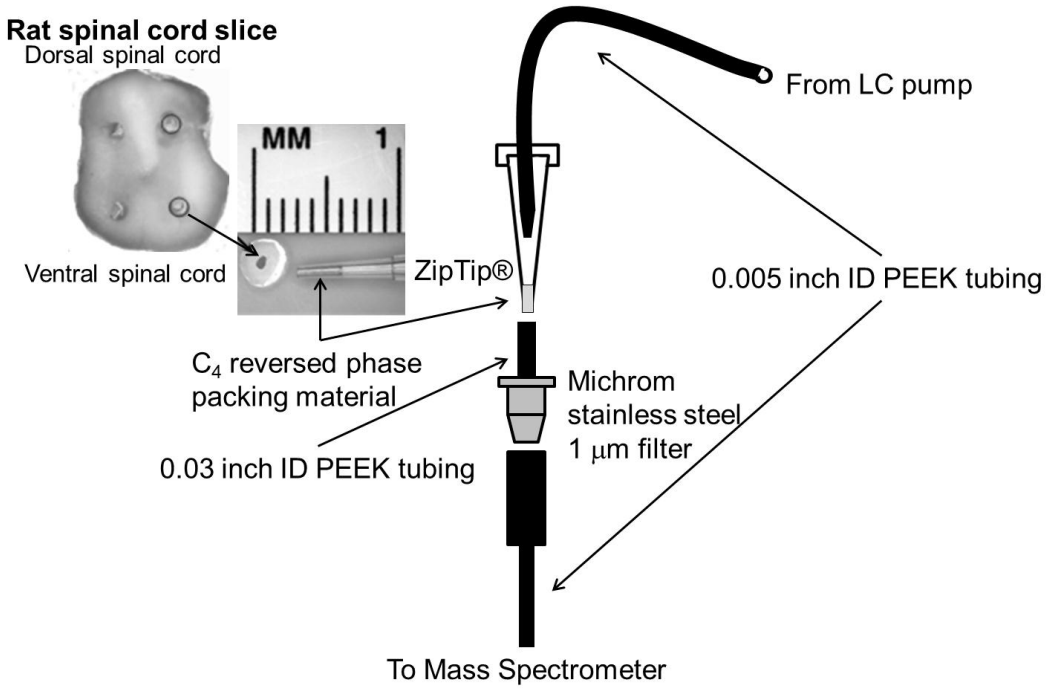

Figure 2.1 Tissue preparation for Ziptip® assay with mass spectrometer interface. A 500 micron biopsy punch is taken from a 1 mm spinal cord slice, thawed in buffer and adsorbed onto a Ziptip. Solvent from an HPLC pump flowed through 0.005 inch interior diameter PEEK tubing that was inserted snugly into the back of the Ziptip. The end of the Ziptip was inserted into a second short segment of PEEK tubing with an interior diameter of 0.03 inches that had been slightly expanded with a dissecting needle to fit the end of the Ziptip snuggly. A stainless steel 1 μm microfilter was inserted between the Ziptip and the mass spectrometer inlet to trap large particulates released from the Ziptip.

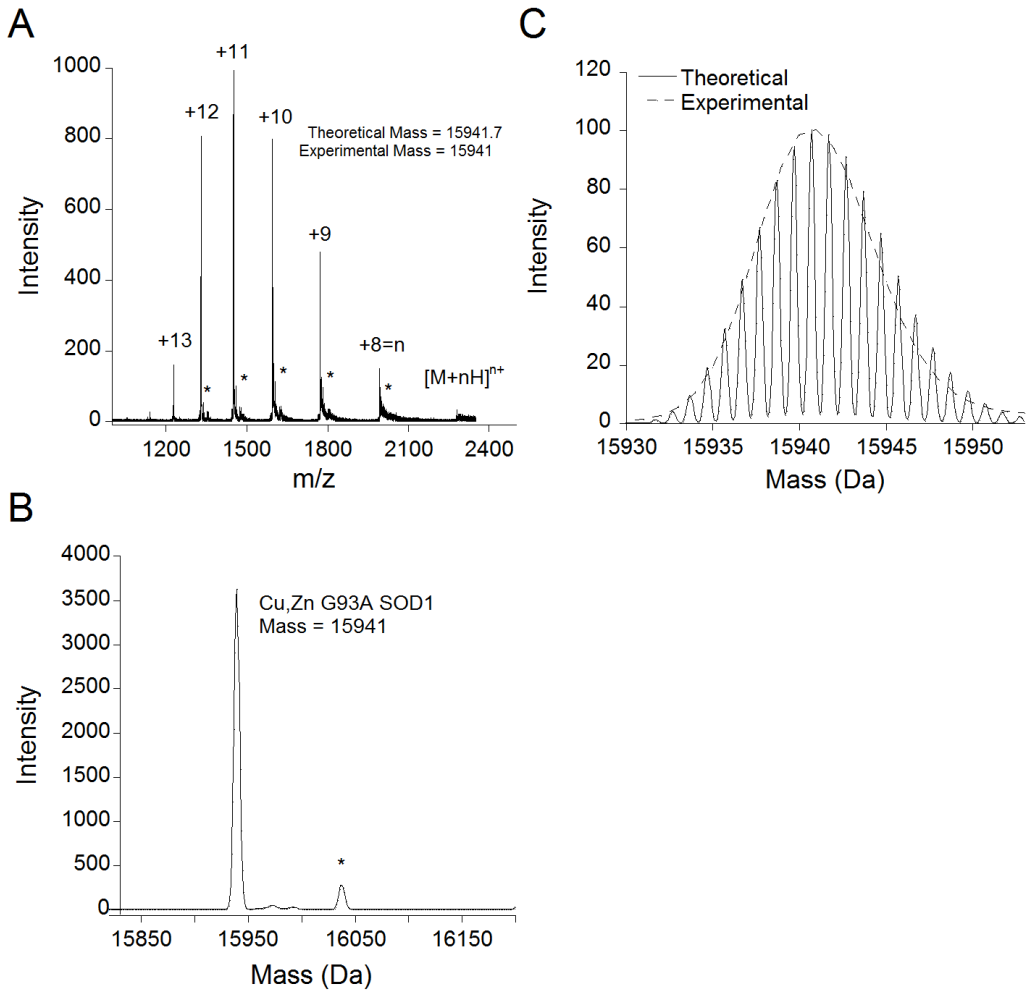

Figure 2.2 Mass spectra of G93A SOD1. A. The Ziptip m/z spectrum of 1 μM G93A SOD1 in 10 mM ammonium acetate, showing the charge state distribution of the protein, with the 10th-12th charge states being the most prominent. **B.** Mathematical deconvolution of the m/z spectrum yields the parent mass spectrum, showing a singular peak centered at a mass of 15941. *The spectrum also contained a small peak centered at 16039 (observable in A as well). This peak, which is 98 mass units larger than Cu,Zn G93A SOD1, likely corresponding to a sulfate (H_2SO_4) adduct remaining from the purification process. **C.** Overlay of the experimental mass spectrum with the theoretical high resolution mass spectrum calculated from the empirical formula for G93A SOD1 with the program *iMass*. The high resolution theoretical spectrum is used to illustrate the effects of isotopic broadening, primarily due to the natural isotope distribution.

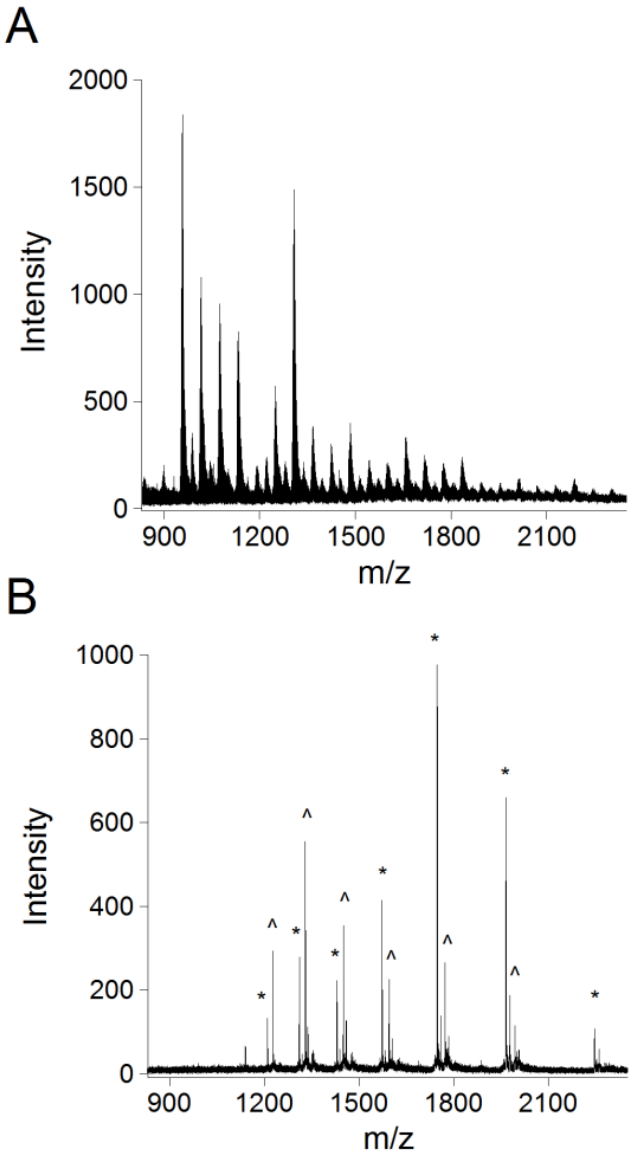

Figure 2.3 Elimination of salt interference using a Ziptip to bind G93A SOD1. A. Mass spectrum of bovine and G93A SOD1 directly injected in the presence of 100 mM sodium chloride. **B.** Mass spectrum of bovine (*) and G93A (^) SOD1 with 100 mM sodium chloride after washing with the Ziptip.

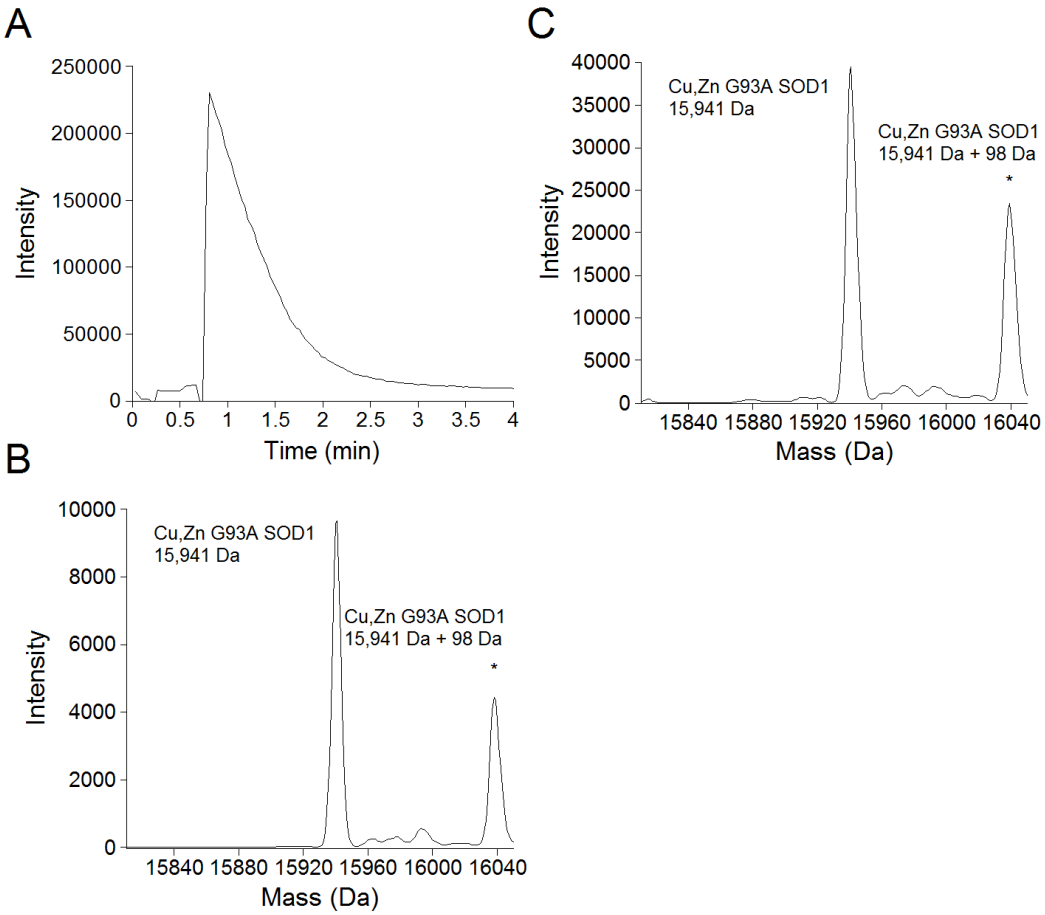

Figure 2.4 Stability of metal binding of G93A SOD1 in elution solvent. **A.** Chromatogram of G93A SOD1 eluting from the Ziptip. **B.** Parent mass spectrum of G93A SOD1 mixed immediately in elution solvent and directly injected into the mass spectrometer. **C.** Parent mass spectrum of G93A SOD1 incubated in elution solvent for 5 minutes to mimic the maximum exposure of SOD1 to solvent when bound to a Ziptip. *In both B and C, the sulfate-bound SOD1 peak was more prominent probably due to the absence of the washing step used with the Ziptip.

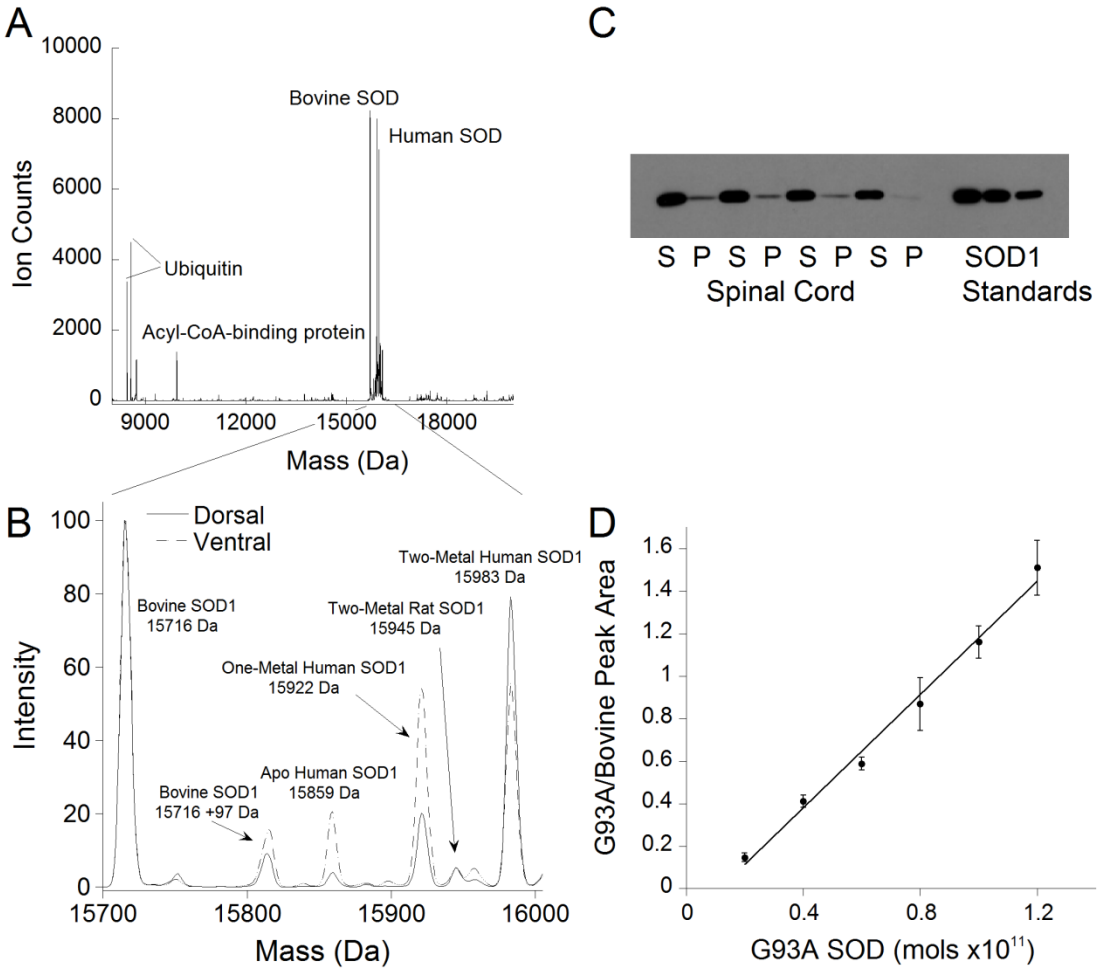

Figure 2.5 Metal content of G93A SOD1 in transgenic rats with symptoms of motor neuron degeneration. A. Deconvoluted mass spectrum of a ventral tissue punch from the lumbar spinal cord of a G93A SOD1-overexpressing rat shown over the mass range 8000 to 24000 Da. Several other proteins, including ubiquitin, ubiquitin minus two glycine residues (-114 Da), and acyl-CoA binding protein were observable in addition to SOD1. **B.** Overlay of the mass spectra of dorsal and ventral tissue punches from the lumbar spinal cord of a G93A SOD1 overexpressing rat. Prominent peaks are identified in the spectrum, including the endogenous rat SOD1. **C.** Western blot of tissue punch supernatant (S) and pellet (P) fractions used to verify the release of SOD1 into the supernatant. The SOD1 standards were 4, 2, and 1 pmol, respectively. **D.** Standard curve using bovine SOD1 as an internal standard at a concentration of 800 nM and varying the G93A SOD1 over a concentration range of 200 nM-1.2 μM. The ratio of the peak integrations of the G93A SOD1 over the bovine SOD1 was plotted against the amount of G93A SOD1 in the sample to produce the standard curve.

Chapter 3

Using theoretical protein isotopic distributions to parse small-mass-difference post-translational interactions via mass spectrometry

Timothy W. Rhoads, Jared R. Williams, Nathan I. Lopez, Jeffrey T. Morré, C. Samuel Bradford, Joseph S. Beckman

Submitted to *Journal of the American Society for Mass Spectrometry*

3.1 Abstract

Small-mass-difference modifications to proteins are obscured in mass spectrometry by the natural abundance of stable isotopes such as ^{13}C that broaden the isotopic distribution of an intact protein when observed by mass spectrometry. Using a Ziptip to remove salt from proteins in preparation for high resolution mass spectrometry, the theoretical isotopic distribution intensities calculated from the protein's empirical formula could be fit to experimentally acquired data and used to differentiate between multiple low-mass modifications to proteins. We could distinguish copper from zinc bound to a single-metal superoxide dismutase (SOD1) species; copper and zinc only differ by an average mass of 1.8 and have overlapping stable isotope patterns. In addition, proteins could be directly modified while bound to the Ziptip. For example, washing 10 mM S-methyl methanethiosulfonate over the Ziptip allowed the number of free cysteines on proteins to be detected as S-methyl adducts. Alternatively, washing with 10 mM diamide could quickly reestablish disulfide bridges. Using these methods, we could resolve the relative contributions of copper and zinc binding, as well as disulfide reduction to intact SOD1 protein present from <100 µg of the lumbar spinal cord of a transgenic, SOD1 overexpressing mouse. Although techniques like ICP-MS have provided solution metal amounts, this is the first method able to assess the metal-binding and sulfhydryl reduction of SOD1 at the individual subunit level and is applicable to many other proteins.

3.2 Introduction

Many mass spectrometers in principle have sufficient resolution to distinguish 1-2 Da mass differences in intact proteins that result from small post-translational modifications such as disulfide bond formation [108]. However, the natural abundance of ^{13}C and other stable isotopes in proteins obscures such low mass modifications because the same number of protein ions are distributed over dozens of isotopic mass peaks [109,110]. The intensities of the isotopic peaks can be predicted from the empirical formula of a protein with sufficient accuracy to distinguish even the addition of a single hydrogen atom [101,102,110]. Experimentally obtained intensities therefore contain a significant amount of information regarding the empirical formula of the molecule in question. Senko *et al*. used an experimental distribution based on a model amino acid, averagine, to assign the monoisotopic peak and empirical formula of myoglobin [110]. However, while the averagine method they used can calculate a distribution that closely matches the experimentally acquired data, the determined empirical formula did not match the correct formula exactly. Assigning the oxidation status of a metal ion, a single dalton mass change, has also been accomplished using isotopic distributions [111]. In this case, however, the authors looked at distributions that contained only one species. Green *et al*. distinguished between two species differing by 1 Da by identifying the tallest peak via the calculation of a centroid of the isotopic distribution over 50% of the maximum height [112]. This limits the ability to differentiate between differences in low abundance species that may contribute to less than 50% of the isotopic distribution, as could be the case when measuring proteins from in vivo samples. The challenge then is whether or not the isotopic distributions of proteins could be used to quantify multiple, simultaneous modifications to proteins isolated from tissue.

Our interest stems from the need to measure the metal content of the antioxidant protein copper, zinc superoxide dismutase (SOD1), a protein genetically linked to amyotrophic lateral sclerosis (ALS), from in vivo samples. We have previously shown that a C_4-reversed phase Ziptip® could be used to measure SOD1 from less than 100 μg of spinal cord from transgenic rats [113]. The Ziptip allowed salts and other contaminants that would otherwise interfere with mass spectrometry to be removed by washing with water. After washing, the Ziptip was mounted directly into the electrospray interface of a Time-of-Flight (ToF) mass spectrometer and proteins were eluted with a small amount of acetonitrile.

Although conditions for electrospray ionization could be made sufficiently gentle with the Ziptip method to keep metals bound to SOD1, a majority of the protein isolated from the spinal cord of transgenic animals was missing one metal. The missing metal from SOD1 in these tissues could be either copper or zinc, whose average masses differ by only 1.8 Daltons. Our method using ToF mass spectrometry lacks the resolution to distinguish such overlapping species. Determining whether the remaining metal was copper or zinc *in vivo* is important because we have previously shown that copper-containing, zinc-deficient SOD1 is toxic to motor neurons [94], but have no means of assaying zinc-deficient SOD1 from transgenic animal model tissue.

The measurement of zinc-deficient SOD1 is further complicated because the protein has an unusually stable intrasubunit disulfide bond restraining the zinc-binding loop. Additionally, the disulfide is known to be partially reduced in transgenic SOD1 overexpressing animals [103,107,114-117]. The extent of disulfide reduction in vivo is controversial because of differences in measurement methods between laboratories.

No method has been able to simultaneously determine which metals remain bound to disulfide-reduced versus oxidized SOD1 subunits in vivo. To address these issues, we adapted the Ziptip-based assay for use with a

Fourier transform ion cyclotron resonance (FT-ICR) mass spectrometer to accurately measure the isotopic intensity distributions of intact proteins. By comparing the predicted isotope distribution calculated from the empirical formula to the experimental high-resolution mass spectrum, it is possible to distinguish the contributions that each metal ion makes to the experimental isotopic distribution of SOD1. Reduction of the disulfide bond was independently assessed by modifying reduced cysteines with S-methyl methanethiosulfonate (MMTS). The combination of these methods could also be useful for probing multiple modifications to other proteins in addition to SOD1.

3.3 Materials and Methods

3.3.1 Reagents and Equipment

All chemicals were obtained from VWR, unless otherwise noted. Chicken lysozyme, bovine ubiquitin, and MMTS were obtained from Sigma-Aldrich. Bovine SOD1 from erythrocytes was obtained from Sigma. Its concentration was determined spectrophotometrically at 258 nm (ε= 5150 $M^{-1}cm^{-1}$ for the Cu,Zn containing monomer). Wild type and pseudo-wild type C111S human SOD1 expressed in *Escherichia coli* (recombinant SOD1) with coexpression of the copper chaperone for SOD1 (CCS) were used for developing many of the assays. C111S SOD1 is more stable than wild-type human SOD1 and was used here to verify the rapid modification of a single thiol was due to C111. The SOD1 protein was purified as described in Hayward *et al* [96], and the concentration was determined spectrophotometrically at 265 nm (ε= 9200 $M^{-1}cm^{-1}$ for the Cu,Zn containing monomer) [88]. Recombinant forms of human SOD were not acetylated on the N-terminus.

To generate copper- or zinc-containing single metal SOD1 standards, both metals were stripped from Cu,Zn SOD1 by incubating the protein (>1 mg/mL) in 50 mM acetate pH 3.7 with 1.5 mM EDTA. Once metal-free, copper-containing SOD1 was prepared by multiple additions of 15 µM copper nitrate atomic absorption standard (Sigma-Aldrich), in 10 mM potassium acetate at pH 4.15 with 10 mM sodium chloride, to the SOD1 in an Amicon Ultra 0.5 mL centrifugal filter with a 3k MWCO. This was centrifuged for 10 minutes at 16,000 rcf after each addition. Zinc-containing SOD1 was prepared in a similar manner through multiple additions of 15 µM zinc chloride atomic absorption standard (Sigma-Aldrich), in 10 mM potassium acetate at pH 4.6 with 10 mM sodium chloride. The number of metal additions was determined by monitoring metal incorporation into SOD after each addition via mass

spectrometry. All buffer solutions and water were run through a Chelex 100 (50-100 dry mesh, Sigma) column prior to use.

The solvent used for the mass spectrometric experiments was 30% acetonitrile, 70% water and 100 μM formic acid, delivered isocratically at a flow rate of 20 μL/min from a single pump (Shimadzu, Kyoto, Japan). The solvent was degassed for 10 minutes with helium and was changed each week. HPLC-grade solvents were used for all mass spectrometer experiments. Water was obtained from Burdick and Jackson (Muskegon, MI, USA).

3.3.2 Ziptip Method

SOD1 was also measured from tissue samples of wild-type SOD1-overexpressing transgenic mice (B6SJL-Tg(SOD1)2Gur/J). In eukaryotic sources, SOD1 is acetylated on the amino-terminus, increasing the protein mass by 42.1 Da. All animal procedures and housing arrangements were approved by IACUC (institutional animal care and use committee). Fresh spinal cord tissues from transgenic wild-type-SOD1 mice were extracted via dissection of euthanized animals and frozen at -80 °C until use. Frozen necropsy punches taken from 1 mm thick spinal cord slices were thawed in 10 mM ammonium acetate, pH 5.1, via centrifugation. The buffer, containing the soluble proteins, was adsorbed onto a C_4 reversed-phase Ziptip® (Millipore, Billerica, MA, USA), and then introduced into the mass spectrometer as described previously [113].

Probing the oxidation status of free cysteines was done using either MMTS or diamide. Diamide is a thiol oxidant, and could be used to ensure all disulfide bonds were oxidized [118]. This served as a negative control for using MMTS to determine if a disulfide bond was oxidized or reduced. MMTS modifies accessible free thiols with a methylthiol group. In developing the MMTS assay, lysozyme pre-incubated with 100 μM TCEP was used. Proteins were first adsorbed onto the Ziptip as above, but before rinsing with water the

tip was rinsed once with 10 µL of 10.6 mM MMTS. The short (<5 seconds) exposure time was sufficient to modify all free thiols on the protein of interest.

3.3.3 ^{13}C Measurements

The ratio of ^{13}C incorporated into a protein can vary depending on the source of carbon in either the bacterial media or in the mouse diet, which in turn reflects differences in carbon fixation between C3 and C4 plants [119]. Stable isotope analysis of tissues and purchased proteins was carried out by the Stable Isotope Research Unit (SIRU), Department of Crop and Soil Sciences, Oregon State University. Samples were analyzed for total carbon and ^{13}C on a PDZ Europa 20-20 isotope ratio mass spectrometer interfaced with a SerCon GSL elemental analyzer (SerCon, Crewe, UK). To determine % carbon, dry sample material was weighed to the nearest microgram on a Cahn microbalance prior to combustion. Liquid samples were pipetted onto an inert sorbant material (Chromosorb, SerCon, Crewe, UK). Samples were packaged in pressed tin capsules (Elemental Microanalysis, Devon, UK). The laboratory-working standard was NIST SRM1547 peach leaves (45.54% C, $\delta^{13}C$ VPDB -25.99). To correct for possible drift in the EA/IRMS combination with time, drift correction standards of equal mass were run every 10 samples. Additional standards were run as after every 10 samples. Stable isotope ratios were reported in delta notation as parts per thousand deviation from the international standard V-PDB. Typical precision for the SIRU 20-20 IRMS was <0.2 parts per thousand deviation for ^{13}C. These values were incorporated into the theoretical protein isotopic distribution calculations.

3.3.4 Mass Spectrometry

Proteins were detected using a LTQ-FT Ultra hybrid linear ion trap-Fourier transform ion cyclotron resonance mass spectrometer (Thermo, San Jose, CA) with a Finnigan™ Ion Max™ API source configured for electrospray

ionization (ESI) interface in positive ion mode. Measurements to determine the specific metals bound to the protein were accomplished in the ICR cell at a chosen resolution of 100,000 defined at 400 m/z, while quantitation of total protein levels using bovine SOD1 as an internal standard was performed in the linear ion trap.

Spectra were collected using Tune-Plus (Thermo, v. 2.2) page of Xcalibur (Thermo, v. 2.0.5) using the parameters given in Table 1. Spectra were averaged over the 3 minutes of the elution of SOD1 from the Ziptip using the Qual Browser (Thermo, v. 2.0). The data were exported as text files containing two columns of m/z versus intensity to be analyzed by custom programs written in *MatLab*™. The baseline was subtracted and centroids calculated from the experimental data using programs provided in the *Bioinformatics Toolbox* of *MatLab*. The parent mass distribution of SOD was reconstructed by summing the spectral regions containing individual charge states of SOD multiplied by their charge after subtracting the number of hydrogen atoms corresponding to the charge state [120]. Bayesian deconvolution of the mass/charge spectra as previously used with our ToF measurements was not necessary due to the clarity and high signal/noise ratio of the data.

3.3.5 Matlab Programming and Data Analysis

Intensities of theoretical isotopic distributions were calculated for apo, copper-containing, zinc-containing and Cu,Zn SOD1 via the Rockwood algorithm [102] using only the empirical formulas of the particular SOD mutant protein under investigation and the experimentally determined $^{13}C/^{12}C$ ratios (Table 3.2). The theoretical isotopic distributions calculated for SOD1 were calculated for electrically neutral parent molecules, so a hydrogen ion was removed for each charge carried by the metal ions bound to SOD1. Two hydrogen atoms were subtracted for the reduction of the intra-molecular

disulfide bond between C57 and C146. The theoretical spectra also were calculated with multiple additions when SOD was treated with the sulfhydryl-modifying agent MMTS.

Fitting of experimental to theoretical data was done in two steps. The predicted m/z centroids from the theoretical isotopic spectra were first matched to the closest m/z values for experimental centroid peaks for each charge state of SOD1 in the experimental spectra. The Levenberg-Marquardt fitting algorithm was then used to determine the optimal scaling of the normalized intensities of theoretical spectra with overlapping distributions to match experimentally measured centroid data. The fit was constrained to allow only positive intensities. Predicted isotope intensities less than 1% were ignored in the fitting program. The scaling factors were summed over all observable charge states to determine the relative contribution of each species to the overall observed spectrum.

3.4 Results

3.4.1 Optimization of Mass Spectrometry Parameters

As illustrated with lysozyme, the Ziptip interface worked well with the FT-ICR for many small proteins, enabling collection of isotopically resolved spectra that could then be combined into a parent mass spectrum (Figure 3.1). The isotopic intensities predicted from the empirical formula of lysozyme with four disulfide bonds accurately fit to the experimentally acquired isotope distribution (Figure 3.2), so long as the number of ions filling in the FT cell was kept below an empirically determined limit. Increasing the ion fill beyond this level distorted the isotopic distribution as seen with ubiquitin (Figure 3.3A-C). At lower ion fill levels, sensitivity decreased and the decreased signal to noise resulted in worse fitting to the predicted spectra. Consequently, the ion fill needed to be experimentally optimized for each type of protein, with smaller proteins generally fitting better with lower ion fills.

Copper-deficient and zinc-deficient SOD1 standards were used to validate the fitting program's ability to differentiate between copper and zinc in a one-metal peak (Figure 3.4-3.6). C111S SOD1 prepared with only zinc fit as exclusively zinc-containing SOD1 (Figure 3.4). C111S SOD1 prepared with only copper fit as mostly copper-containing SOD1 with 6% of the peak corresponding to zinc-containing SOD1 (Figure 3.5). These two single-metal standards, when combined in equimolar amounts, produced an isotopic distribution that was fit containing 48% copper-containing and 52% zinc-containing (Figure 3.6). Copper can also be reduced by one electron, a phenomenon often observed for iron-containing heme proteins in the gas phase. As a result, the fit required the inclusion of a second species for the CuZn protein one mass unit heavier as a result of the additional proton compensating for the loss of a charge on the copper [121]. The amount of copper reduction observed varied among the samples.

3.4.2 Sulfhydryl Oxidation Status Determination with MMTS

The intramolecular disulfide bond of SOD1 could be either reduced or oxidized, shifting the isotopic distribution by two Daltons. Although the difference could be parsed by the fitting program, the presence of other potentially overlapping species, such as zinc vs. copper, or Cu^{1+} vs. Cu^{2+}, confounded the fit. For measurements of those species from tissue samples, we included the thiol oxidant diamide in the buffer. Diamide rapidly oxidized disulfide bonds, thereby preventing any overlap within the isotopic distribution with the zinc or copper measurements. Diamide was not necessary with recombinant protein samples as the disulfide bonds were fully oxidized.

A separate assay was developed to determine the level of reduced disulfide present. After testing many sulfhydryl modifying reagents, we found that MMTS was particularly well suited to modify free thiols of proteins bound on the Ziptip. Each MMTS added 47.1 Da to every free thiol within seconds of exposure. The reduced disulfide bond increased a protein mass by 94.2 Da relative to those with an oxidized disulfide bond, allowing disulfide-reduced proteins to be clearly resolved from those with intact disulfide bridges.

Using tris(2-carboxyethyl)phosphine as a reductant, MMTS was utilized to determine the number of disulfide bonds of lysozyme that had been reduced over a given period of time (Figure 3.7). Lysozyme contains four disulfide bonds and does not bind metals like SOD1, making it a convenient molecule for perturbing disulfide bond status and validating MMTS for use as a free-thiol probe. A 100 mM concentration of tris(2-carboxyethyl)phosphine was sufficient to fully reduce one disulfide bond and partially reduce a second (Figure 3.7B), leading to a majority of the protein modified by 2 MMTS molecules and a small population modified by 4. Recombinant wild-type SOD1, when reacted with MMTS, was modified at one cysteine only as the disulfide bond was entirely oxidized, while C111S SOD1 was not modified (data not shown).

3.4.3 Detection of SOD1 from Tissue

Human SOD1 could be observed above the background soluble proteins of a 100 μg punch of SOD1-overexpressing mouse spinal cord, as had previously been observed in transgenic rats [113]. Surprisingly, the one-metal SOD1 peak comprised almost 60% of total SOD1 while 38% of the SOD1 contained both copper and zinc (Figure 3.8). Apo SOD1 represented less than 2% of the total SOD1. Without diamide present, the one-metal SOD1 peak showed a systematic shift to a slightly higher mass relative to the predicted isotopic distribution, indicating the existence of a population containing a reduced disulfide bond. MMTS modification revealed 15% of the one-metal SOD1 contained a reduced disulfide bond, closely matching the fit of 13%. In the presence of diamide, the shift to higher mass was absent, indicating oxidation of the disulfide bond. The one-metal peak fits entirely as zinc-containing SOD1 with no copper present.

3.5 Discussion

The Ziptip offers a simple, fast, and reliable method to isolate proteins in complex samples sufficiently free of interference to allow accurate measurement of the isotopic distribution. The isotopic distribution calculated from the empirical formula of several small proteins can match experimental data with a root-mean square of 1-2%, which provides sufficient accuracy to potentially resolve low mass post-translational interactions to a protein. In addition, the proteins bound to the Ziptip can also be reacted with specific modifying reagents. For example, free protein thiols were modified within seconds with MMTS on the Ziptip, which allowed thiol reduction to be probed independently of other modifications. These methods allowed us to simultaneously probe the metal content as well as the reduction of a key disulfide bridge in the same subunits of SOD1 directly from spinal cord tissues from transgenic mice.

Controlling the number of ions in the FTICR proved to be important for accurately resolving the isotopic distribution and the ion fill needs optimization for each type of protein. The upper limit likely results from space charge repulsion between protein ions that affects the course of the free-induction decay used to measure the mass to charge of protein ions [122,123]. Overfilling of the ion cell causes the central isotopic peaks of the protein's distribution to become magnified, while the smaller peripheral peaks were deemphasized [124]. These deviations can be identified from a residual plot of deviations (Figure 3.3A). As the ion fill levels were lowered, the isotopic distributions more closely matched the theoretical distributions but the signal-to-noise ratio eventually limited detection.

In developing the Matlab^{TM} programs to fit predicted isotopic distributions to experimental data, we customized the Rockwood algorithm [101] for calculating isotopic intensity distributions to allow different

abundances of isotopes to be included. The largest contribution to the isotopic distribution is the ratio of ^{13}C to ^{12}C incorporated into proteins, which can vary significantly in nature [119]. The major source of this variation results from different photosynthetic processes used to fix carbon dioxide. Due to compartmentalization of different steps of carbon fixation, plants such as corn that use the C4 pathway discriminate against the incorporation of ^{13}C less than plants relying entirely on the C3 Calvin cycle [125]. Proteins from animals fed diets enriched in corn can have a significantly greater amount of ^{13}C incorporated, which can be observed in the spectra [126,127]. These ratios can be independently measured by inductively coupled plasma mass spectrometry and incorporated in the calculation of the predicted spectra. The overall effect resulted in relatively small corrections in the RMS for the fitted plots of up to 0.5%. Such corrections could be relevant when measuring low-abundance species.

The isotopic distributions of copper and zinc add considerable complexity to the spectrum of SOD1 and are challenging to resolve because copper and zinc are neighbors on the periodic chart. Yet distinguishing how much copper can be lost compared to zinc from SOD1 in vivo is crucial for understanding how this enzyme malfunctions to cause motor neuron death in ALS. Tests with mixtures of metal-deficient SOD1s showed that fitting the predicted isotopic distributions allows copper-containing SOD1 to be readily distinguished from zinc-containing SOD1.

An additional potential confounding factor is the reduction of copper from Cu^{2+} to Cu^{1+} that is the key event in the standard catalytic cycle of SOD1. Reduction of copper by one electron increases the uncharged protein mass by one hydrogen ion. Thus, copper reduction will increase the mass of SOD1 containing the two stable ^{63}Cu and ^{65}Cu isotopes to equal the mass of SOD1 containing the ^{64}Zn isotope (48% abundance) or ^{66}Zn isotope (28% abundance). Hence, zinc-deficient cuprous-containing SOD would not be

distinguished from SODs containing the two predominant zinc isotopes and the method will underestimate the amount of copper-containing SOD1. Fortunately, this issue appears to be minor because reduction of copper in purified zinc-deficient SOD1 during electrospray ionization was not observed in any of our zinc-deficient SOD standards. Experiments with chemically reduced, purified zinc-deficient SOD1 also appeared to be completely oxidized in the mass spectrometer. This is consistent with copper being more exposed in zinc-deficient SOD and able to be reoxidized during the electrospray ionization process.

However, this does appear to be a problem for Cu,Zn SOD1, which becomes partially reduced during ionization, as can be observed in Figure 3.8. The observed spectrum for Cu,Zn SOD1 could only be reasonably fit by assuming a fraction of the copper was reduced. The reduction happened during the ionization process, because it was observed with both purified bovine and human SOD1 that were fully oxidized. These purified SOD1s were confirmed to be fully oxidized before introduction into the mass spectrometer by measuring the cuprous d-d* band (λ_{max}=680 nm). Reduced SOD1 has no absorbance at this wavelength. These fits typically found that 20-50% of Cu,Zn SOD1 was reduced. Chemically reduced purified Cu,Zn SOD1 also appeared to be a mixture of reduced and oxidized SOD. These results might be explained by the oxidation of formate within the steel electrospray needle to formate radical that will reduce oxygen to superoxide. The superoxide produced would result in a rapid reduction of oxidized SOD1 as well as oxidation of reduced SOD1 to produce a mixture of reduced and oxidized Cu,Zn SOD1 from whichever was present at the start.

A further challenge to resolve is the potential reduction of the disulfide bond of SOD, which is known to occur in SOD1 transgenic mice [107]. The addition of two hydrogens upon reduction almost perfectly overlaps the difference between copper and zinc. Parsing the difference between the two

concurrently is not directly possible by mass measurements alone. For tissue measurements, we could include diamide to oxidize disulfide bonds, allowing us to ignore any contribution the two additional protons on a reduced disulfide would make to the isotopic distribution. The fitting program could easily parse zinc and copper bound to SOD1 in this case. However, the measurement of thiol reduction in SOD1 necessitated the development of another approach. The majority of thiol modifying agents, including iodoacetamide, iodoacetic acid, vinyl pyridine, and maleimides, reacted too slowly to be useful in the present assay. In addition, many modifiers introduced adducts whose mass overlapped with other metal-binding states of SOD1. MMTS, in contrast, modifies free thiol groups in less than five seconds and added a methyl thiol group (-SCH_3; 47.1 Da). Hence, MMTS could be washed over SOD1 bound to the Ziptip and was simple to incorporate into the assay. Purified SOD1 bound one methyl thiol group immediately, which we concluded was due to modification of cysteine residue 111 since the modification did not occur using the pseudo-wild type SOD1 containing the mutation of cysteine 111 to serine. One caveat with MMTS is that the methyl thiol adduct is the intermediate formation of a mixed disulfide and could exchange with another cysteine to reoxidize the disulfide bridge [128]. This was minimized by using 10 mM MMTS to modify all free thiols within seconds.

In summary, isotopically-resolved protein mass spectrometry data offer a simple means to measure non-covalent protein post-translational interactions via mass spectrometry. The method is exquisitely sensitive, allowing us to even measure metal contents of SOD1 from samples as small as a few hundred cells collected by laser capture (Figure 3.9). It has also proved useful in assessing the correct expression and formation of disulfides of other recombinant proteins. The Ziptip method also allowed bound proteins to be probed with classical biochemical protein modifying reagents to examine other modifications.

3.6 Acknowledgements

We are grateful to Rockie Yarwood of the Stable Isotope Research Unit for ^{13}C measurements. We would also like to acknowledge the Environmental Health Sciences Center Mass Spectrometry Core Facility for infrastructure support. This work was supported by the National Institute for Environmental and Health Sciences (NIEHS P30ES000210), the National Institutes of Neurological Disorders and Stroke (NINDS R01NS058628A), and the National Center for Complementary and Alternative Medicine (NCCAM P01AT002034).

3.7 Abbreviations

SOD1, Cu,Zn superoxide dismutase; ALS, amyotrophic lateral sclerosis; ToF, time-of-flight; FT-ICR, fourier transform ion cyclotron resonance; MMTS, S-methyl methanethiosulfonate; CCS, copper chaperone for SOD1; IACUC, institutional animal care and use committee; SIRU, stable isotope research unit; ESI, electrospray ionization.

Table 3.1. Instrumental parameters for LTQ-FT Ultra mass spectrometer.

ESI Source	
Sheath Gas	2 arb units
Auxillary Gas	1 arb units
Sweep Gas	1 arb units
Spray Voltage	5 kV
Capillary Temp.	200 °C
Capillary Voltage	36 V
Tube Lens	205 V
Scan Parameters	
Mass Range	800-2000 m/z
Resolution	100000
Scan Type	Full
Microscans	1
Max. Inject Time	8000 ms
ICR Cell Parameters	
Trapping Voltage	Pos 0.51 Neg -0.40
Excite Amplitude	fm>190(+): 0.64
	fm>98(+): 0.5
	fm>50(+): 0.75
Injection Control	
Full MS	8.00×10^5 ion current

Table 3.2. $\delta^{13}C$ values for proteins from different sources.

Protein Source	$\delta^{13}C$
Recombinant	-20.24
Bovine/Chicken	-11.94
Rodent	-19.56

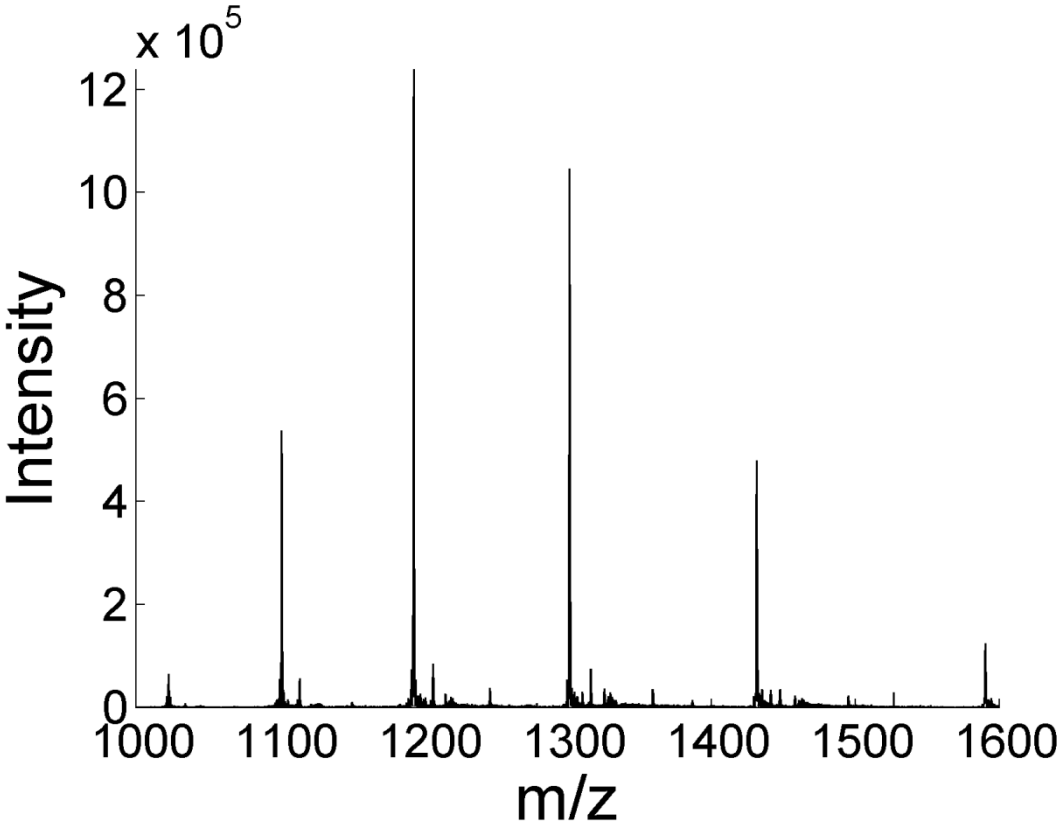

Figure 3.1 Charge-state spectrum of chicken lysozyme. The m/z distribution of chicken lysozyme eluted from the Ziptip, showing charge states 9-14.

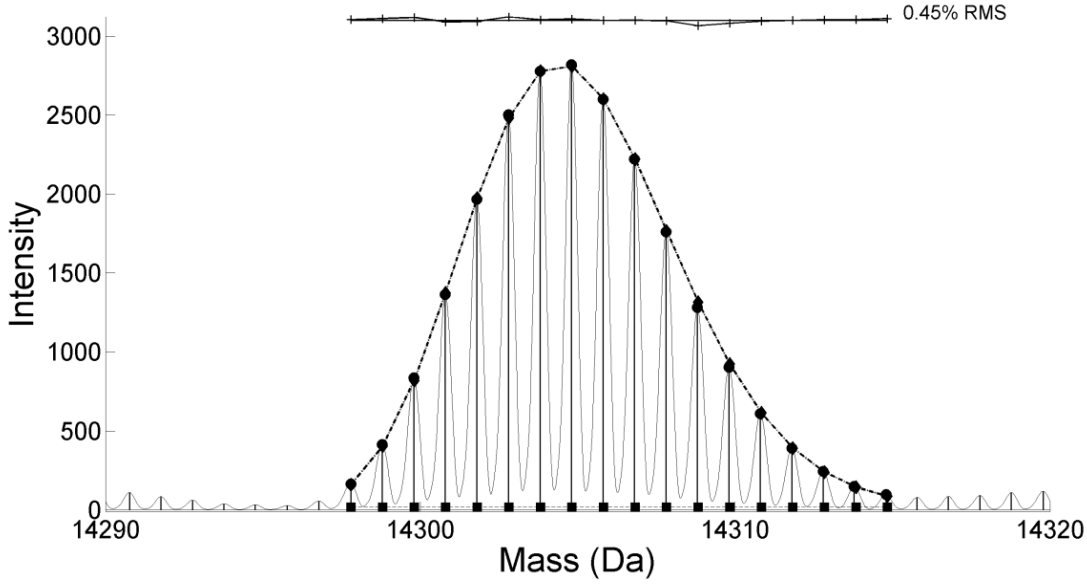

Figure 3.2 The parent mass spectrum of chicken lysozyme derived from Figure 3.1. The theoretical isotope distribution of chicken lysozyme, based on the empirical formula $C_{613}H_{951}N_{193}O_{185}S_{10}$, was fit to the experimental distribution, showing excellent agreement. $\delta^{13}C$ of -11.94 was used for the theoretical isotopic distribution calculation.

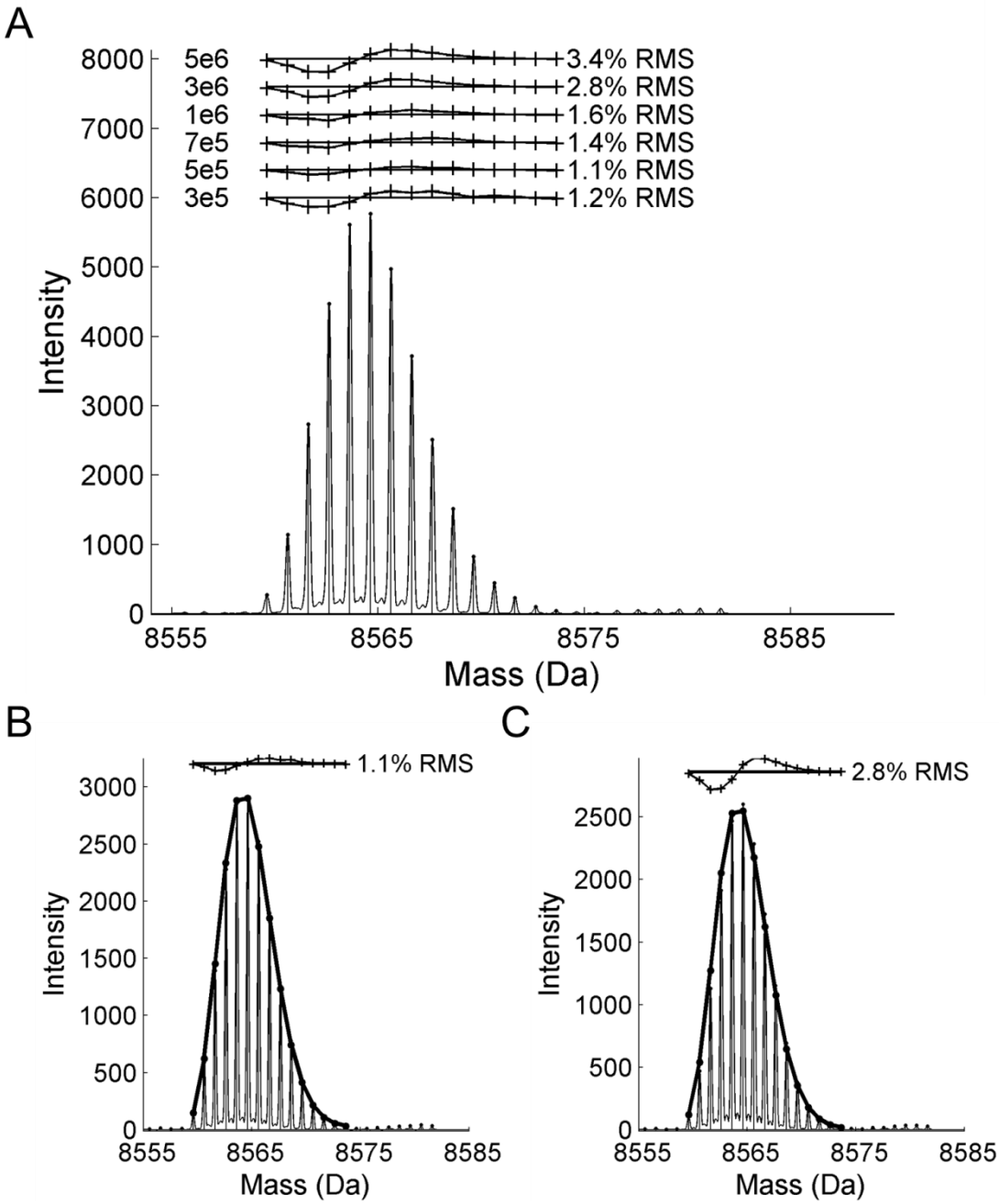

Figure 3.3 Effect of ion cell fill on the isotopic distribution of ubiquitin. A. Bovine ubiquitin was fit with the program at ICR cell AGC settings from $3x10^5$ to $5x10^6$, demonstrating a systematic deviation from the expected distribution at ion fill levels below and above $5\text{-}7x10^5$. B. Ubiquitin fit at the optimal $5x10^5$ ion fill. C. Ubiquitin fit at $3x10^6$ ion fill, showing the systematic deviation. $\delta^{13}C$ of -11.94 was used for the theoretical isotopic distribution calculation.

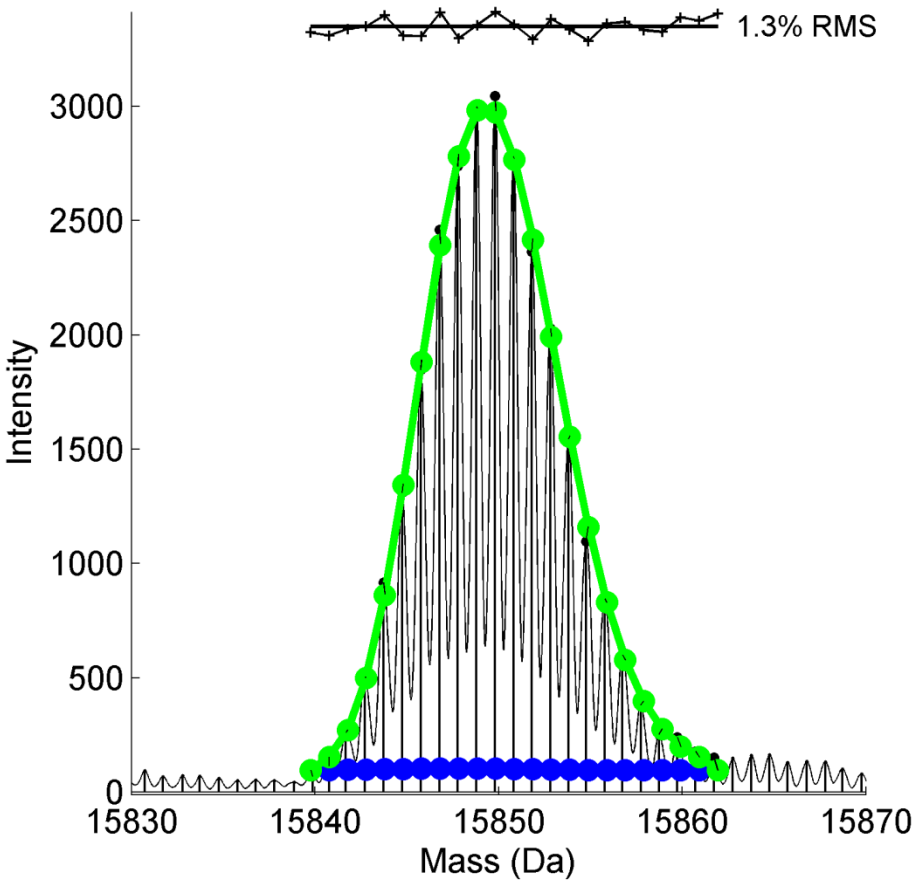

Figure 3.4 C111S SOD1 prepared with only zinc. C111S mutant SOD1 single-metal standard was prepared with only zinc (green fit) as described in the methods. The fit was 100% zinc-containing. $\delta^{13}C$ of -20.24 was used for the theoretical isotopic distribution calculation.

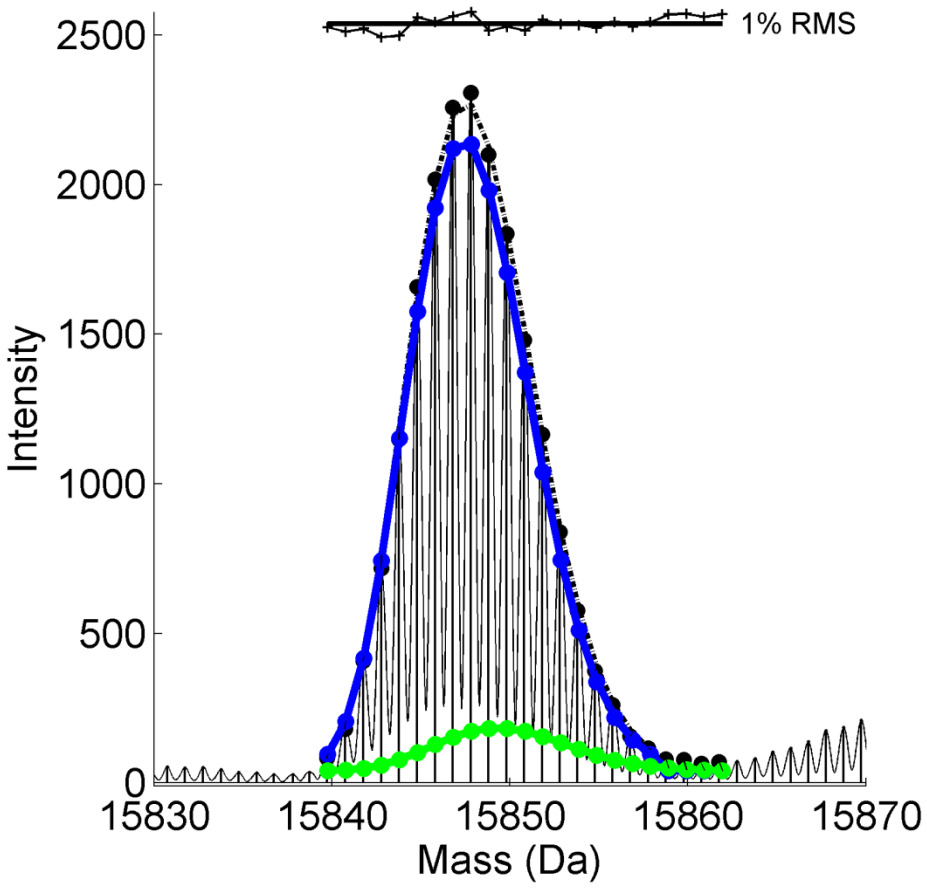

Figure 3.5 C111S SOD1 prepared with only copper. C111S mutant SOD1 single-metal standard was prepared with only copper (blue fit) as described in the methods. A small amount of residual zinc (green fit) that varied with the preparation was consistently present that we were unable to remove, 6.6% in this case. $\delta^{13}C$ of -20.24 was used for the theoretical isotopic distribution calculation.

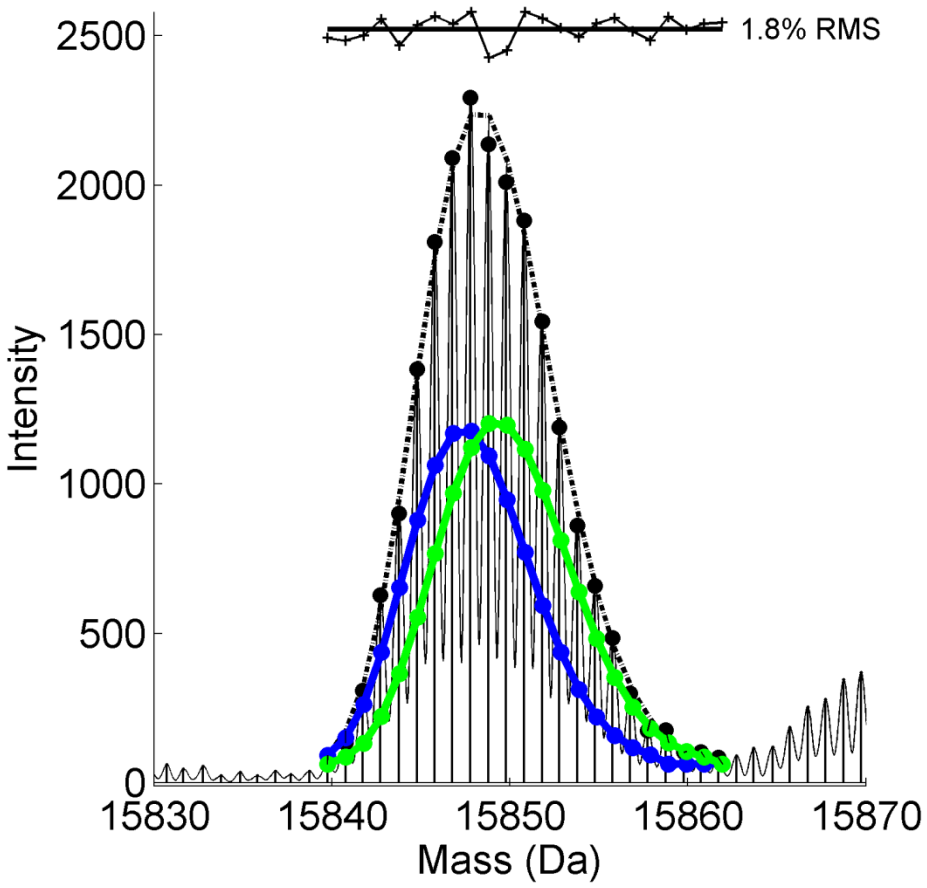

Figure 3.6 50-50 mixture of C111S SOD1 single-metal standards. C111S mutant SOD1 single-metal standard prepared with only zinc (green) or only copper (blue) were combined in equimolar amounts and the resulting distribution fit to the theoretical isotope distributions, which returned a ratio of 48% copper containing and 52% zinc containing SOD1. $\delta^{13}C$ of -20.24 was used for the theoretical isotopic distribution calculation.

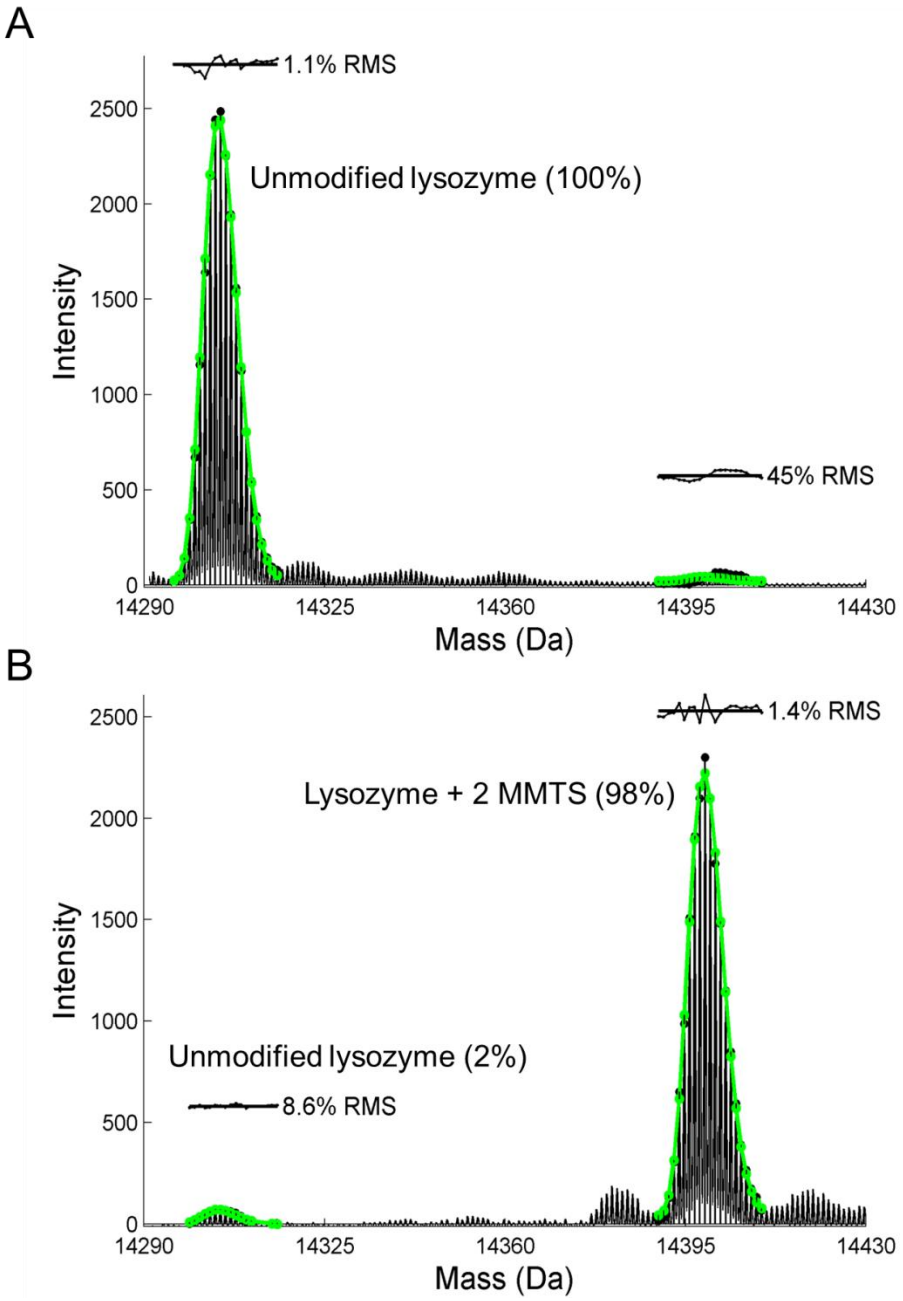

Figure 3.7 Use of MMTS to determine thiol oxidation status of lysozyme. Lysozyme was subjected to MMTS treatment on the Ziptip as described in the methods after incubation with TCEP for 0 minutes (**A**) or 30 minutes (**B**), demonstrating the complete reduction of one disulfide bond. $\delta^{13}C$ of -11.94 was used for the theoretical isotopic distribution calculation.

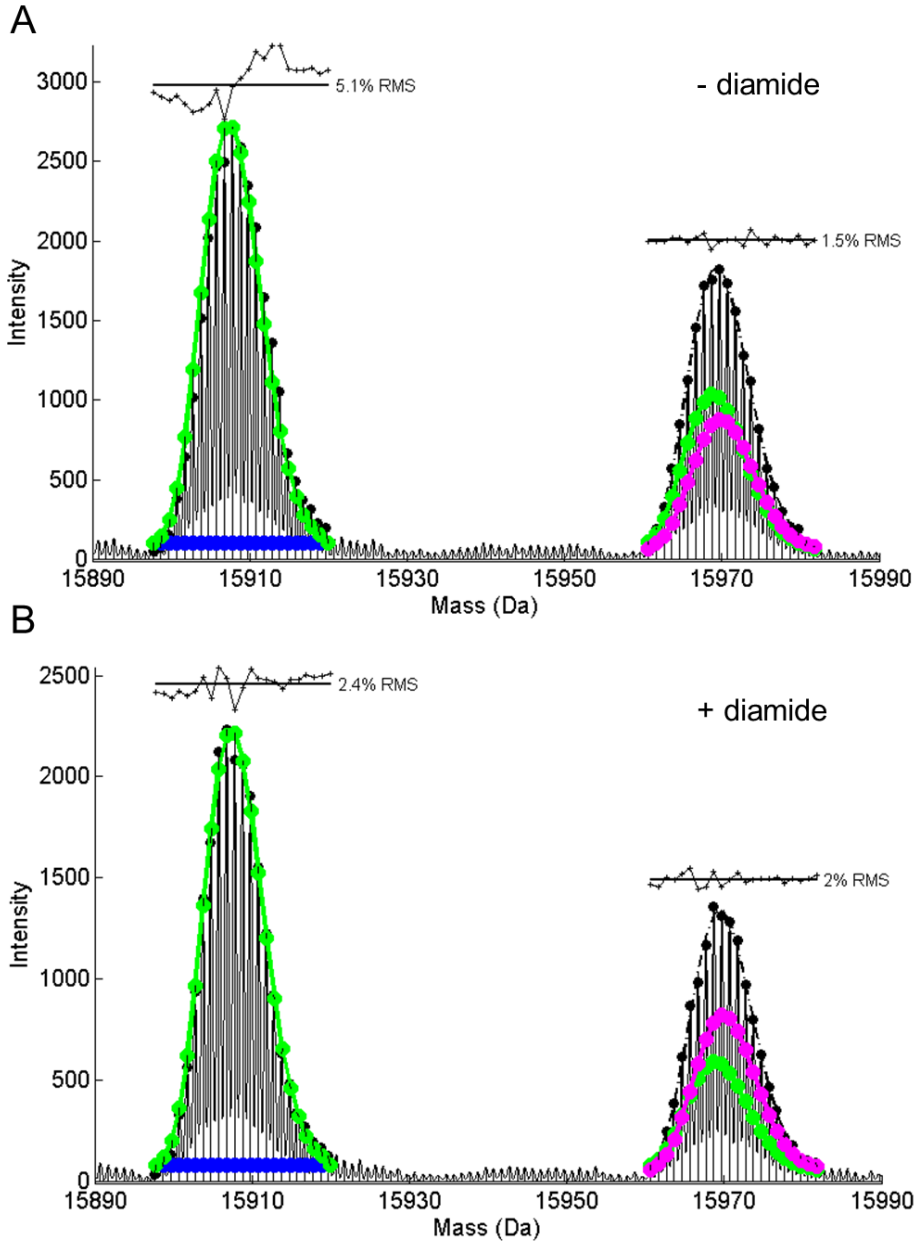

Figure 3.8 SOD1 isolated from the ventral spinal cord of a wild-type transgenic mouse with and without diamide. A ventral spinal cord punch was analyzed via the ziptip assay as described in methods. **A.** The one-metal SOD1 peak without diamide shows a systematic shift towards the right, indicating the presence of some disulfide reduction. **B.** The same tissue run with diamide present does not contain that shift, indicating the complete oxidation of the disulfide bond. The amount of disulfide reduction was confirmed with our MMTS assay. $\delta^{13}C$ of -19.56 was used for the theoretical isotopic distribution calculation.

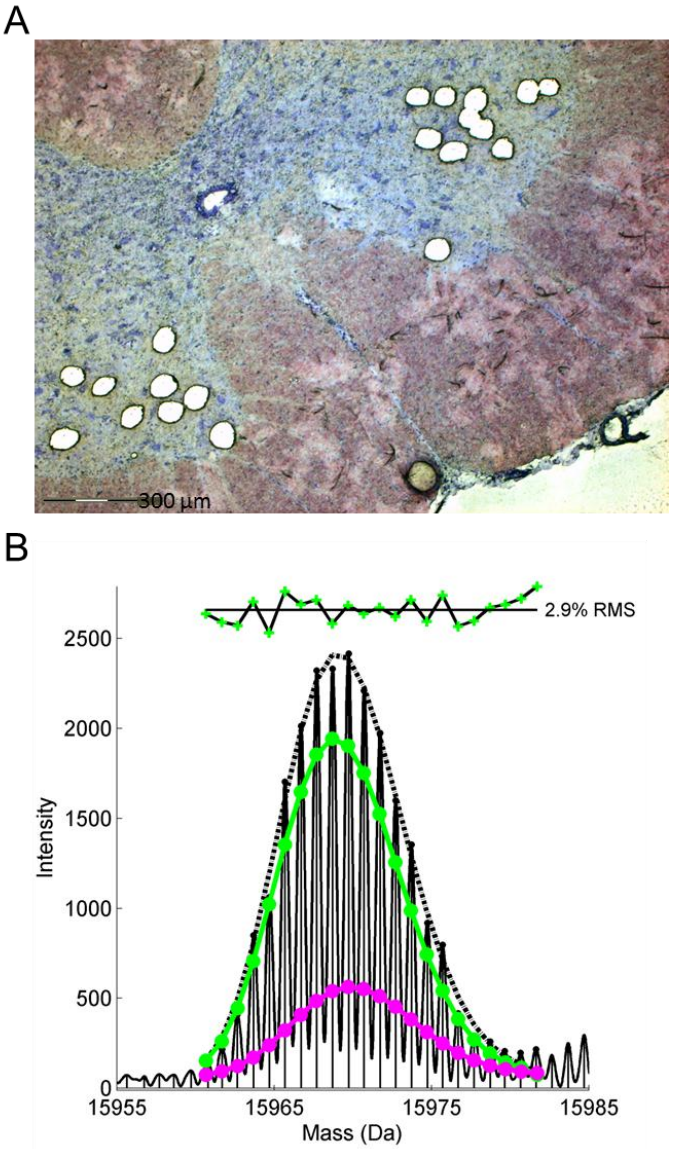

Figure 3.9 SOD1 isolated from 400 motor neurons captured via laser capture microdissection. The spinal cord from a wild-type transgenic rat was frozen and embedded in O.C.T.™ (Optimal Cutting Temperature) sectioning medium. 20 µm thick sections were cut using a cryostat and then stained with Cresyl violet. **A.** A Zeiss Laser Capture Microdissection instrument was used to cut and capture approximately 400 motor neurons from eight sections into 20 µL of 10 mM ammonium acetate. A 50X magnification of one section is shown. Scale bar is 300 µm. **B.** A mass spectrum of the capture buffer was acquired using a Ziptip, showing Cu,Zn SOD1 from the motor neurons.

Chapter 4

Assessing the impact of metal-binding and disulfide status of superoxide dismutase on amyotrophic lateral sclerosis

Timothy W. Rhoads, Jared R. Williams, Nathan I. Lopez, Joseph S. Beckman

Formatted for Publication

4.1 Abstract

The relevance of the metal-binding of Cu,Zn superoxide dismutase (SOD1) to mutant-SOD1-linked amyotrophic lateral sclerosis (ALS) remains controversial. The metals have a larger influence on the folding and stability of SOD1 than any single mutation. However, they are frequently ignored in discussions of how partially unfolded intermediates of mutant SOD1 may cause ALS. We have previously demonstrated that exogenous zinc-deficient SOD1 is toxic to motor neurons in cell culture, but it has not been possible to measure which metal-bound species of SOD1 are present *in vivo*. The development of a Ziptip-based, high resolution mass spectrometry assay to measure SOD1 from small amounts of spinal cord tissue while keeping metal-binding intact now allows us to determine how the presence of zinc-deficient SOD1 in disease-affected tissue correlates with the progression of ALS. We present here a combined approach to quantify the metal-binding and disulfide oxidation status of SOD1 in a mouse model of ALS. This provides a detailed look at the partially unfolded intermediates of SOD1 present in the spinal cord both in pre-symptomatic, end-stage, and control SOD1 transgenic mice. We found that wild-type SOD1 mice contain more of all forms of the partially unfolded intermediate species of SOD1 except for copper-containing, zinc-deficient SOD1. Zinc-deficient SOD1 was present at a toxic level in G93A mice, while the wild-type mice contained a substantially lower, likely non-lethal level of zinc-deficient SOD1.

4.2 Introduction

The mechanism by which mutant forms of Cu,Zn superoxide dismutase (SOD1) cause amyotrophic lateral sclerosis (ALS) has remained controversial since the involvement of the protein in the disease was first discovered in 1993 [9]. As of 2012, 165 different mutations to SOD1 that lead to the development of the disease have been identified (http://alsod.iop.kcl.ac.uk/). The rate of progression of the disease can vary widely, depending on the mutation, but the age of onset is generally uncorrelated with any mutation [52,53]. Both the pattern of inheritance and experiments with transgenic animals clearly establish that the mutations confer a toxic gain of function rather than resulting in a loss of superoxide scavenging activity [23,129]. Much of the research has focused on SOD1-immunoreactive aggregates that are readily observed in animal models at the last stages of the disease. These aggregates of SOD1 may be a result of the gross overexpression of mutant SOD1 in the most common ALS models [43,46,130-134]. Although these aggregates are purported to be cytotoxic, evidence of direct toxicity is lacking. Some ALS models involving low expression of SOD1 show no evidence of aggregation even in terminally ill animals [50,135]. Thus aggregates of SOD1 may be a symptom rather than the driver of toxicity.

The presence of aggregates in the disease has led to increased scrutiny of the mechanics of SOD1 folding and unfolding. The folding pathway for SOD1 includes four post-translational modifications. The first is binding of the zinc cofactor [136,137]. The zinc ion organizes a significant loop structure that contributes to the dimer interface of the protein. Once the protein has acquired zinc, it has enough structure to interact with the copper chaperone for SOD1 (CCS), an interaction that is mediated by an SOD1-like domain in CCS that forms a dimer with the zinc-containing SOD1 subunit. The second modification is insertion of a copper ion and the third is oxidation of the

disulfide bond, both of which are mediated by CCS [138,139]. The completely folded monomer is then able to dimerize with another folded SOD1 subunit.

The unfolding process is thought to proceed through a two-state mechanism: dimer dissociation followed by monomer unfolding [140]. Mutations to SOD1 destabilize the protein, presumably making this process more likely to occur [141]. The destabilization leads to a shift in the folding equilibrium towards increased population of soluble, partially unfolded intermediate species [142]. The toxicity of mutant SOD1 may arise from such partially unfolded species that can arise either via incomplete folding and activation or via unfolding from an active state. The partially unfolded species present *in vivo*, however, are not well characterized.

The metal cofactors in particular play a significant role in SOD1 stability and folding [55,140,143,144]. The metal-replete enzyme has an unfolding half-life on the order of 200 years, whereas the apo protein unfolds in hours [140]. Zinc loss, in particular, dramatically decreases the stability of SOD1, and is thought to be the first metal lost as the protein unfolds [55,140]. Nevertheless, the metal content of SOD1 *in vivo* is often ignored or unknown. Techniques such as activity gels often serve as surrogates for actual metal-binding measurements, although the activity assay demonstrates only the ability to inhibit the reaction of superoxide with an indicator molecule, not that copper is actually bound to the protein [145]. An additional problem is that high levels of metal chelators, such as millimolar amounts of EDTA, are often used to prevent additional bands from appearing on an activity gel [30]. The bands are ascribed to spurious metal-binding to the protein, but the levels of chelators used may in fact impact the specifically-bound cofactors as well.

Although the metal-binding of SOD1 is frequently ignored *in vivo*, there are several examples of SOD1 metal-binding playing a role in causing toxicity in cell culture models. The zinc chelating ability of the folded apo SOD1 was shown to mediate the toxicity of SOD1 to cultured human neuroblastoma cells

[146]. The role of copper in toxicity has also been studied. The loss of zinc from SOD1 resulted in a copper-containing zinc-deficient protein that could induce motor neuron apoptosis in cell culture similar to trophic factor withdrawal [69,147]. The toxicity also required the production of nitric oxide, leading to peroxynitrite production. Zinc-deficient SOD1 can catalyze protein tyrosine nitration via peroxynitrite [57]. Crucially, the zinc-deficient protein was toxic whether or not it carried an ALS-mutation, evidence that may help explain the mechanism of sporadic ALS.

The lack of knowledge concerning the *in vivo* metal-binding of SOD1 is due in part to the difficulty in assessing the native metal-binding of a protein i*n vivo.* This is especially true of SOD1, as copper and zinc are similar in mass and electronic structure. The intrasubunit disulfide bond is an additional confounding factor that is intrinsically related to the metal-binding. One side of the disulfide linkage is located on the zinc-binding loop of the protein, making it necessary to understand the role the disulfide bridge may play in metal-binding. The level of disulfide reduced SOD1 protein in general has been the subject of debate, as different levels of disulfide reduction in transgenic animals are found depending on the methods used, although the metal content is not known [107,116,148].

We have recently developed a series of techniques to measure the metal-binding and disulfide oxidation status of proteins from *in vivo* samples using high resolution mass spectrometry [113]. SOD1 can be extracted from small location-specific punches from disease-affected or non-affected areas of spinal cord tissue from transgenic rats or mice. A C4 Ziptip® allowed physiological salts to be washed off, enabling the detection of proteins via electrospray mass spectrometry. We observed that almost half of the SOD1 from the spinal cord of a wild-type SOD1 overexpressing transgenic mouse bound only a single zinc ion and was missing the copper cofactor. Almost 25% of that single metal SOD1 contained a reduced disulfide. Zinc-deficient SOD1

was not observed. These results illuminate the need to understand how the metal-distribution of SOD1 is different in disease-affected G93A mice, as well as how it might change as the disease progresses. We present here the application of our previous methods to measure SOD1 metal-binding and disulfide oxidation status from G93A and wild-type mouse tissues over the course of the disease progression.

4.3 Materials and Methods

4.3.1 Animal Care and Use

All animal studies were carried out with strict adherence to the recommendations in the Guide for the Care and Use of Laboratory Animals of the National Institutes of Health. Oregon State University Laboratory Animal Resources Center personnel provided husbandry services in an Association for Assessment and Accreditation of Laboratory Animal Care accredited environment. All animal handling and procedures were approved and overseen by the Institutional Animal Care and Use Committee. The most commonly used transgenic ALS SOD1 model, G93A SOD (B6SJL-Tg(SOD1*G93A)1Gur/J) mice, grow and develop normally until around 110 days of age when symptoms of the disease first become apparent. The progression usually starts with an altered hind limb gait, proceeding in a few days with noticeable weight loss and partial paralysis. The end stage of the progression was complete paralysis of the hind limbs, typically by 120-125 days of age. The control wild-type SOD1-overexpressing (B6SJL-Tg(SOD1)2Gur/J) mice do not display any of these symptoms and are reported to contain about 60% of the SOD1 mRNA level of the G93A mice [23]. The mice were maintained in separate colonies by breeding hemizygous transgenic males to non-transgenic (B6SJLF1/J) females. New transgenic male mice and non-transgenic female mice were periodically ordered from Jackson Labs to maintain background consistency with others using this model.

Animals sacrificed for tissue harvest were placed under isofluorane anesthesia followed by pericardial perfusion with heparinized PBS and decapitation. Brain, kidney, lung, leg muscle, stomach and heart were extracted via dissection and snap frozen in liquid nitrogen. The spinal cord was removed by inserting a 26 gauge needle into the base of the spinal

column and pushing PBS with a syringe to force the cord out the top. Although the cord came out intact, the roots were generally sheared off. Animals were sacrificed at 30 days, 60 days, 90 days, and 120 days or when they became symptomatic (110-120 days). The weakened structural integrity of the spinal cord in terminal animals (120-125 days) meant that the spinal cord could be easily damaged when removed. As a result, the animals chosen for the 120 day age group for this study were sacrificed while symptomatic, but not yet terminal. Tissues were stored at -80 °C prior to use.

4.3.2 Tissue Measurements

Four types of SOD1 measurements were performed on the tissues collected: SOD1 quantitation via mass spectrometry, determination of relative copper and zinc levels via high resolution mass spectrometry, disulfide bond oxidation status determination, and SOD1 extraction efficiency via reducing and non-reducing gels and Western blots. SOD1 quantitation via mass spectrometry was accomplished by including a known concentration of bovine SOD1 in the buffer. Additionally, the measurements were performed in the low resolution linear ion trap of our hybrid LTQ-FT instrument due to concerns about overfilling the ICR cell when the standard bovine SOD1 was present and a desire to measure the level of apo SOD1, which was not observable with the m/z cutoff used for the FT measurements (see Chapter 3). As such, quantitation measurements only provided levels of apo, one-metal, and two-metal SOD1. The disulfide oxidation status measurements were performed in the linear ion trap. The determination of copper or zinc bound to SOD1 was performed in the high resolution ICR cell.

For spinal cord measurements, punches were taken from five 1 mm thick transverse sections from the lumbar region using a 300 μm biopsy punch (Zivic Instruments, Pittsburgh, PA, USA) with an air-filled syringe attached to the rear of the punch to expel the tissue as previously described [113]. All five

slices were laid out on an insulating plastic plate on top of dry ice to warm to about -20 °C as the tissue was too brittle at liquid nitrogen temperatures to manipulate. From each slice, one punch from each area (ventral left, ventral right, dorsal left, dorsal right) was taken with the biopsy punch; all 5 punches from each area were combined into one tube. The tissue from the left side was placed directly into 50 µL of 10 mM ammonium acetate with 10 mM diamide and centrifuged at 15000 rcf. The tissue from the right side was placed in a micro weigh boat (VWR #12577-060) and weighed on a Cahn 25 Automatic Electrobalance (Cerritos, CA, USA) with a sensitivity of 0.1 µg. After weighing, the weigh boat was flattened in the top of a microcentrifuge tube and the tissue was spun down to the bottom of the tube containing 50 µL of 10 mM ammonium acetate. For brain measurements, 6 punches were taken from a 1 mm thick coronal section of the (rostral) cortex region. Three punches were combined into one tube and prepared as described above for the spinal cord tissue. After centrifugation the supernatant was removed from the tissue pellet, separated into 10 µL aliquots, frozen and held in liquid nitrogen before mass spectrometry analysis. For all other tissues, single punches were thawed in 10 µL of 10 mM ammonium acetate, pH 5.2.

Mass spectrometric analysis using a Ziptip was performed on a LTQ-FT Ultra mass spectrometer (Thermo, San Jose, CA, USA) as previously described (Chapter 3). The mass spectrometry running solvent was either 30:70 acetonitrile:water or 25:75 acetonitrile:water, depending on the tissue being assayed, delivered isocratically via a single Shimadzu HPLC pump. In both cases the running solvent contained 100 µM formic acid to more efficiently ionize SOD1. The left-side tissue was analyzed in the ICR cell to provide high-resolution isotopic distributions that could be fit with our custom Matlab programs (Chapter 3). Three of the five aliquots were run, and individual aliquots were replaced if the fitting program was unable to find data to fit. The right-side tissue was analyzed in the linear ion trap to provide

quantitation data with bovine SOD1 used as an internal standard. One of the LTQ aliquots was modified on the Ziptip with MMTS for 5 seconds before being analyzed via the mass spectrometer to determine thiol oxidation status. For determining total SOD1 concentration spinal cord, brain, kidney, leg muscle, heart or liver was sectioned as above and a single punch was weighed on the electrobalance. After flattening the weigh boat in the top of the microcentrifuge tube, the tube was frozen for 3 seconds in liquid nitrogen. This was done because many of the non-CNS tissues would not release cleanly from the weigh boat upon centrifugation without freezing. The tube was then centrifuged and analyzed as above in the linear ion trap. This was repeated two more times for each tissue. We only report the levels of two-metal, one-metal, and apo SOD1 in those tissues.

4.3.3 Statistical Analysis

The level of zinc-deficient SOD1 was tested for statistical significance using Statgraphics (v. 16.1.03, StatPoint Technologies, Warrenton, VA, USA). Because the data in some cases did not fit a parametric distribution, The Kolmogorov-Smirnov test was used.

4.3.4 Western Blot Analysis

The amount of SOD1 released from tissue was verified by western blot analysis on non-reducing and reducing SDS-PAGE. We used both reducing and non-reducing gels to confirm the quantitation from the mass spectrometry analysis, how much SOD1 remained in the pellet after our extraction procedure, and whether thiol or non-thiol crosslinked oligomers could be observed from spinal cord tissue matched to that used for mass spectrometry analysis. The supernatants from three punches were combined to provide enough sample per lane for the Western blot. The punches were thawed in 20 μL of 10 mM ammonium acetate at pH 5.1, vortexed for 10 seconds, and

centrifuged for 1 minute at 15000 rcf. The tissue supernatant and pellet fractions were separated, and the pellet was rinsed with an additional 10 μL of thaw buffer. The rinse was combined with the supernatant. The supernatant fraction was diluted with 5X Laemmli buffer, bringing the Laemmli buffer to a 1X concentration. The pellet was brought up to the same volume as the supernatant fraction with 1X Laemmli buffer [100]. For the non-reducing gels, Laemmli buffer without β-mercaptoethanol was used. The samples were heated for 5 min at 95 °C. Samples were then run on a 10% SDS-PAGE at 150 V for 60 min in a Bio-Rad Mini Protean II system. Gels were transferred to a polyvinylidene fluoride membrane (Bio-Rad Product No. 162-0177) for 60 min at 100 V. SOD1 was detected using rabbit polyclonal antibodies raised in our laboratory against human SOD1 (1:10000). Affinity-purified antibodies retained cross reactivity with mouse and rat SOD1. The secondary antibody was goat anti-rabbit IgG heavy plus light chain horseradish peroxidase conjugate (Bio-Rad No. 170-6515).

4.4 Results

4.4.1 SOD1 Distribution and Metal Content in Tissues

The total amount of SOD1 was higher in wild-type mice than in G93A mice in spinal cord, brain, kidney and liver, whereas the reverse was true for the muscle tissues (Figures 4.1 and 4.2). The majority of the SOD1 contained both copper and zinc with the amount missing one metal being largest in the spinal cord and brain tissues of both G93A and wild-type SOD1 transgenic mice. In these tissues, one-metal forms accounted for 20-30% of the total SOD1 in G93A mice, but 45-55% in wild-type mice. The SOD1 missing one-metal comprised less than 15% in the other tissues. These measurements were the average of 3 independent tissue punches, likely contributing to the high variability observed in some cases. The amount of apo-SOD, which is missing both copper and zinc, was less than 5% in all tissues assayed.

The high resolution of the FT-ICR mass spectrometer allowed the theoretical isotopic distributions for zinc and copper-containing SOD1 to be fit to isotopically resolved spectra of SOD1. The amounts of each SOD1 metal-state were 30% lower than in Figures 4.1 and 4.2; the extraction method for assays to determine the metal bound to SOD1 contained one less freeze-thaw step due to concerns about the stability of one-metal SOD1s. In initial experiments, the one metal-containing SOD1 fit best to only zinc-containing SOD1 for both genotypes, with no measurable copper-containing SOD1 (Figure 4.3A,C). Close examination of the m/z spectra also showed small evidence of oxidation of the SOD protein, manifested as the addition of 1-3 oxygens to the protein. We did not observe glutathione adducts or other modifications to the C111 thiol. Such modifications were readily detected in recombinant SOD1, particularly when subjected to treatments adding copper to metal-deficient SOD involving dialysis (data not shown).

4.4.2 Diamide Prevents Copper Loss from Zinc-deficient SOD1

We were initially unable to measure any copper-containing, zinc-deficient SOD1 from the spinal cord, even in early symptomatic G93A transgenic animals (Figure 4.3A). Because of the toxicity of zinc-deficient SOD1 to motor neurons in cell culture, we tested whether tissues might contain compounds that would remove copper from zinc-deficient SOD1 during isolation by adding recombinant zinc-deficient SOD1. The copper was in fact quickly removed from zinc-deficient SOD1 and ultrafiltration showed the copper–removing activity would pass through a 3-kDa membrane. A variety of reagents and methods were tested to prevent the loss of copper from recombinant zinc-deficient SOD. Inclusion of the sulfhydryl oxidant diamide directly in the thaw buffer used for the frozen tissue punches was the most effective at preserving copper in recombinant zinc-deficient SOD1. Diamide treatment also effectively oxidized the intracellular disulfide bond in SOD1, further simplifying the isotopic analyses by eliminating overlapping disulfide-reduced species from the mass spectrum (Chapter 3).

With the inclusion of diamide, copper-containing, zinc-deficient SOD1 could be measured in the spinal cord, particularly in G93A SOD1 mice (Figure 4.3B). Less was found in wild-type SOD1 mice where the amounts observed were generally close to background (Figure 4.3C). Separate experiments using recombinant SOD1s showed that diamide treatment had no effect on the isotopic distribution of Cu,Zn SOD1, copper-deficient, zinc-containing SOD1 or apo-SOD1 for either wild-type, ALS mutant or C111S pseudo-wild-type SOD1 proteins. Thus, the appearance of zinc-deficient, copper-containing SOD1 in tissues was unlikely to be caused by the oxidation of another moiety on SOD1 that might thereby have decreased the mass by two Daltons to overlap with that of zinc-deficient SOD1. It also did not result in a significant amount of zinc-deficient SOD1 becoming detectable in wild-type SOD transgenic tissues.

Importantly, addition of diamide even 2 minutes after thawing the punch in buffer resulted in no detectable copper-containing SOD1.

4.4.3 Metal Content of G93A SOD1 from Spinal Cord

In G93A mice, CuZn SOD1 was 6.3 ± 0.8 pmol/mg tissue at 30 days old and increased to 16 ± 1.5 pmol/mg tissue at 120 days old in ventral spinal cord (Figure 4.4). Only 3-5% of the Cu,Zn SOD1 contained a reduced disulfide bond, which was unchanged as the mice aged. Zinc-containing, copper-deficient SOD1 was the major species in the ventral spinal cord, particularly in 60- and 90-day-old mice. A larger fraction of the disulfide in zinc-containing SOD1 (35%) was reduced compared to Cu,Zn SOD1.

The amount of copper-containing, zinc-deficient SOD1 was consistent across all ages in the ventral and dorsal spinal cord, ranging from average concentrations of 0.6 to 0.7 pmol/mg tissue. The requirement for diamide to retain copper prevented measuring the proportion of zinc-deficient SOD1 that contained a reduced disulfide bond. Apo SOD1 ranged between 0.1 ± 0.02 pmol/mg tissue to 1.4 ± 0.2 pmol/mg tissue. These low levels of apo-SOD1 suggest that there was not a substantially larger pool of zinc-deficient SOD1 that had shed its copper during isolation.

The metal contents of SOD1 in the dorsal horn essentially mirrored the ventral spinal cord. The concentration of total SOD1 peaked at 27 ± 6.1 pmol/mg tissue (Figure 4.5). The concentration of zinc-containing SOD1 in the dorsal horn was large compared to other tissues, though the fraction of zinc-containing SOD1 was less than in ventral spinal cord (30-40%).

4.4.4 Metal Content of Wild-type SOD1 from Spinal Cord

The ventral and dorsal spinal cord from wild-type mice contained substantially more SOD1 protein at 30 and 60 days than G93A mice, but total SOD1 levels became comparable to those found in G93A mice at later ages

(Figure 4.6 and 4.7). This did not hold true when we made more rigorous attempts to extract all of the SOD1, in which case the wild-type animals had larger amounts of SOD1, although the proportions of the number of metals bound to SOD1 remained the same (data not shown). Remarkably, wild-type SOD1 contained substantially more zinc-containing SOD1 at all ages from 30 to 120 days than G93A mice. Furthermore, 45% of the zinc-containing SOD1 had a reduced disulfide bond at all ages, which was far greater than found in G93A SOD1 spinal cord. This was statistically significant by one-way ANOVA (F-ratio 47.99, p-value <0.001 at the 95% confidence interval). CuZn SOD1 levels were similar to those found in G93A mice, around 10-13 pmol/mg tissue in both regions and at all ages. The disulfide of wild-type CuZn SOD1 was only 6-7% reduced, compared to 3-5% for the G93A mice. Apo wild–type SOD1 ranged from 0.3 pmol-mg tissue in 30-day-old mice to 1.7 pmol/mg tissue in 120-day-old mice.

The amount of copper-containing wild-type SOD1 was significantly lower than the G93A mice and was consistent at all ages in both ventral and dorsal spinal cord, about 0.1 pmol/mg tissue. The standard error of mean of all of the copper-containing wild-type SOD1 measurements was extremely high due to the levels measured being close to the noise level. Thus, the distribution of zinc-deficient SOD1 was very close to 0 and the fitting program did not allow negative numbers for any value. The distribution was non-parametric as a result and so the Kolmogorov-Smirnov test was used to test for significance. Many of the individual wild-type SOD1 replicate spectra did not fit any copper in the one-metal SOD1 peak.

4.4.5 Amount of SOD1 Assessed by Western Blots

The release of SOD1 from spinal cord tissues punches was also monitored by western blot as a way to verify some aspects of our mass spectrometry assays (Figure 4.8). Spinal cord tissue from representative

animals of the cohort used for the mass spectrometry assays was used. The gels were run both with (reducing) and without (non-reducing) β-mercaptoethanol to account for and be able to monitor the presence of disulfide reduced species. We also used longer exposures to determine if small amounts of oligomerized SOD1 was present (Figure 4.9). Pseudo-wild-type C111S SOD1 was used for a standard curve.

Rough quantitation of the amount of SOD1 in the soluble fraction by eye agreed well with the mass spectrometry measurements, reflecting the population of SOD1 that is extracted via the more gentle method. For example, the SOD1 concentration in the 30 day old G93A mouse used for the western blot was 15.1 pmol/mg tissue via mass spectrometry. The amount in the pellet fraction was ~5-15% of the total SOD1, which generally matched the increase in SOD1 concentration from the spinal cord observed when we included the additional freeze/thaw cycle to ensure complete extraction. We could not see any higher molecular weight species at 1-3 second exposure times. However, longer exposure times revealed the presence of a series of higher molecular weight bands immunoreactive for SOD1. The bands were more intense in the non-reducing gel, as well as generally tending to increase with age.

4.4.6 SOD1 in Cerebral Cortex

In G93A SOD1 mice, the brain contained similar total SOD1 levels as the spinal cord (Figure 4.10). The majority of the SOD1 contained copper and zinc in the cerebral cortex with 2-3 pmol/mg tissue of zinc-containing SOD1. The concentrations of copper-containing, zinc-deficient SOD1 in cortex were roughly equivalent to those found in spinal cords.

The zinc-containing SOD1 from wild-type brain cortex was 8-11 pmol/mg tissue, which was substantially higher than found in G93A SOD1 cortex and paralleled the results from spinal cord (Figure 4.11). The SOD1 in

brain contained a similar fraction of disulfide-reduced protein as found in spinal cords and significantly less copper-containing SOD1 compared to G93A SOD1 brain of spinal cord. The amount of apo SOD1 was less than 2 pmol/mg tissue in brain at all ages for both genotypes (Figures 4.10-4.11).

4.4.7 Metal Content of SOD1 in Leg Muscle

Total SOD1 from G93A muscle stayed relatively consistent (35-39 pmol/mg tissue) for 30-90 days, but then increased to 52 pmol/mg tissue at 120 days old mice (Figure 4.12). At this stage, the muscle was undergoing severe shrinkage due to the disease. Total SOD1 concentrations from wild-type muscle (35-42 pmol/mg tissue) were similar to that in G93A SOD1 mice and did not rise at 120 days. CuZn SOD1 accounted for 70-80% present in muscle at all ages in G93A and wild-type mice with ~5% containing a reduced disulfide bond. As in the spinal cord and in the brain, there was more one-metal SOD1 in the leg muscle in wild-type mice than in G93A mice (30% in the wild-type, 15% in the G93A mice) (Figure 4.13). The low signal-to-noise ratio in muscle tissue made the fit of copper or zinc in the one-metal peak unreliable (RMS>6%), thus we used the linear ion trap data and reported only the total amount of one-metal SOD1.

4.5 Discussion

The mass spectrometry assay allowed the binding of copper and zinc as well as reduction of the C57-C146 disulfide bridge to be simultaneously determined in SOD1 from specific spinal cord regions of transgenic mice, yielding the first quantitative distribution of partially unfolded intermediates of SOD1 throughout ALS disease progression. Far more soluble, partially unfolded intermediates of SOD1 reside in the ventral gray spinal cord than in dorsal gray spinal cord, brain, muscle, heart, liver, kidney, lung or stomach. The surprising result was that wild-type SOD mice had substantially more of every partially folded intermediate SOD1 species than in G93A SOD1 mice, with the sole exception of zinc-deficient SOD (Figure 4.4-4.7 and 4.14).

The concentrations of SOD1 protein in both wild-type and G93A SOD1 are astonishing in all tissues assayed. The reporting of SOD1 as picomols protein per milligram-wet-weight corresponds to an equivalent concentration in micromolar protein. Thus, the average total SOD1 concentration in the ventral horn of the spinal cord corresponded to 38 μM in G93A mice and 69 μM in wild-type mice at 60 days of age. Western blot data reported by Jonsson *et al*. yields even higher estimates in 100 day old mice of 69 μM in the total mouse spinal cord of G93A mice and 101 μM in wild-type mice [107]. Clearly SOD1 is highly overexpressed to the point where its cellular concentration is comparable to that of molecular oxygen in tissues. Furthermore, these estimates of SOD1 concentrations average multiple cell types together. Immunohistology reveals SOD1 is several fold higher in motor neurons relative to the surrounding neuropil [149,150]. SOD1 is also present in the axons of motor neurons, which may constitute 99% of the volume of a motor neuron that extends beyond the ventral gray horn [151,152].

The average concentration of SOD1 is even higher in the heart and livers of 60 day-old G93A mice, corresponding to ~69 μM and 83 μM Cu,Zn

SOD1 respectively. In non-CNS tissues, 80-90% of the SOD1 was mature, Cu,Zn SOD1 desite having higher SOD1 concentrations than in brain and spinal cord. This suggests that copper import into the CNS is much slower than in other tissues. Indeed, the turnover of copper in rat brain is estimated to have a half-life of over 400 days [153]. Zinc import is also closely regulated in the CNS. Excessive free zinc accumulation in the nanomolar range has been shown to be toxic in the CNS [154,155].

Several groups have measured the zinc and copper levels in transgenic mouse spinal cord. Tokuda *et al*. found 36 μM copper and 66 μM zinc in 56 day old G93A mice via inductively coupled plasma mass spectrometry. Lelie, *et al*., found significantly higher amounts of copper and zinc in end-stage animals, 95 and 214 μM respectively, amounts sufficient to achieve full copper and zinc incorporation into the SOD1. This difference might reflect the different age of the mice and in part the G93A line used as Tokuda *et al*. used the B6SJL-Tg(SOD1-G93A)^{dl} 1Gur/J line. This line contains about 30% fewer copies of the G93A transgene and therefore express less SOD1, which may reduce the import of copper and zinc into the spinal cord of these animals [156].

The increased amount of zinc-containing SOD1 in the wild-type mice suggests that sequestering of zinc is not sufficient for toxicity as has been suggested [146]. Johansson *et al.* found the ability of apo SOD1 to deplete zinc from cell culture growth media was toxic to cultured human neuroblastoma cells. However, the total level of zinc reported by Lelie, *et al*. indicates that the SOD1 concentration in the spinal cord would require only 20% of the available zinc to be fully zinc replete. Even using the lower amount of zinc determined by Tokuda *et al*., fully zinc replete SOD1 does not require all of the available zinc in the spinal cord. This is borne out by the fact that the majority of the protein does contain zinc, indicating zinc is not limiting. However, what is not clear from the data is which direction of the SOD

maturation/unfolding pathway the various intermediates are moving towards. The folding pathway of the in vitro protein usually involves incorporation of zinc as one of the first steps, consistent with zinc-containing SOD1 representing immature SOD1 that has not received copper yet.

The mass spectrometry assay also reveals much about modifications to SOD1 that we did not see. Oxidation and glutathionylation have been hypothesized to contribute to SOD1-linked toxicity [157-159]. These modifications are typically thought to occur on the cysteine residue located at position 111, possibly with the involvement of ectopic copper binding at this location [160]. In our assay, such modifications would be readily apparent by the increase in mass the addition of oxygen or glutathione would add to the protein. However, we observed no evidence of glutathionylation to SOD1 in any of the tissues assayed via mass spectrometry. We did see small amounts of SOD1 that contained 1-3 additional oxygens. However, the SOD1 with additional oxygens was less than 2% of the total protein and was discernible in only about 30% of the animals. It was equally abundant in wild-type SOD1-expressing mice as in G93A SOD1 mice. The oxidized species could overlap with our measurement of disulfide reduction, slightly increasing the amount of one-metal SOD1 found to be reduced. However this only resulted in an increase of 2% zinc-containing SOD1 reduced.

The difference in SOD1 total concentrations depending on the extraction method from tissue is interesting because we did not observe this previously when working with rat tissue [113]. The metal cofactors play such a significant role in the stability of SOD1 that partially unfolded intermediate species, which may be missing one or both metals, are likely to be marginally stable. Indeed we have already observed that diamide is a necessary component of the thaw buffer in order to measure zinc-deficient SOD1. We have also noticed that it is difficult to prepare recombinant G93A zinc-deficient SOD1, indicating that it is less stable than CuZn SOD1 and quickly inactivated

in tissue lysates. As such, we designed an extraction protocol that was as gentle as possible, essentially only involving a single freeze-thaw step. The fact that a more rigorous extraction protocol involving an additional freeze-thaw results in the release of more SOD1 from the tissue suggests that the amounts of partially unfolded intermediates of SOD1 measured with the first method are underestimates of the actual tissue concentration.

In contrast to our previous work, we observed an increased proportion of the SOD1 from the transgenic mouse spinal cord in the pellet fraction via Western blots [113]. We did not observe this in the rat model animals. It may be that this is a species-specific effect that will require more investigation in the mouse model. The blots did reveal when grossly overexposed, also unlike the rats, small amounts of higher molecular weight oligomeric species of SOD1 existed and could be observed if the blot was exposed for long enough. However, the proportion was exceedingly minor compared to the total SOD1, and was generally higher in the wild-type mice until the late stages of disease in the G93A mice, suggesting it is not relevant to disease toxicity. The higher molecular weight species may represent disulfide cross-linked versions of SOD1. The level of disulfide reduced SOD1 was significantly higher in wild-type mice than in G93A mice and this may tend to lead to the formation of disulfide cross-linked species in small amounts.

Zinc-deficient SOD1 is not stable in spinal cord samples, which has made detection challenging. It could only be measured by including the sulfhydryl oxidant diamide directly in the buffer used to thaw tissue punches. If the addition of diamide was delayed for even 30 seconds after the centrifugation step, zinc-deficient SOD1 could not be measured. Diamide has two major effects in this assay. Diamide oxidizes cysteines C57 and C146 to reestablish the disulfide bond that stabilizes the zinc-binding loop as we previously described (Chapter 3). Because copper is on average two Daltons smaller than zinc, the two additional hydrogens added by the reduction of the

disulfide makes thiol-reduced, zinc-deficient SOD1 overlap completely with thiol-oxidized, copper-deficient SOD1 in the mass spectrometer. Hence, addition of diamide reversed that overlap, allowing any thiol-reduced zinc-deficient SOD1 to become measurable by the mass spectrometer.

The second major action of diamide is oxidation of a low molecular weight compound in spinal cord that removes copper from zinc-deficient SOD1. A likely candidate for this compound is glutathione, which is quickly oxidized by diamide to glutathione disulfide [118]. Glutathione is an excellent copper chelator as well as a sulfhydryl reductant [87]. We had previously found that glutathione removed copper from recombinant zinc-deficient SOD1 in vitro and could remove copper from Cu,Zn SOD1 in addition to reducing the disulfide bond.

Among many other antioxidant functions, glutathione may also serve as a major protective factor by removing zinc-deficient SOD1. Motor neurons depend on astrocytes to synthesize glutathione [161]. Knockouts of parts of the glutathione synthetic pathway dramatically accelerate the disease when crossed with G93A SOD1 overexpressing mice, with death occurring in 60 rather than 130 days [33]. In contrast, activation of the transcription factor Nrf2 that increases GSH synthesis is protective in both astrocyte/motor neuron co-cultures and in G93A mice [34,35]. Depletion of glutathione levels in the motor neuron or interruption of the supply of glutathione precursors from astrocytes may affect the onset of toxicity by failing to prevent the accumulation of zinc-deficient SOD1.

We have previously shown that the copper in recombinant zinc-deficient SOD1 catalyzes tyrosine nitration when delivered to motor neurons in culture [70]. More recent unpublished results (A.G. Estévez, University of Central Florida) show that as little as 0.5 μM of purified zinc-deficient SOD1 delivered directly to cultured motor neurons is sufficient to induce motor neuron death. The G93A mouse spinal cord and brain contained zinc-deficient SOD1 close

to or above this value while the wild-type SOD1 mouse spinal cord and brain were consistently well below the threshold (Figure 4.15). Zinc-deficient SOD1 was also present in mice at 30 days of age, well before onset of observable symptoms in the G93A mice. However, spinal cord pathology has been reported in these animals as early as 30 days of age, along with subtle signs of injury in the motor cortex [162].

In G93A SOD1 mice, zinc-deficient SOD1 was also found in the dorsal spinal cord and brain in amounts similar to ventral spinal cord. The actual toxic effect may occur early on while the phenotypic effects are not observed until later [162]. Activation of cell death in motor neurons by zinc-deficient SOD1 depended upon the simultaneous generation of nitric oxide to generate peroxynitrite [94]. Thus the animals may carry zinc-deficient SOD1 throughout their lifespan, but realize minimal injury without the presence of nitric oxide. Ye *et al*. showed that motor neuron death from trophic factor deprivation or from expression of mutant SOD1 depended upon tyrosine nitration [71]. Raoul *et al*. have described a Fas-ligand signaling pathway specific to motor neurons that involves the upregulation of neuronal nitric oxide synthase and a vicious cycle involving chronic, low-level activation of a Fas/nitric oxide feedback loop that eventually activates cell death in motor neurons [163,164]. Thus, zinc-deficient SOD1 appears to amplify nitrative stress to levels that eventually activate death cascades in motor neurons.

A crucial next step for this research is to use the tools we have developed to examine other ALS-model animals. Four other SOD1-overexpressing ALS mouse-models are commercially available, thus representing important targets in which to determine if the trends we have noted are also present. Our mass spectrometry assay also enables measurements of the metal-binding distribution from modified disease models such as CCSxG93A SOD1 overexpressing animals, which develop and die from ALS symptoms by 30 days of age [32]. Such measurements are

important for understanding how CCS hastens disease onset. Additionally, knockdown of a portion of the glutathione synthesis pathway also increases disease onset, to 50 days of age [33], and our results reveal the possibility that glutathione may be a key player in the disease progression. Experiments to measure the levels of partially unfolded intermediates in these animals are therefore essential objectives to determine how glutathione may influence the disease. The distributions of intermediates also represent important targets for therapeutic interventions. Compounds that alter the levels of partially unfolded intermediates, particularly by removing zinc-deficient SOD1, are important areas of research for developing treatments for ALS. Finally the methods reported here could be applied to protein post-translational modifications in other neurodegenerative disorders, potentially providing a greater understanding of how such modifications may contribute to disease pathology.

4.6 Acknowledgements

We wish to acknowledge the Environmental Health Sciences Center Mass Spectrometry Core Facility for instrument support, as well as funding from the National Institute for Environmental and Health Sciences (NIEHS P30ES000210), the National Institutes of Neurological Disorders and Stroke (NINDS R01NS058628A), the National Center for Complementary and Alternative Medicine (NCCAM P01AT002034), and the ALS Association.

4.7 Abbreviations

SOD1, Cu,Zn superoxide dismutase; ALS, amyotrophic lateral sclerosis; CCS, copper chaperone for SOD1; wild-type, wild-type; HPLC, high performance liquid chromatography; FT-ICR, fourier transform ion cyclotron resonance; MMTS, S-methyl methanethiosulfonate; SDS-PAGE, sodium dodecyl sulfate polyacrylamide gel electrophoresis; GSH, glutathione.

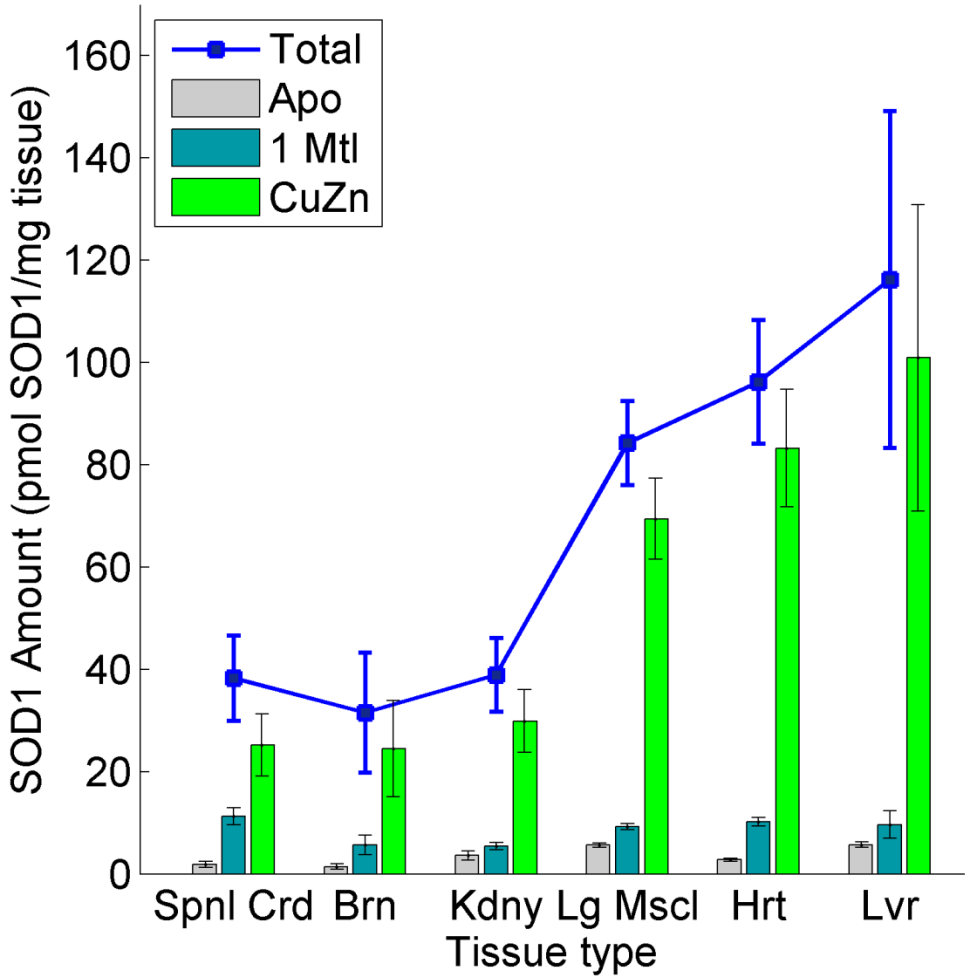

Figure 4.1 SOD1 metal state levels from various tissues from 60 day old G93A mice. The total amount of SOD1, broken down by metal state, was measured from 6 different tissues using 3 replicates from each of three 60 day old G93A mice: spinal cord (Spnl Crd), brain (Brn), Kidney (Kdny), Leg Muscle (Lg Mscl), Heart (Hrt), Liver (Lvr). Error bars are ± SEM.

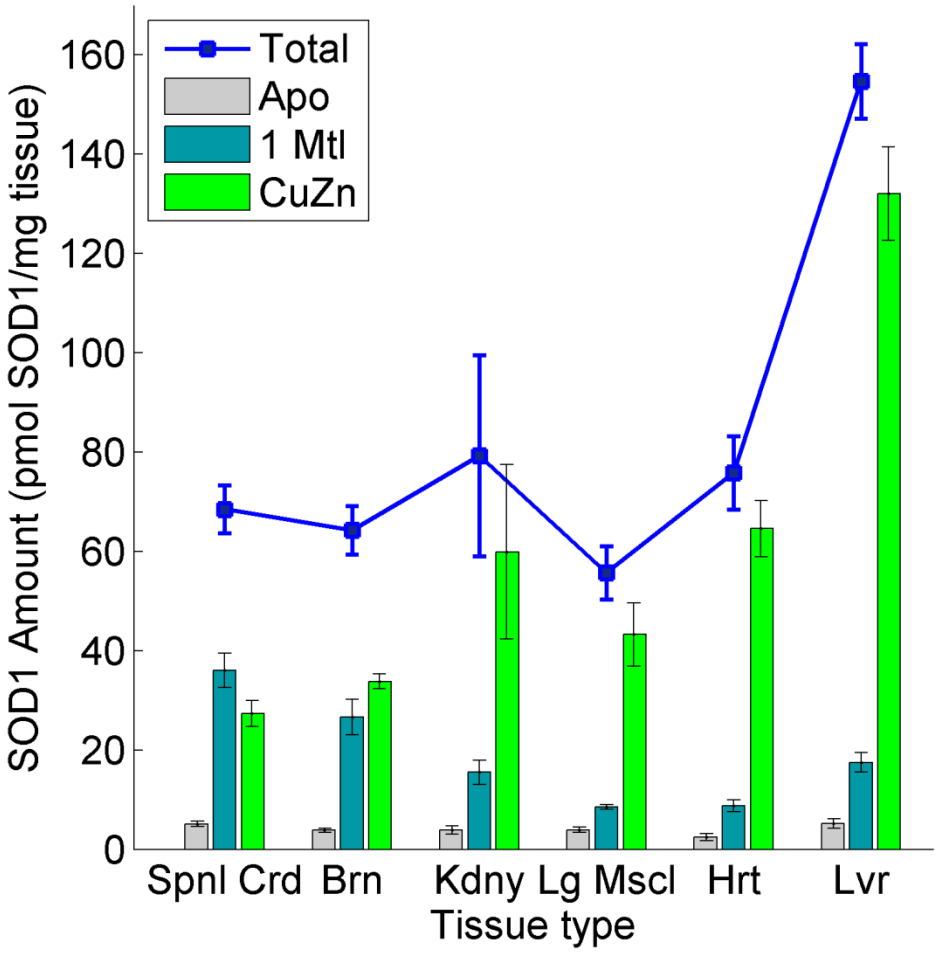

Figure 4.2 SOD1 metal state levels from various tissues from 60 day old wild-type mice. The total amount of SOD1, broken down by metal state, was measured from 6 different tissues using 3 replicates from each of three 60 day old wild-type mice: spinal cord (Spnl Crd), brain (Brn), Kidney (Kdny), Leg Muscle (Lg Mscl), Heart (Hrt), Liver (Lvr). Error bars are ± SEM.

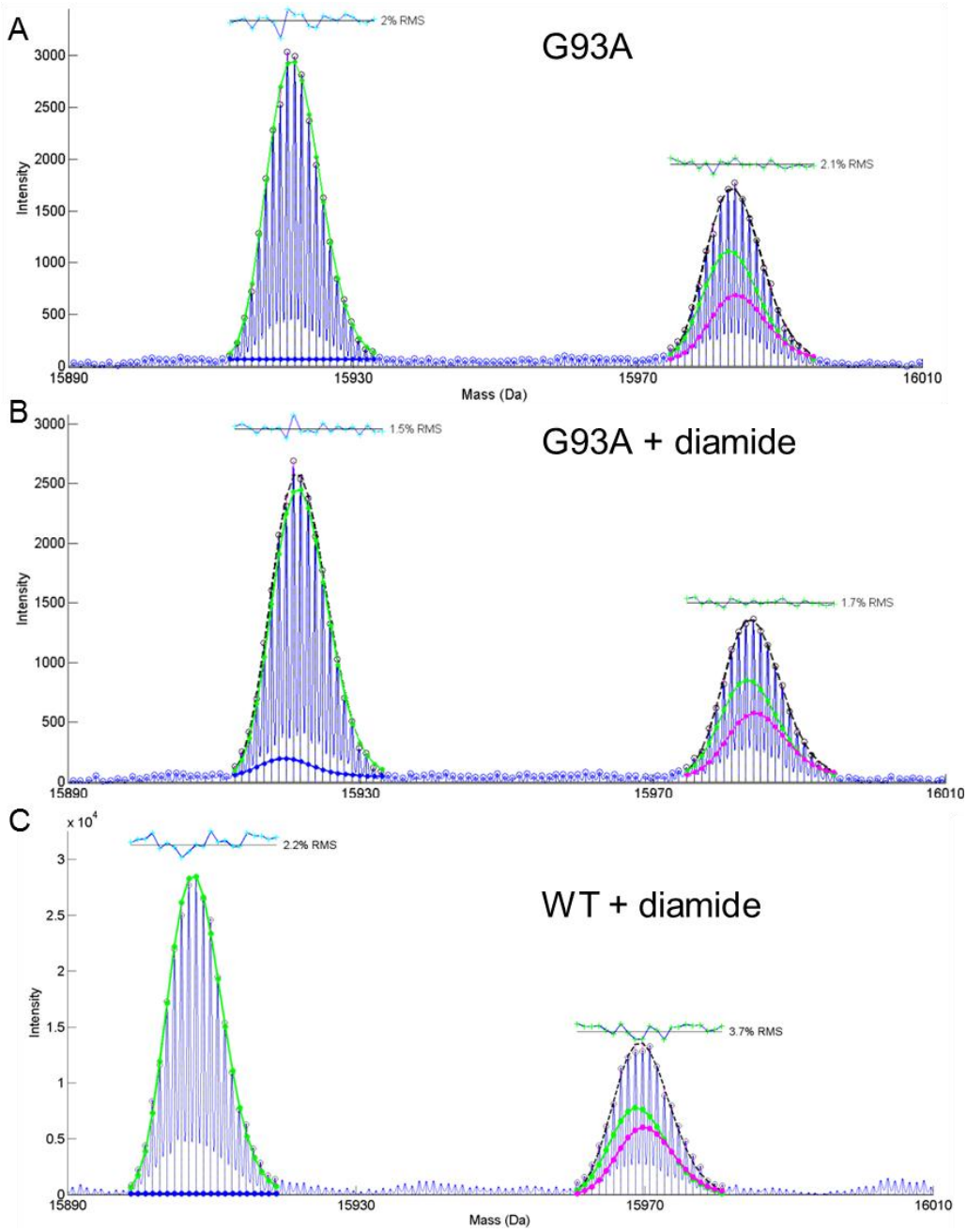

Figure 4.3 Impact of diamide. The one-metal peak on the left can contain either copper (blue) or zinc (green). The CuZn peak on the right can contain copper in the +2 (green) or +1 (magenta) oxidation state. **A.** A punch from the ventral spinal cord of a G93A mouse without diamide in the thaw buffer. **B.** A punch from the same animal with 10 mM diamide in the thaw buffer. **C.** A punch from the ventral spinal cord of a wild-type mouse with 10 mM diamide in the thaw buffer. Note that the wild-type SOD1 spectra are 14 Da less in mass due to the absence of the CH_2 introduced by the G93A mutation.

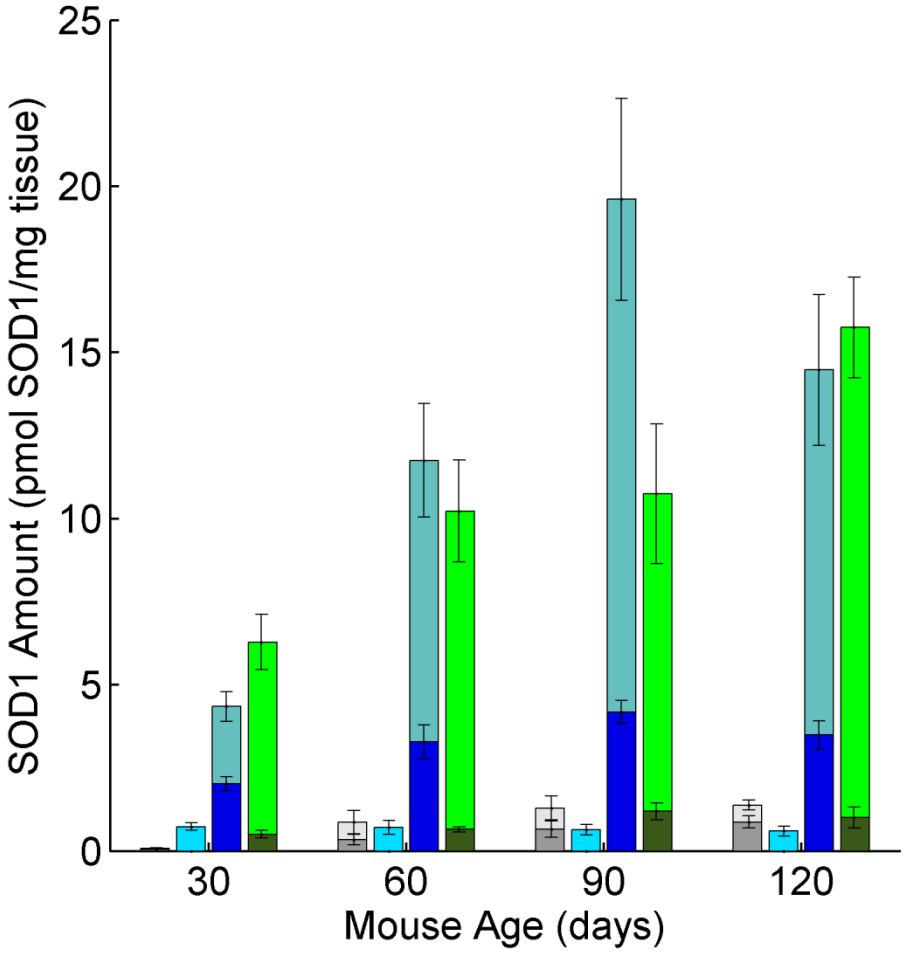

Figure 4.4 SOD1 distribution in the ventral spinal cord of G93A mice. The SOD1 at 30, 60, 90, and 120 days in G93A mouse spinal cord is broken down by metal state: apo (grey), copper-containing (cyan), zinc-containing (blue), and CuZn (green). The proportion of each species that is disulfide reduced is represented by the darker-shaded bar. All error bars are ± the standard error of mean (SEM).

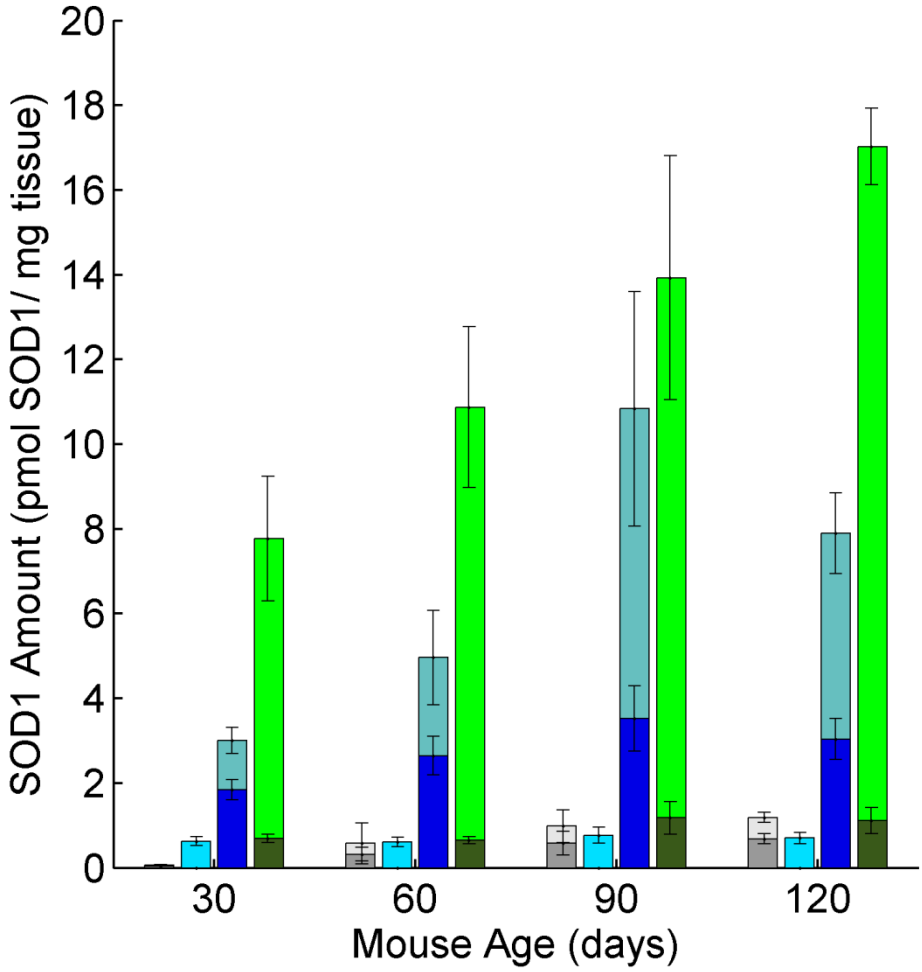

Figure 4.5 SOD1 distribution in the dorsal spinal cord of G93A mice. The SOD1 at 30, 60, 90, and 120 days in G93A mouse spinal cord is broken down by metal state: apo (grey), copper-containing (cyan), zinc-containing (blue), and CuZn (green). The proportion of each species that is disulfide reduced is represented by the darker-shaded bar. All error bars are ± SEM.

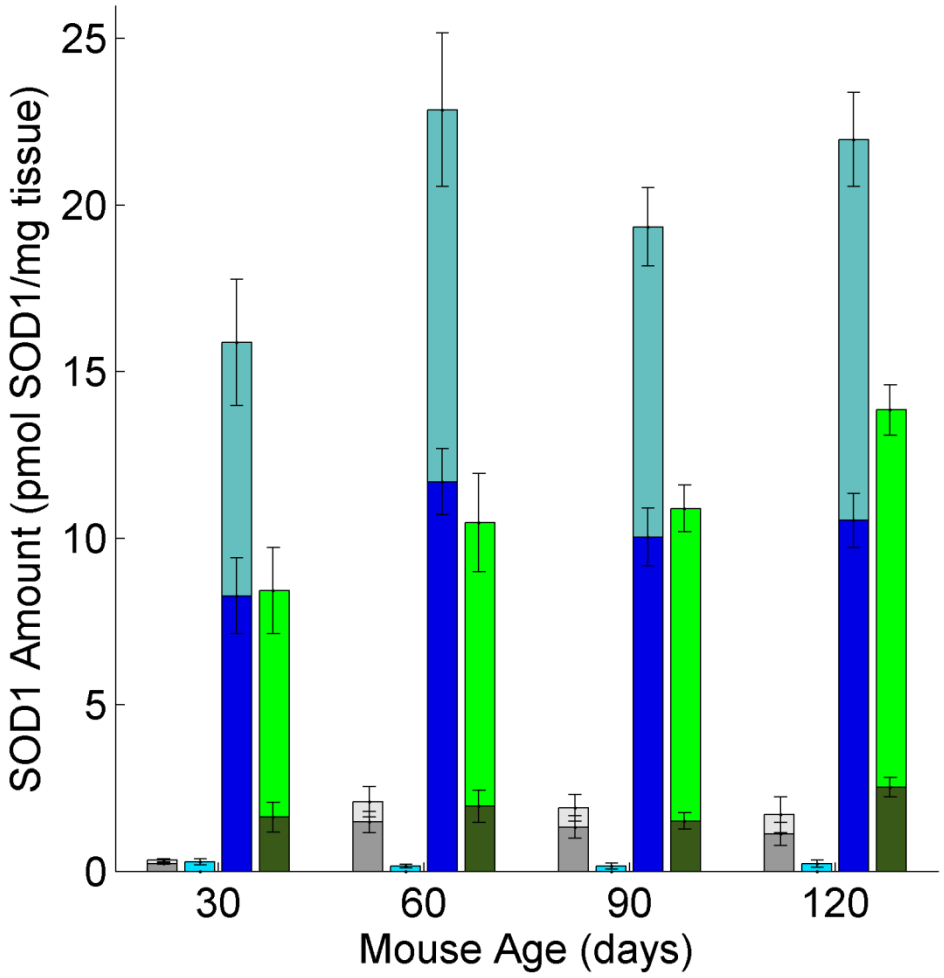

Figure 4.6 SOD1 distribution in the ventral spinal cord of wild-type mice. The SOD1 at 30, 60, 90, and 120 days in wild-type mouse spinal cord is broken down by metal state: apo (grey), copper-containing (cyan), zinc-containing (blue), and CuZn (green). The proportion of each species that is disulfide reduced is represented by the darker-shaded bar. All error bars are ± SEM.

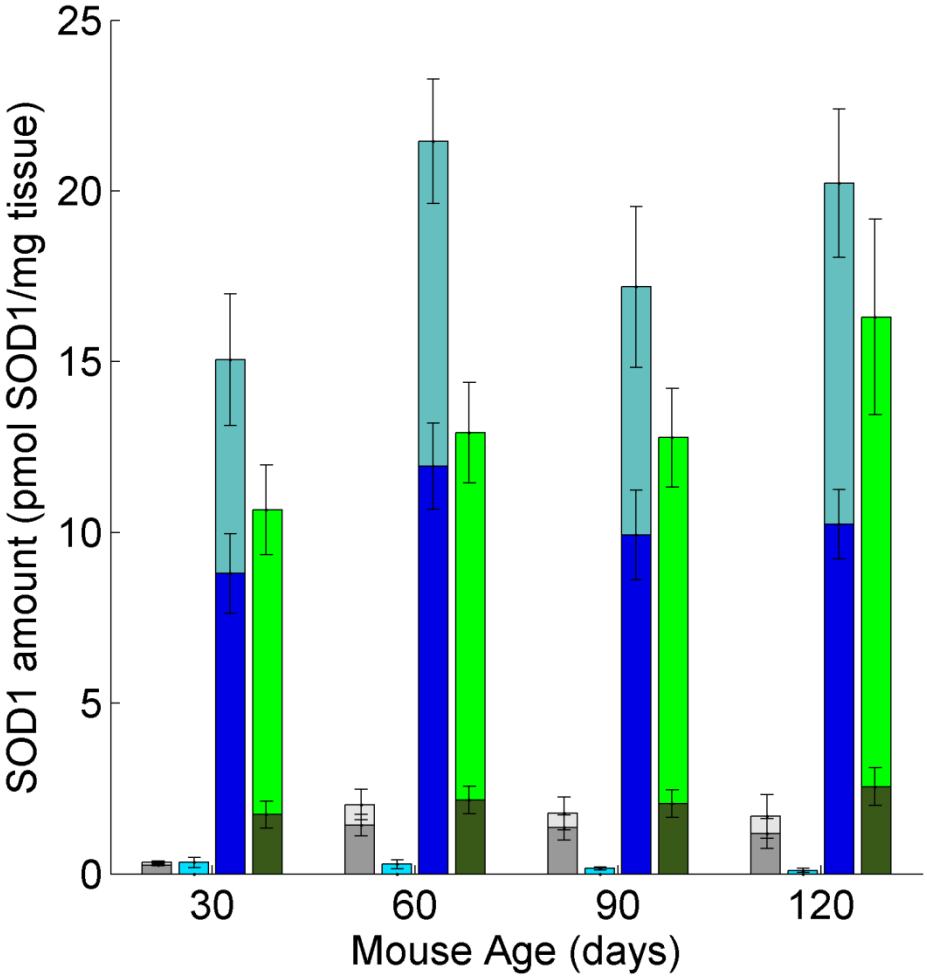

Figure 4.7 SOD1 distribution in the dorsal spinal cord of wild-type mice. The SOD1 at 30, 60, 90, and 120 days in wild-type mouse spinal cord is broken down by metal state: apo (grey), copper-containing (cyan), zinc-containing (blue), and CuZn (green). The proportion of each species that is disulfide reduced is represented by the darker-shaded bar. All error bars are ± SEM.

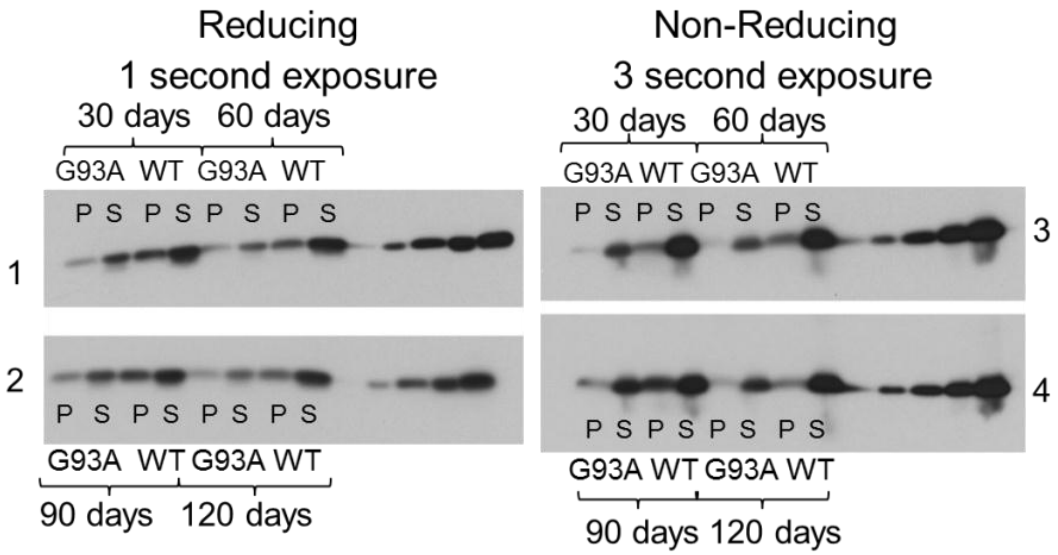

Figure 4.8 Western blots of reducing and non-reducing gels of spinal cord punches. The amount of SOD1 released from the tissue punches was monitored by reducing and non-reducing gels followed by Western blot with our anti-SOD1 antibody. Blot 1 is the pellet (P) and supernatant (S) fraction from a 30 day old G93A and wild-type and a 60 day old G93A and wild-type mice, followed by a standard curve using C111S SOD1 (as read left to right). The standard curve was 10 ng (0.6 pmol), 30 ng (1.9 pmol), 100 ng (6.3 pmol), 300 ng (19 pmol), and 1000 ng (63 pmol). Blot 3 contains the same only the gel was run without β-mercaptoethanol. Blots 2 and 4 are identical treatment of tissue from 90 and 120 day old animals.

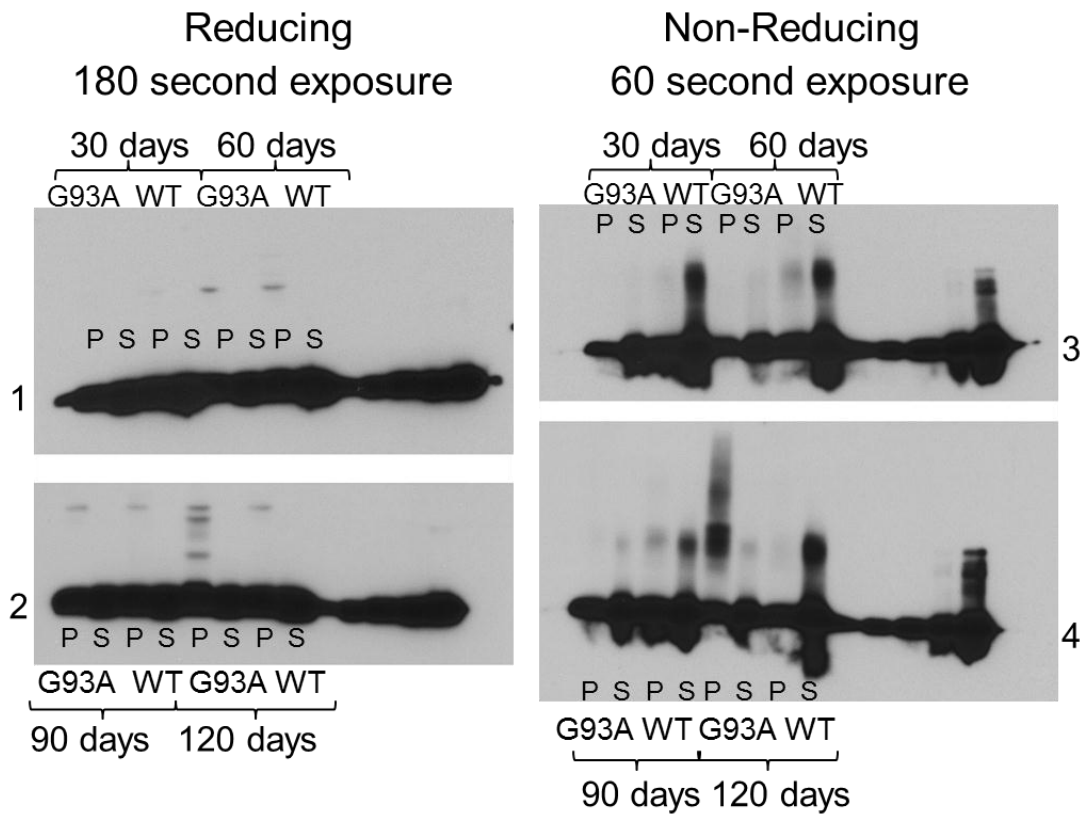

Figure 4.9 Overexposed Western blots of reducing and non-reducing gels of spinal cord punches. The same blots as Figure 4.7 were exposed for longer periods to look for low abundance species of SOD1.

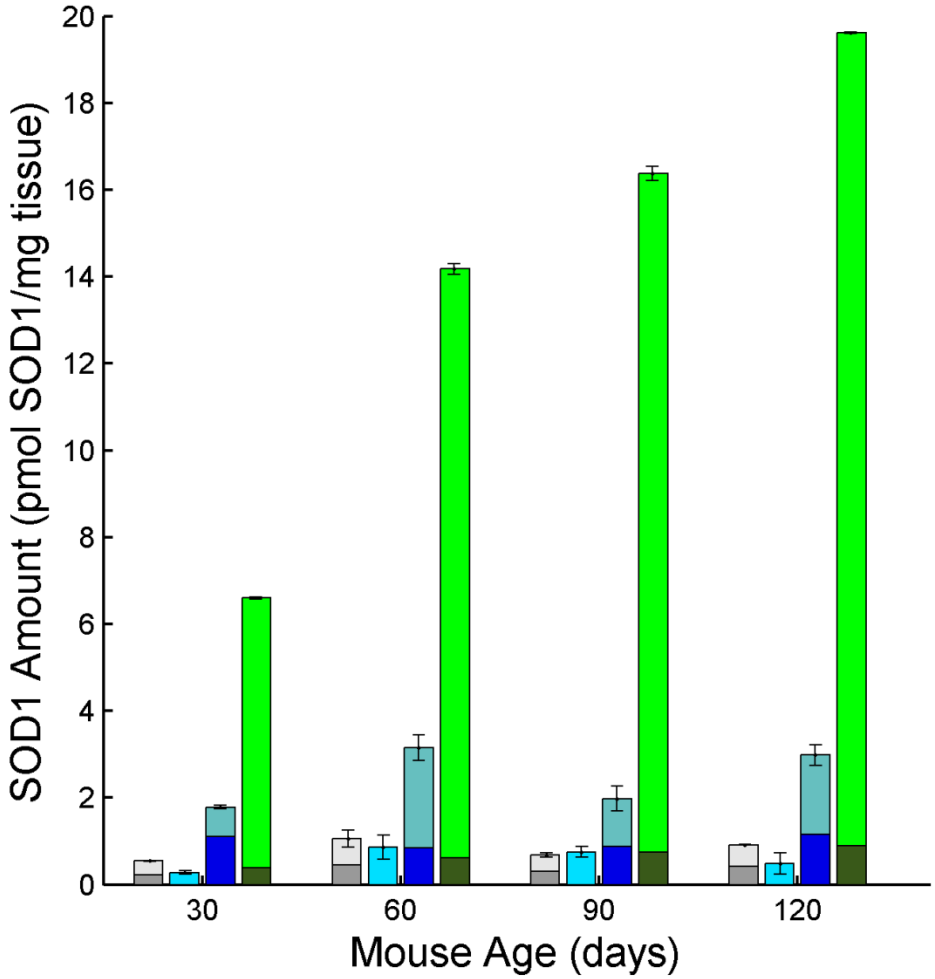

Figure 4.10 SOD1 distribution in the cerebral cortex of G93A mice. The SOD1 at 30, 60, 90, and 120 days in G93A cerebral cortex is broken down by metal state: apo (grey), copper-containing (cyan), zinc-containing (blue), and CuZn (green). The proportion of each species that is disulfide reduced is represented by the darker-shaded bar. All error bars are ± SEM.

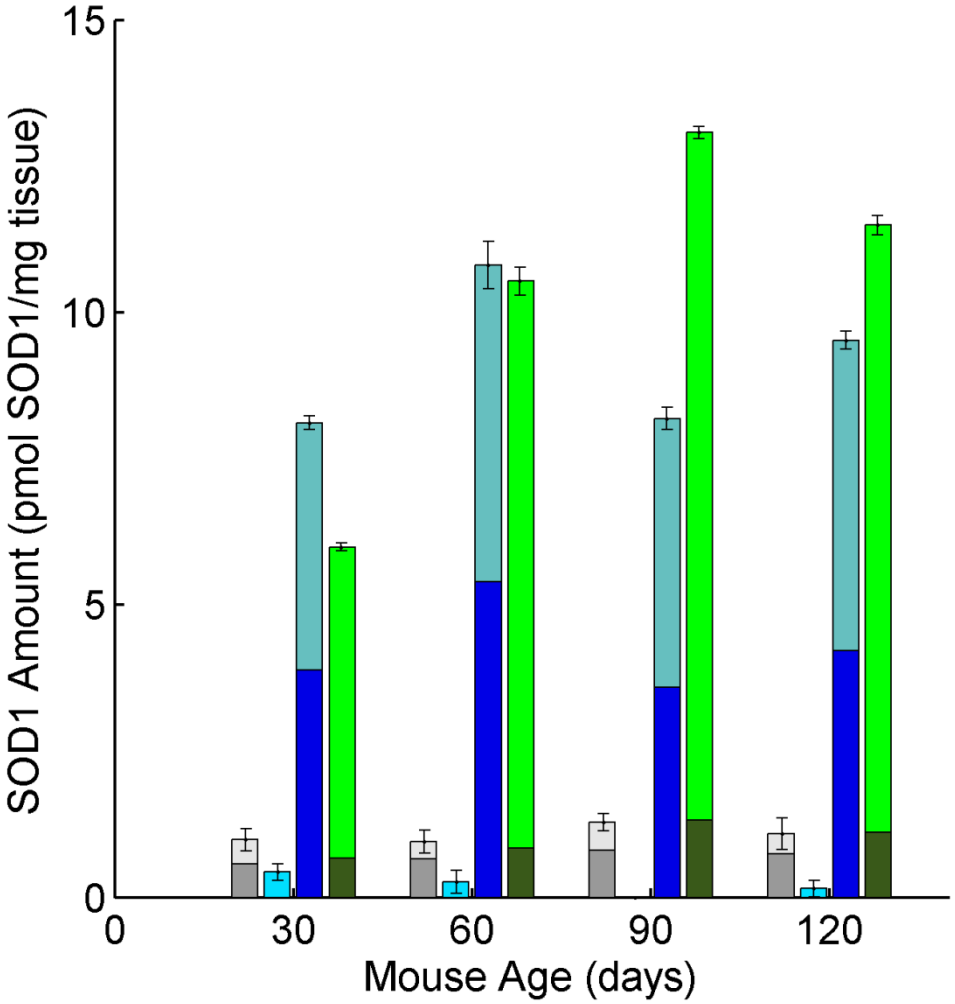

Figure 4.11 SOD1 distribution in the cerebral cortex of wild-type mice. The SOD1 at 30, 60, 90, and 120 days in wild-type mouse cerebral cortex is broken down by metal state: apo (grey), copper-containing (cyan), zinc-containing (blue), and CuZn (green). The proportion of each species that is disulfide reduced is represented by the darker-shaded bar. All error bars are ± SEM.

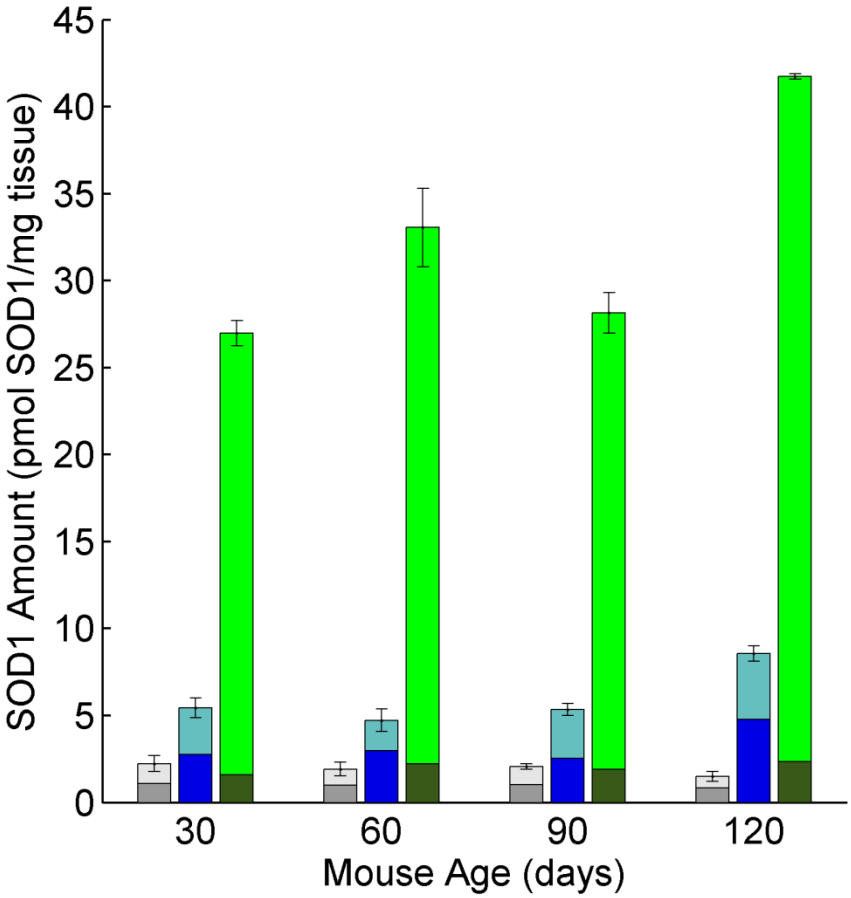

Figure 4.12 SOD1 distribution in the leg muscle of G93A mice. The SOD1 at 30, 60, 90, and 120 days in G93A mouse leg muscle is broken down by number of metals bound: no-metals (grey), one-metal (blue), two metals (green). The proportion of each species that is disulfide reduced is represented by the darker-shaded bar. Each age is 3 measurements of one representative animal. All error bars are ± 1 standard deviation.

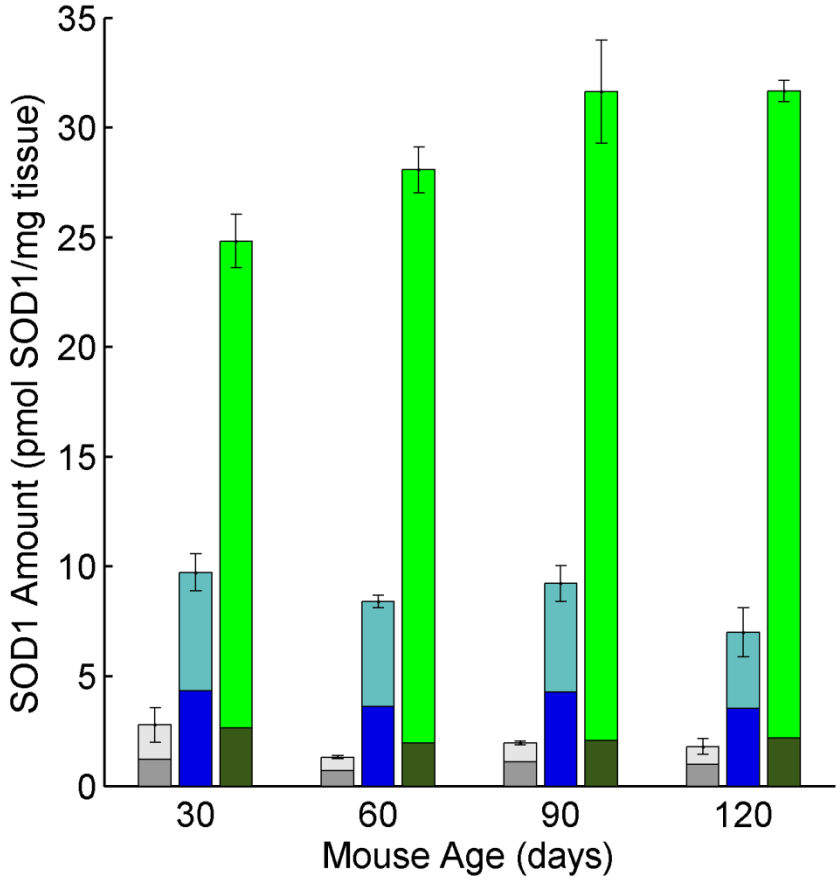

Figure 4.13 SOD1 distribution in the leg muscle of wild-type mice. The SOD1 at 30, 60, 90, and 120 days in wild-type mouse leg muscle is broken down by number of metals bound: no-metals (grey), one-metal (blue), two metals (green). The proportion of each species that is disulfide reduced is represented by the darker-shaded bar. Each age is 3 measurements of one representative animal. All error bars are ± 1 standard deviation.

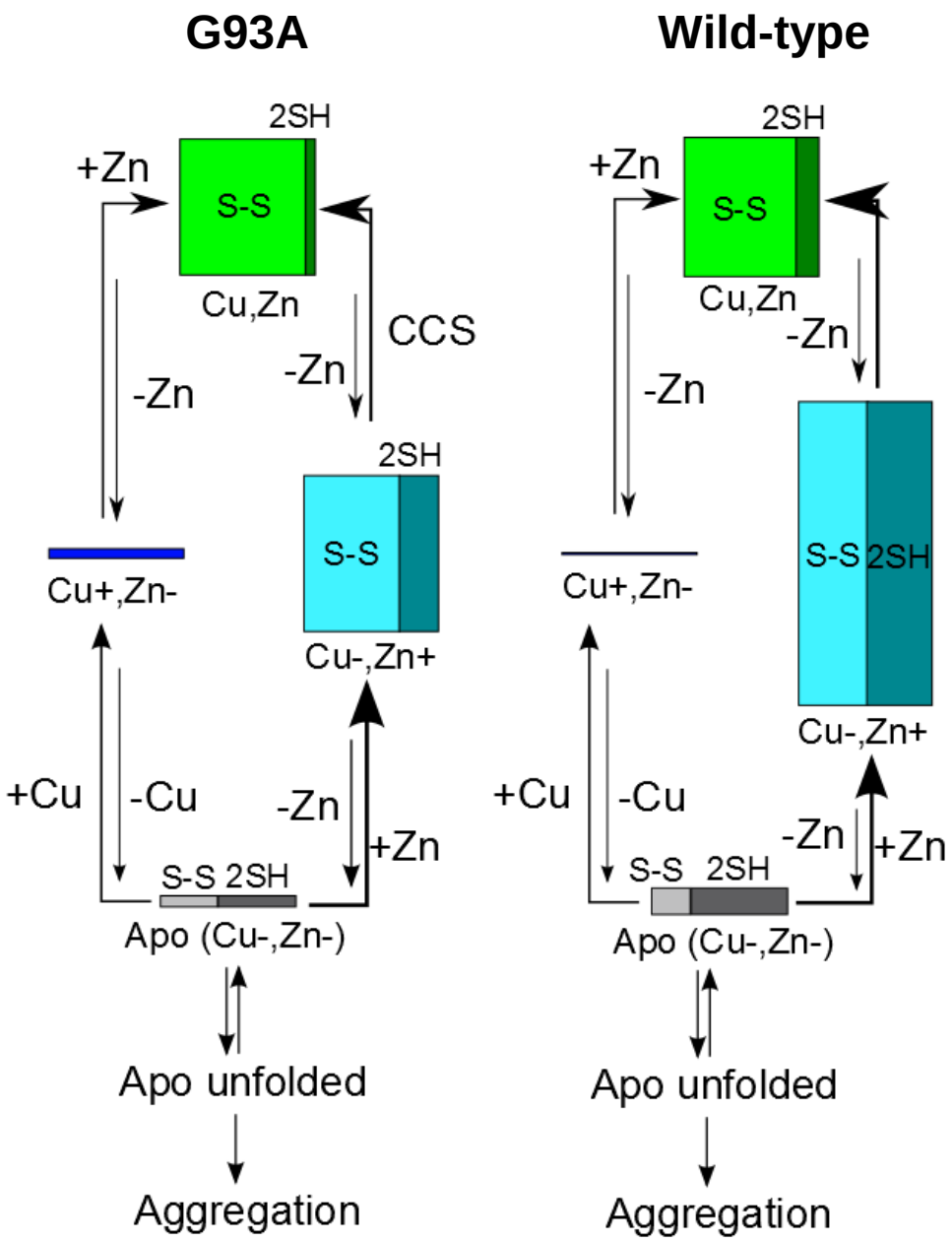

Figure 4.14 Partially unfolded intermediates of SOD1 in transgenic mouse spinal cord. The average levels of each intermediate from the 60 day old mouse spinal cords are proportionally represented by the colored boxes, with the lighter fraction representing the proportion of each species that contains a reduced disulfide bond.

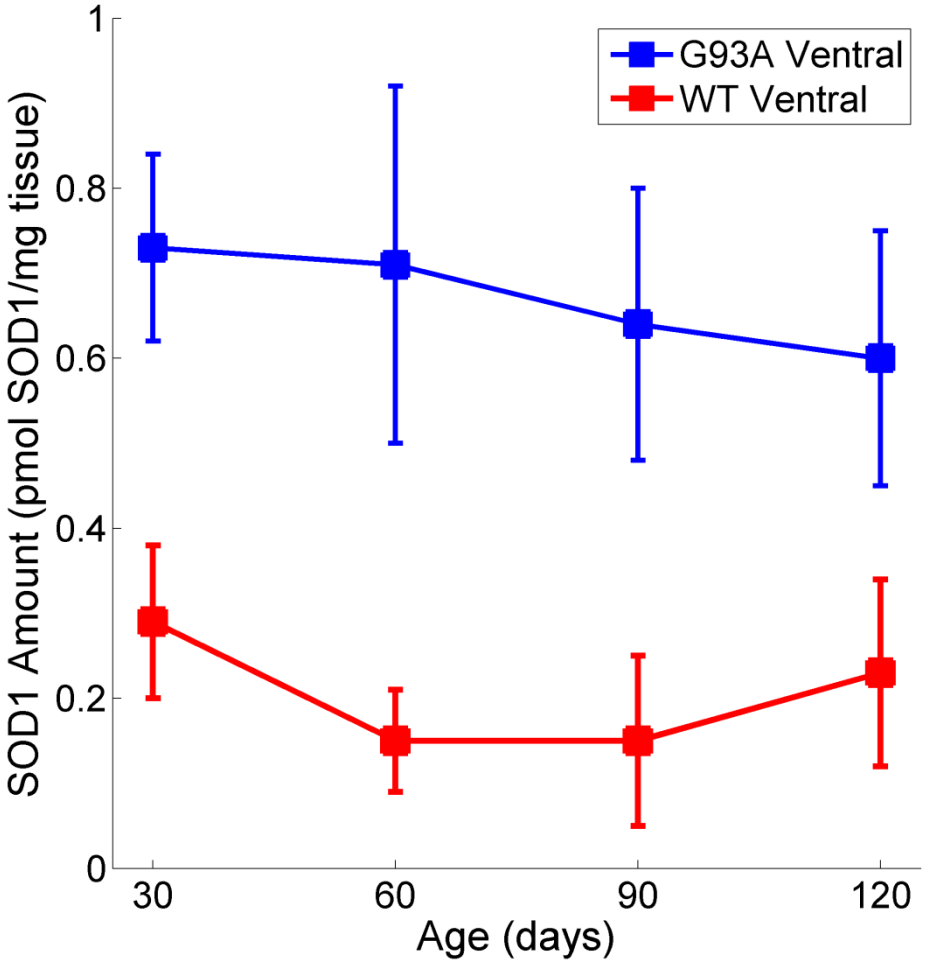

Figure 4.15 Levels of zinc-deficient SOD1 in transgenic mouse spinal cord. The amount of zinc-deficient SOD1 in G93A and wild-type ventral spinal cord at 4 different ages are represented by each colored marker and line. The measurement of pmol SOD1/mg tissue roughly corresponds to a concentration in micromolar. 0.5 μM zinc-deficient SOD1 was necessary for toxicity to motor neurons *in vitro*. Error bars represent ± SEM.

Chapter 5

Conclusions and Outlook

5.1 Summary

My dissertation presents the development of methods to measure the metal-binding of SOD1 from transgenic disease-model tissue. The development of a Ziptip-based assay that allowed rapid quantification of SOD1 from small punches of spinal cord tissue (Chapter 2), and the extension of that assay to high resolution mass spectrometry (Chapter 3) led to a larger-scale characterization of the metal-binding of SOD1 in G93A and wild-type mice at several time points (Chapter 4). We made several key observations, including the high level of zinc-containing SOD1 in both genotypes, the higher level of disulfide reduced SOD1 in the wild-type animals, that G93A mice contained more copper-containing SOD1 at all ages and in all regions than wild-type mice, and that apo SOD1 did not seem to be an abundant species relative to the other forms of SOD1 in any region tested. The wider impacts of this work and the future directions of the research are summarized below.

5.2 Impacts

A critical component of the work presented in my dissertation is the development of a series of methods to measure modifications to intact proteins via mass spectrometry. These methods were developed for determining the metal-binding of SOD1 from tissue, but can also be applied to other proteins. We have used the Ziptip as an interface to observe many recombinant proteins, including CCS, GFP, the coat-protein from turnip yellow mosaic virus, symerythrin, and cysteine dioxygenase. The Ziptip is particularly useful as the protein can remain in high strength buffers or salts yet still be amenable to electrospray mass spectrometry. Jared Williams, a current graduate student in the lab, has even succeeded in using 8 M urea and guanidine to probe protein denaturation via mass spectrometry. Versions of

the C4 Ziptip with different chromatography material, such as C18, are available that could enable many other proteins to be studied in this manner. The Ziptip method provides similar information as an SDS-PAGE gel or Western blot, but it is more rapid, provides better resolution, and is more sensitive. The assay provides anyone with access to a mass spectrometer the means to rapidly assess the molecular weight of a protein of interest along with any modifications that may be present.

The ability to use high resolution mass spectrometry to parse small-mass-difference protein modifications extends the utility of the Ziptip assay even further. Small changes to a protein can be monitored even if they represent only a fraction of the protein under investigation. This technique could be used to monitor amino acid deamidation (Δ1 Da), disulfide formation or reduction (Δ2 Da), or several amino acid substitutions that result in mass differences of less than 5 Da, among other modifications. The simplicity of the Ziptip assay and the increasing availability of mass spectrometers capable of acquiring high resolution, isotopically-resolved data enables such analyses to become routine, simplifying the characterization of proteins and their modifications.

The high expression level of mutant SOD1 in the transgenic animals was part of the original rationale to try mass spectrometry to detect SOD1 from spinal cord, but we also routinely observe other abundant proteins from tissue, such as ubiquitin and the endogenous rat SOD1 in the course of our assays. This represents the other major impact of the work in this dissertation. We have described a series of methods that enable the determination of protein metal-binding at the subunit level from in vivo samples. This is an important advantage over other techniques such as ICP-MS that rely on complete acid digestion of samples and therefore yield only solution measurements of the metals. Knowing which metals are specifically bound to a protein is crucial for

understanding how the metals impact the structure and function of the protein in vivo.

Chapter 4 revealed significant information about the role of partially unfolded intermediates of SOD1 in ALS. The asymptomatic wild-type SOD1 mice contained more partially unfolded intermediate SOD1 species than the G93A mice except for copper-containing, zinc-deficient SOD1. Zinc-containing SOD1 and disulfide reduced SOD1 were higher in wild-type spinal cords and brains, indicating that a model of toxicity that entails the formation of partially unfolded species leading to aggregation is not sufficient to explain the disease. The metal-binding clearly plays a substantial role in the stability of the protein and altered metal-binding forms of SOD1 are toxic to motor neurons, yet the metals receive far less attention. Part of the reason for this is the difficulty of measuring the specific metal-binding of a protein from in vivo samples. Some groups have determined average metal-binding of SOD1 from whole tissue, most notably Lelie *et al*., who used size-exclusion chromatography leading to ICP-MS to determine the metal-binding of SOD1 from transgenic tissue [104]. The data were presented as metal occupancy per SOD1 dimer. They found roughly 3.0 zinc ions and 1.0 copper ion per dimer of SOD1. The numbers we present in Chapter 4 are generally in good agreement with the occupancy they reported. However, what is not clear from Lelie *et al*. is the exact distribution of the metals in SOD1 subunits.

Quantitative measurements of the partially unfolded intermediate species of SOD1 present in the spinal cord are absolutely essential to any determination of which misfolded intermediate is toxic and the mechanism through which the intermediate exerts toxicity. We have now quantitatively measured for the first time the levels of the various partially unfolded intermediates present in disease-affected tissue regions as the disease develops. More specifically, we have shown that a small amount of zinc-deficient SOD1 is present in the G93A mouse spinal cord and that the level is

significantly more than the control wild-type mice. This adds to the evidence that zinc-deficient SOD1 plays a role in the development of the disease. The amount of zinc-deficient SOD1 appears to be sufficient to be toxic in G93A spinal cord, but is generally below the toxic threshold in wild-type SOD1 mice.

Zinc-deficient SOD1 functioning as the source of toxicity for ALS is not immediately apparent from the data presented in my dissertation. The G93A mice contain more zinc-deficient SOD1 than the wild-type mice, but they also maintain this level over much of their lifespan, including a significant portion where they do not display overt symptoms. The translation from the mice to human cases of the disease also becomes difficult. Since humans need only a single copy of mutant SOD1 to acquire the disease, the proportions in the mice would yield substantially less zinc-deficient SOD1, possibly an amount below the toxic threshold. I think the evidence for zinc-deficient SOD1 toxicity is too strong to ignore, which therefore suggests that the mechanism entails several more factors involved in the process. The participation of nitric oxide has already been elucidated, but the process to arrive at zinc-deficient SOD1 in the first place is still nebulous and could involve a number of factors. Although it has become somewhat of a punch line in the lab, the idea that ALS etiology is significantly more complex and involves more factors than just zinc-deficient SOD1 (or SOD1 aggregates) is consistent with the human forms of the disease, which can display a wide range of onset ages and progression times that I suspect will be poorly correlated with any single factor. Additional experiments to elucidate the other players in ALS are therefore crucial.

5.3 Future Research

Like many experiments, the results of my dissertation research have produced additional questions that are worth pursuing further. With the tools developed in chapters 2 and 3, we can now investigate several questions

about the role of SOD1 in ALS and what other factors may impact the disease progression. I describe four areas needing further investigation below.

5.3.1 The Role of CCS

How CCS impacts and modulates SOD1-mediated ALS progression is not entirely clear. CCS has been used as evidence both for and against the zinc-deficient SOD1 hypothesis. CCS null G93A mice had lower enzymatic activity, which the authors extended to mean lower copper incorporation, and yet the same disease onset and progression. This became evidence that copper cannot be involved in the disease, despite the protein retaining 20% of its activity. On the other side, CCS overexpressing G93A mice had a dramatically faster disease onset and progression. Whether this is from increased copper incorporation is not yet clear. However, we now have the methods to address this by measuring the metal-binding of SOD1 and directly determine how the distribution of the metal-binding changes in response to CCS overexpression. Jared Williams has in fact begun looking at a cross between the CCS overexpressing mice first described by Son, *et al*. [32], and our G93A mice, G6SJL-Tg(SOD1*G93A)1Gur/J, which normally develop symptoms around 100-110 days old and are terminal at 120-130 days old. Preliminary results show that the double transgenic animals display symptoms as early as eight days old and become terminal before 15 days old. Furthermore, the cross of the CCS mice with the wild-type SOD1 overexpressing mice results in animals that also show neurological symptoms around 10-14 days old, a phenomenon that Son *et al*. did not observe. Determining how CCS changes the metal-distribution in SOD1 may help us to understand how the toxic gain of function originates.

An additional facet of this project is that CCS is important not only for insertion of copper into SOD1, but also for modulating the status of SOD1's disulfide bond. Son *et al*., in further characterizing the CCS-SOD1 transgenic

crosses, have described an increase in the amount of G93A disulfide reduced protein, while the opposite was true in the wild-type SOD1 mice [32,50]. The data presented in this dissertation would seem to suggest that disulfide reduction is not related to the disease, as the non-disease affected wild-type mice had more SOD1 with a reduced disulfide. However, this still requires more investigation. CCS overexpression provides a way to influence the SOD1 disulfide, and with the tools developed in this dissertation we have the methods necessary to monitor the disulfide bond of each metal-state of SOD1.

5.3.2 Glutathione, Diamide, and Zinc-deficient SOD1

Another molecule that may play a role in ALS is the abundant antioxidant glutathione. I observed the impact that glutathione could have on the metal-binding of SOD1 during my first summer in the lab. I was initially testing it to see if reduction of the SOD1 disulfide bond by glutathione could lead to loss of the zinc and thus a zinc-deficient SOD1 species. I did indeed see loss of the zinc ion; however, concurrent with zinc-loss I observed copper loss leading to the apo protein. We speculated that this was due to the ability of glutathione to chelate copper; however I was moving on to other labs for rotations and did not further pursue this idea. The concept returned while gathering the data for chapter 4. Initially, we could not measure any zinc-deficient SOD1 in G93A mouse spinal cord. Upon further investigation we found that a small-molecule present in the tissue homogenate appeared to be pulling copper out of zinc-deficient SOD1, an activity we could partially prevent by including the thiol oxidant diamide in the buffer. This has led to the idea that glutathione may be able to prevent zinc-deficient SOD1-mediated toxicity. Additional evidence for this is the effect of knock out of the γ-glutamylcysteine ligase modulatory subunit (GCLM) on G93A SOD1 mice lifespan, which die at 50-60 days of age when GCLM is knocked out. This acceleration of disease progression may be due to the 80% reduction in glutathione that results from

GCLM knockout. We have collected data from the spinal cords of two GCLM$^{-/-}$ xG93A SOD1 transgenic mice, and were able to measure a significant amount of copper-containing, zinc-deficient SOD1 even with a 10-fold reduction in diamide concentration. These results suggest that glutathione may be a potent modulator of ALS disease progression, either through its ability to chelate copper, influence the oxidation status of the disulfide bond of SOD1, or function as an antioxidant.

Elucidating the role of glutathione in ALS progression may also help to define the interactions between motor neurons and the surrounding cells such as astrocytes. Astrocytes can become reactive over the course of the disease, and have been shown to be toxic to motor neurons if exposed to zinc-deficient SOD1. Whether the toxicity originates in the astrocytes or in the motor neurons *in vivo*, however, is not clear. Motor neurons are generally reliant on astrocytes to provide precursors for glutathione synthesis, and this may be one of the connections between the two cell types that could explain how zinc-deficient SOD1 in the motor neurons leads to reactive astrocytes and motor neuron death. The GCLM$^{-/-}$ G93A SOD1 mice are an important model for determining what role glutathione has and whether or not it could serve as a therapeutic agent. We have plans to acquire more of these animals; however the breeding necessary to generate them is substantial and thus it will take significantly more time before we have them available.

5.3.3 Laser Capture Microdissection to look at Motor Neurons

A concern with the methods described in this dissertation is the level of dilution that the SOD1 from motor neurons undergoes by the time we are able to observe it. The punch method described in Chapter 2 is an improvement over the more common methods involving homogenization of an entire spinal cord as we are extracting specifically disease affected areas of the spinal cord, a distinction that is lost when the whole cord is used. Motor neurons are

known to be particularly rich in SOD1 [149], yet the ventral spinal cord contains a heterogeneous cell population and the SOD1 we observe cannot be assumed to only reflect the distribution in motor neurons. It is possible that the amount of zinc-deficient SOD1 we find is an underestimate due to the contribution of SOD1 from other cell types (astrocytes, microglia, etc.). Addressing this requires being able to extract only motor neurons from the spinal cord of transgenic mice, an ability that Oregon State University has recently acquired with the purchase of a laser capture microdissection instrument. With a demonstration model, we were able to measure SOD1 from approximately 200 cells using the Ziptip assay. The cells so extracted contained more zinc-deficient SOD1 than we have seen in the conventional tissue punches. Advancing this ability will allow us to specifically monitor the metal-binding of SOD1 in only motor neurons or other cell types, enabling us to determine with significantly more accuracy how SOD1 causes toxicity to motor neurons.

5.3.4 The Connection to Nitrated HSP90

The nitration of HSP90 potentially represents the putative downstream target of zinc-deficient SOD1 and peroxynitrite; however the pathway between SOD1 and HSP90 has yet to be fully elucidated. Nitrated HSP90 was one of several proteins identified from peroxynitrite-treated PC12 cells that were then tested to see if the nitration had any role in peroxynitrite-mediated cell death. Peroxynitrite-treated HSP90, upon delivery to cultured motor neurons, induced cell death in 60% of the cells. In an effort to understand which tyrosine residues participated in this toxicity (HSP90 has 24 tyrosines), Alvaro Estévez's lab identified 5 tyrosines in the protein that were prone to nitration. Thanks to the unnatural amino acid incorporation system of Ryan Mehl, HSP90 could be generated with a nitrotyrosine residue at each of those locations. I was able to participate in these experiments by confirming the

incorporation of the nitrotyrosine at the desired position via tandem mass spectrometry. Delivery of each nitrated form to cultured motor neurons revealed that only nitration at positions 33 or 56 was able to initiate cell death. Nitration of HSP90 at one of those two positions clearly causes the protein to gain a toxic function that results in a Fas-mediated cellular death cascade that appears to be distinct in motor neurons.

HSP90 can become nitrated via peroxynitrite *in vitro* and in cell culture models and this may represent a mechanism involved in ALS disease progression. What remains to be worked out is the direct role that zinc-deficient SOD1 might play in this pathway. Some of the preliminary work from Alvaro Estévez's lab suggests that SOD1 and HSP90 may physically interact; such proximity would potentially facilitate nitration. Surface plasmon resonance experiments have shown that CuZn SOD1 does not bind to HSP90, and that zinc-only SOD1 binds weakly. Importantly, copper-containing zinc-deficient SOD1 binds quite strongly, with 20 nM affinity. HSP90 is an abundant cellular protein, thus the levels of zinc-deficient SOD1 we have found in the spinal cord (~800 nM) are certainly sufficient for this interaction to happen *in vivo*. Determining if the interaction does indeed happen *in vivo*, and what the consequences are for motor neurons, represents the next step in the research. Now that we have a quantitative picture of the partially unfolded intermediates present in the cell throughout disease development, the interactions between HSP90 and all of those intermediates can be probed to determine if any of the interactions results in toxicity.

5.4 Final Thoughts

My dissertation work has consisted of development of methods to measure the specific, subunit-level protein binding of two similar metals. I then applied that methodology to determine the distribution of the partially unfolded

intermediate species of SOD1 from the spinal cord of transgenic, SOD1-overexpressing ALS-model mice. This work has generated several novel methods that can be applied to other proteins and small-mass-difference protein modifications. Finally, we now have a detailed look at the potential involvement of differential metal-binding in ALS disease progression, opening many new avenues for research.

Bibliography

1. ALSA What is ALS? Washington, D.C.: ALS Association.

2. MLB Lou Gehrig Hall of Fame Biography. Cooperstown, NY: MLB Hall of Fame.

3. Barbara Haberman MH, Joe McGowan Official Lou Gehrig Web Site.

4. Rowland LP, Shneider NA (2001) Amyotrophic lateral sclerosis. N Engl J Med 344: 1688-1700.

5. Wong PC, Rothstein JD, Price DL (1998) The genetic and molecular mechanisms of motor neuron disease. Curr Opin Neurobiol 8: 791-799.

6. ALSA ALS: Facts you should know. Washington D.C.: ALS Associtation.

7. Charcot J-M (1874) De la sclerose laterale amyotrophique: Symptomatologie. Prog Med 2: 325-327, 341-342, 453-455.

8. Rowland LP (2001) How amyotrophic lateral sclerosis got its name: the clinical-pathologic genius of Jean-Martin Charcot. Arch Neurol 58: 512-515.

9. Rosen DR, Siddique T, Patterson D, Figlewicz DA, Sapp P, et al. (1993) Mutations in Cu/Zn superoxide dismutase gene are associated with familial amyotrophic lateral sclerosis. Nature 362: 59-62.

10. Siddique T, Figlewicz DA, Pericak-Vance MA, Haines JL, Rouleau G, et al. (1991) Linkage of a gene causing familial amyotrophic lateral sclerosis to chromosome 21 and evidence of genetic-locus heterogeneity. N Engl J Med 324: 1381-1384.

11. Rosen DR, Siddique T, Patterson D, Figlewicz DA, Sapp P, et al. (1993) Mutations in Cu/Zn superoxide dismutase gene are associated with familial amyotrophic lateral sclerosis. Nature 362: 59-62.

12. Andersen PM (2001) Genetics of sporadic ALS. Amyotroph Lateral Scler Other Motor Neuron Disord 2 Suppl 1: S37-41.

13. Andersen PM (2000) Genetic factors in the early diagnosis of ALS. Amyotroph Lateral Scler Other Motor Neuron Disord 1 Suppl 1: S31-42.

14. Strange RW, Antonyuk S, Hough MA, Doucette PA, Rodriguez JA, et al. (2003) The structure of holo and metal-deficient wild-type human Cu, Zn superoxide dismutase and its relevance to familial amyotrophic lateral sclerosis. J Mol Biol 328: 877-891.

15. Richardson J, Thomas KA, Rubin BH, Richardson DC (1975) Crystal structure of bovine Cu,Zn superoxide dismutase at 3 A resolution: chain tracing and metal ligands. Proc Natl Acad Sci U S A 72: 1349-1353.

16. Forman JH, Fridovich I (1973) On the stability of bovine superoxide dismutase. J Biol Chem 248: 2645-2649.

17. Lepock JR, Arnold LD, Torrie BH, Andrews B, Kruuv J (1985) Structural analyses of various Cu2+, Zn2+-superoxide dismutases by differential scanning calorimetry and Raman spectroscopy. Arch Biochem Biophys 241: 243-251.

18. Beyer WF, Jr., Fridovich I, Mullenbach GT, Hallewell R (1987) Examination of the role of arginine-143 in the human copper and zinc superoxide dismutase by site-specific mutagenesis. J Biol Chem 262: 11182-11187.

19. Fisher CL, Cabelli DE, Tainer JA, Hallewell RA, Getzoff ED (1994) The role of arginine 143 in the electrostatics and mechanism of Cu,Zn superoxide dismutase: Computational and experimental evaluation by mutational analysis. Proteins: Structure, Function, and Genetics 19: 24-34.

20. Forman HJ, Fridovich I (1973) Superoxide dismutase: a comparison of rate constants. Arch Biochem Biophys 158: 396-400.

21. Borchelt DR, Lee MK, Slunt HS, Guarnieri M, Xu Z-S, et al. (1994) Superoxide dismutase 1 with mutations linked to familial amyotrophic lateral sclerosis possesses significant activity. Proc Natl Acad Sci USA 91: 8292-9296.

22. Elchuri S, Oberley TD, Qi W, Eisenstein RS, Jackson Roberts L, et al. (2005) CuZnSOD deficiency leads to persistent and widespread

oxidative damage and hepatocarcinogenesis later in life. Oncogene 24: 367-380.

23. Gurney ME, Pu H, Chiu AY, Dal Corto MC, Polchow CY, et al. (1994) Motor neuron degeneration in mice that express a human Cu,Zn superoxide dismutase mutation. Science 264: 1772-1775.

24. Epstein CJ, Avraham KB, Lovett M, Smith S, Elroy-Stein O, et al. (1987) Transgenic mice with increased Cu/Zn-superoxide dismutase activity: animal model of dosage effects in Down syndrome. Proc Natl Acad Sci USA 84: 8044-8048.

25. Tu PH, Raju P, Robinson KA, Gurney ME, Trojanowski JQ, et al. (1996) Transgenic mice carrying a human mutant superoxide dismutase transgene develop neuronal cytoskeletal pathology resembling human amyotrophic lateral sclerosis lesions. Proc Natl Acad Sci U S A 93: 3155-3160.

26. Jankowsky JL, Savonenko A, Schilling G, Wang J, Xu G, et al. (2002) Transgenic mouse models of neurodegenerative disease: opportunities for therapeutic development. Curr Neurol Neurosci Rep 2: 457-464.

27. Bruijn LI, Becher MW, Lee MK, Anderson KL, Jenkins NA, et al. (1997) ALS-linked SOD1 mutant G85R mediates damage to astrocytes and promotes rapidly progressive disease with SOD1-containing inclusions. Neuron 18: 327-338.

28. Wong PC, Pardo CA, Borchelt DR, Lee MK, Copeland NG, et al. (1995) An adverse property of a familial ALS-linked SOD1 mutation causes motor neuron disease characterized by vacuolar degeneration of mitochondria. Neuron 14: 1105-1116.

29. Culotta VC, Klomp LWJ, Strain J, Casareno RLB, Krems B, et al. (1997) The copper chaperone for superoxide dismutase. J Biol Chem 272: 23469-23472.

30. Subramaniam JR, Lyons WE, Liu J, Bartnikas TB, Rothstein J, et al. (2002) Mutant SOD1 causes motor neuron disease independent of copper chaperone-mediated copper loading. Nat Neurosci 5: 301-307.

31. Beckman JS, Estevez AG, Barbeito L, Crow JP (2002) CCS knockout mice establish an alternative source of copper for SOD in ALS. Free Radic Biol Med 33: 1433-1435.

32. Son M, Puttaparthi K, Kawamata H, Rajendran B, Boyer PJ, et al. (2007) Overexpression of CCS in G93A-SOD1 mice leads to accelerated neurological deficits with severe mitochondrial pathology. Proc Natl Acad Sci U S A 104: 6072-6077.

33. Vargas MR, Johnson DA, Johnson JA (2011) Decreased glutathione accelerates neurological deficit and mitochondrial pathology in familial ALS-linked hSOD1(G93A) mice model. Neurobiol Dis 43: 543-551.

34. Vargas MR, Pehar M, Cassina P, Beckman JS, Barbeito L (2006) Increased glutathione biosynthesis by Nrf2 activation in astrocytes prevents p75-dependent motor neuron apoptosis. J Neurochem 97: 687-696.

35. Vargas MR, Johnson DA, Sirkis DW, Messing A, Johnson JA (2008) Nrf2 activation in astrocytes protects against neurodegeneration in mouse models of familial amyotrophic lateral sclerosis. J Neurosci 28: 13574-13581.

36. Freedman JH, Ciriolo MR, Peisach J (1989) The role of glutathione in copper metabolism and toxicity. J Biol Chem 264: 5598-5605.

37. Lill CM, Abel O, Bertram L, Al-Chalabi A (2011) Keeping up with genetic discoveries in amyotrophic lateral sclerosis: the ALSoD and ALSGene databases. Amyotroph Lateral Scler 12: 238-249.

38. Andersen PM, Nilsson P, Keranen ML, Forsgren L, Hagglund J, et al. (1997) Phenotypic heterogeneity in motor neuron disease patients with CuZn-superoxide dismutase mutations in Scandinavia. Brain 120: 1723-1737.

39. Parton MJ, Broom W, Andersen PM, Al-Chalabi A, Nigel Leigh P, et al. (2002) D90A-SOD1 mediated amyotrophic lateral sclerosis: a single founder for all cases with evidence for a Cis-acting disease modifier in the recessive haplotype. Hum Mutat 20: 473.

40. Xia K, Zhang S, Bathrick B, Liu S, Garcia Y, et al. (2012) Quantifying the kinetic stability of hyperstable proteins via time-dependent SDS trapping. Biochemistry 51: 100-107.

41. Stathopulos PB, Rumfeldt JA, Scholz GA, Irani RA, Frey HE, et al. (2003) Cu/Zn superoxide dismutase mutants associated with amyotrophic lateral sclerosis show enhanced formation of aggregates in vitro. Proc Natl Acad Sci U S A 100: 7021-7026.

42. Bruijn LI, Houseweart MK, Kato S, Anderson KL, Anderson SD, et al. (1998) Aggregation and motor neuron toxicity of an ALS-linked SOD1 mutant independent from Wild-Type SOD1. Science 281: 1851-1854.

43. Johnston JA, Dalton MJ, Gurney ME, Kopito RR (2000) Formation of high molecular weight complexes of mutant Cu,Zn-superoxide dismutase in a mouse model for familial amyotrophic lateral sclerosis. Proc Natl Acad Sci USA 97: 12571-12576.

44. Kato S, Takikawa M, Nakashima K, Hirano A, Cleveland DW, et al. (2000) New consensus research on neuropathological aspects of familial amyotrophic lateral sclerosis with superoxide dismutase 1 (SOD1) gene mutations: inclusions containing SOD1 in neurons and astrocytes. Amyotroph Lateral Scler Other Motor Neuron Disord 1: 163-184.

45. Ligon LA, LaMonte BH, Wallace KE, Weber N, Kalb RG, et al. (2005) Mutant superoxide dismutase disrupts cytoplasmic dynein in motor neurons. NeuroReport 16: 533-536.

46. Watanabe M, Dykes-Hoberg M, Culotta VC, Price DL, Wong PC, et al. (2001) Histological evidence of protein aggregation in mutant SOD1 transgenic mice and in amyotrophic lateral sclerosis neural tissues. Neurobiol Dis 8: 933-941.

47. Vassall KA, Stubbs HR, Primmer HA, Tong MS, Sullivan SM, et al. (2011) Decreased stability and increased formation of soluble aggregates by immature superoxide dismutase do not account for disease severity in ALS. Proc Natl Acad Sci U S A 108: 2210-2215.

48. Lee JP, Gerin C, Bindokas VP, Miller R, Ghadge G, et al. (2002) No correlation between aggregates of Cu/Zn superoxide dismutase and

cell death in familial amyotrophic lateral sclerosis. J Neurochem 82: 1229-1238.

49. Witan H, Kern A, Koziollek-Drechsler I, Wade R, Behl C, et al. (2008) Heterodimer formation of wild-type and amyotrophic lateral sclerosis-causing mutant Cu/Zn-superoxide dismutase induces toxicity independent of protein aggregation. Hum Mol Genet 17: 1373-1385.

50. Proescher JB, Son M, Elliott JL, Culotta VC (2008) Biological effects of CCS in the absence of SOD1 enzyme activation: implications for disease in a mouse model for ALS. Hum Mol Genet 17: 1728-1737.

51. Zetterstrom P, Stewart HG, Bergemalm D, Jonsson PA, Graffmo KS, et al. (2007) Soluble misfolded subfractions of mutant superoxide dismutase-1s are enriched in spinal cords throughout life in murine ALS models. Proc Natl Acad Sci U S A 104: 14157-14162.

52. Lindberg MJ, Bystrom R, Boknas N, Andersen PM, Oliveberg M (2005) Systematically perturbed folding patterns of amyotrophic lateral sclerosis (ALS)-associated SOD1 mutants. Proc Natl Acad Sci U S A 102: 9754-9759.

53. Lindberg MJ, Tibell L, Oliveberg M (2002) Common denominator of Cu/Zn superoxide dismutase mutants associated with amyotrophic lateral sclerosis: Decreased stability of the apo state. Proc Natl Acad Sci U S A 99: 16607-16612.

54. Leinartaite L, Saraboji K, Nordlund A, Logan DT, Oliveberg M (2010) Folding Catalysis by Transient Coordination of Zn(2+) to the Cu Ligands of the ALS-Associated Enzyme Cu/Zn Superoxide Dismutase 1. J Am Chem Soc.

55. Kayatekin C, Zitzewitz JA, Matthews CR (2008) Zinc binding modulates the entire folding free energy surface of human Cu,Zn superoxide dismutase. J Mol Biol 384: 540-555.

56. Banci L, Bertini I, Cantini F, D'Onofrio M, Viezzoli MS (2002) Structure and dynamics of copper-free SOD: The protein before binding copper. Protein Sci 11: 2479-2492.

57. Crow JP, Sampson JB, Zhuang Y, Thompson JA, Beckman JS (1997) Decreased zinc affinity of amyotrophic lateral sclerosis-associated superoxide dismutase mutants leads to enhanced catalysis of tyrosine nitration by peroxynitrite. J Neurochem 69: 1936-1944.

58. Winterbourn CC, Kettle AJ (2003) Radical-radical reactions of superoxide: a potential route to toxicity. Biochem Biophys Res Commun 305: 729-736.

59. Beckman JS, Beckman TW, Chen J, Marshall PM, Freeman BA (1990) Apparent hydroxyl radical production by peroxynitrite: Implications for endothelial injury by nitric oxide and superoxide. Proc Natl Acad Sci (USA) 87: 1620-1624.

60. Nauser T, Koppenol WH (2002) The rate constant of superoxide with nitrogen monoxide: approaching the diffusion limit. J Phys Chem A 106: 4084-4086.

61. Ischiropoulos H, Al-Mehdi AB (1995) Peroxynitrite-mediated oxidative protein modifications. FEBS Lett 364: 279-282.

62. Beckman JS (1996) Oxidative damage and tyrosine nitration from peroxynitrite. Chem Res Toxicol 9: 836-844.

63. Turko IV, Murad F (2002) Protein nitration in cardiovascular diseases. Pharmacol Rev 54: 619-634.

64. Rodriguez-Ariza A, Lopez-Sanchez LM, Gonzalez R, Corrales FJ, Lopez P, et al. (2005) Altered protein expression and protein nitration pattern during d-galactosamine-induced cell death in human hepatocytes: a proteomic analysis. Liver Int 25: 1259-1269.

65. Natal C, Modol T, Oses-Prieto JA, Lopez-Moratalla N, Iraburu MJ, et al. (2008) Specific protein nitration in nitric oxide-induced apoptosis of human monocytes. Apoptosis 13: 1356-1367.

66. Estevez AG, Spear N, Manuel SM, Radi R, Henderson CE, et al. (1998) Nitric oxide and superoxide contribute to motor neuron apoptosis induced by trophic factor deprivation. J Neurosci 18: 923-931.

67. Estevez AG, Jordan J (2002) Nitric oxide and superoxide, a deadly cocktail. Ann N Y Acad Sci 962: 207-211.

68. Roberts BR, Tainer JA, Getzoff ED, Malencik DA, Anderson SR, et al. (2007) Structural Characterization of Zinc-deficient Human Superoxide Dismutase and Implications for ALS. J Mol Biol 373: 377-390.

69. Estévez AG, Crow JP, Sampson JB, Reiter C, Zhuang Y-X, et al. (1999) Induction of nitric oxide-dependent apoptosis in motor neurons by zinc-deficient superoxide dismutase. Science 286: 2498-2500.

70. Sahawneh MA, Ricart KC, Roberts BR, Bomben VC, Basso M, et al. (2010) Cu,Zn superoxide dismutase (SOD) increases toxicity of mutant and Zn-deficient superoxide dismutase by enhancing protein stability. J Biol Chem.

71. Ye Y, Quijano C, Robinson KM, Ricart KC, Strayer AL, et al. (2007) Prevention of peroxynitrite-induced apoptosis of motor neurons and PC12 cells by tyrosine-containing peptides. J Biol Chem 282: 6324-6337.

72. Lynch SM, Boswell SA, Colon W (2004) Kinetic stability of Cu/Zn superoxide dismutase is dependent on its metal ligands: implications for ALS. Biochemistry 43: 16525-16531.

73. Wang J, Slunt H, Gonzales V, Fromholt D, Coonfield M, et al. (2003) Copper-binding-site-null SOD1 causes ALS in transgenic mice: aggregates of non-native SOD1 delineate a common feature. Hum Mol Genet 12: 2753-2764.

74. Valentine JS, Pantoliano MW, McDonnell PJ, Burger AR, Lippard SJ (1979) pH-dependent migration of copper(II) to the vacant zinc-binding site of zinc-free bovine erythrocyte superoxide dismutase. Proc Natl Acad Sci U S A 76: 4245-4249.

75. Prudencio M, Lelie H, Brown HH, Whitelegge JP, Valentine JS, et al. (2012) A novel variant of human superoxide dismutase 1 harboring amyotrophic lateral sclerosis-associated and experimental mutations in metal-binding residues and free cysteines lacks toxicity in vivo. J Neurochem 121: 475-485.

76. Andreini C, Bertini I, Cavallaro G, Holliday GL, Thornton JM (2008) Metal ions in biological catalysis: from enzyme databases to general principles. J Biol Inorg Chem 13: 1205-1218.

77. Waldron KJ, Rutherford JC, Ford D, Robinson NJ (2009) Metalloproteins and metal sensing. Nature 460: 823-830.

78. Holm RH, Kennepohl P, Solomon EI (1996) Structural and Functional Aspects of Metal Sites in Biology. Chem Rev 96: 2239-2314.

79. Hann S, Obinger C, Stingeder G, Paumann M, Furtmuller PG, et al. (2006) Studying metal integration in native and recombinant copper proteins by hyphenated ICP-DRC-MS and ESI-TOF-MS capabilities and limitations of the complementary techniques. Journal of Analytical Atomic Spectrometry 21: 1224-1231.

80. Shi W, Chance MR (2008) Metallomics and metalloproteomics. Cell Mol Life Sci 65: 3040-3048.

81. McCall KA, Fierke CA (2000) Colorimetric and fluorimetric assays to quantitate micromolar concentrations of transition metals. Anal Biochem 284: 307-315.

82. Ayed A, Krutchinsky AN, Ens W, Standing KG, Duckworth HW (1998) Quantitative evaluation of protein-protein and ligand-protein equilibria of a large allosteric enzyme by electrospray ionization time-of-flight mass spectrometry. Rapid Commun Mass Spectrom 12: 339-344.

83. Ganem B, Henion JD (2003) Going gently into flight: analyzing noncovalent interactions by mass spectrometry. Bioorg Med Chem 11: 311-314.

84. Potier N, Rogniaux H, Chevreux G, Van Dorsselaer A (2005) Ligand-metal ion binding to proteins: investigation by ESI mass spectrometry. Methods Enzymol 402: 361-389.

85. Veenstra TD (1999) Electrospray ionization mass spectrometry in the study of biomolecular non-covalent interactions. Biophys Chem 79: 63-79.

86. Deng L, Sun N, Kitova EN, Klassen JS (2010) Direct quantification of protein-metal ion affinities by electrospray ionization mass spectrometry. Anal Chem 82: 2170-2174.

87. Banci L, Bertini I, Ciofi-Baffoni S, Kozyreva T, Zovo K, et al. (2010) Affinity gradients drive copper to cellular destinations. Nature 465: 645-648.

88. McCord JM, Fridovich I (1969) Superoxide dismutase: an enzymic function for erythrocuprein (hemocuprein). J Biol Chem 244: 6049-6055.

89. Nishida CR, Gralla EB, Valentine JS (1994) Characterization of three yeast copper-zinc superoxide dismutase mutants analogous to those coded for in familial amyotrophic lateral sclerosis. Proc Natl Acad Sci USA: 9906-9910.

90. Kim SM, Eum WS, Kang JH (1998) Expression, purification, and characterization of a familial amyotrophic lateral sclerosis-associated D90A Cu,Zn-superoxide dismutase mutant. Mol Cells 8: 478-482.

91. Winterbourn CC, Domigan NM, Broom JK (1995) Decreased thermal stability of red blood cell glu100-->gly superoxide dismutase from a family with amyotrophic lateral sclerosis. FEBS Lett 368: 449-451.

92. Goto JJ, Zhu H, Sanchez RJ, Nersissian A, Gralla EB, et al. (2000) Loss of in vitro metal ion binding specificity in mutant copper-zinc superoxide dismutases associated with familial amyotrophic lateral sclerosis. J Biol Chem 275: 1007-1014.

93. Museth AK, Brorsson AC, Lundqvist M, Tibell LA, Jonsson BH (2009) The ALS-associated mutation G93A in human copper-zinc superoxide dismutase selectively destabilizes the remote metal binding region. Biochemistry 48: 8817-8829.

94. Estevez AG, Crow JP, Sampson JB, Reiter C, Zhuang Y, et al. (1999) Induction of nitric oxide-dependent apoptosis in motor neurons by zinc-deficient superoxide dismutase. Science 286: 2498-2500.

95. Sahawneh MA, Ricart KC, Roberts BR, Bomben VC, Basso M, et al. (2010) Cu,Zn-superoxide dismutase increases toxicity of mutant and zinc-deficient superoxide dismutase by enhancing protein stability. J Biol Chem 285: 33885-33897.

96. Hayward LJ, Rodriguez JA, Kim JW, Tiwari A, Goto JJ, et al. (2002) Decreased metallation and activity in subsets of mutant superoxide dismutases associated with familial amyotrophic lateral sclerosis. J Biol Chem 277: 15923-15931.

97. Leinweber B, Barofsky E, Barofsky DF, Ermilov V, Nylin K, et al. (2004) Aggregation of ALS mutant superoxide dismutase expressed in Escherichia coli. Free Radic Biol Med 36: 911-918.

98. Howland DS, Liu J, She Y, Goad B, Maragakis NJ, et al. (2002) Focal loss of the glutamate transporter EAAT2 in a transgenic rat model of SOD1 mutant-mediated amyotrophic lateral sclerosis (ALS). Proc Natl Acad Sci U S A 99: 1604-1609.

99. Valentine JS, Pantoliano MW (1981) Protein-metal ion interactions in cuprozinc protein (superoxide dismutase). In: Spiro TG, editor. Copper Proteins: Metal ions in biology. New York: John Wiley and Sons. pp. 291-358.

100. Laemmli UK (1970) Cleavage of structural proteins during the assembly of the head of bacteriophage T4. Nature 227: 680-685.

101. Rockwood AL, Vanorden SL, Smith RD (1995) Rapid Calculation of Isotope Distributions. Analytical Chemistry 67: 2699-2704.

102. Rockwood AL, VanOrden SL, Smith RD (1996) Ultrahigh resolution isotope distribution calculations. Rapid Communications in Mass Spectrometry 10: 54-59.

103. Karch CM, Prudencio M, Winkler DD, Hart PJ, Borchelt DR (2009) Role of mutant SOD1 disulfide oxidation and aggregation in the pathogenesis of familial ALS. Proc Natl Acad Sci U S A 106: 7774-7779.

104. Lelie HL, Liba A, Bourassa MW, Chattopadhyay M, Chan PK, et al. (2010) Copper and zinc metallation status of copper-zinc superoxide dismutase from ALS-transgenic mice. J Biol Chem.

105. Huber CG, Premstaller A, Kleindienst G (1999) Evaluation of volatile eluents and electrolytes for high-performance liquid chromatography-electrospray ionization mass spectrometry and capillary

electrophoresis-electrospray ionization mass spectrometry of proteins. II. Capillary electrophoresis. J Chromatogr A 849: 175-189.

106. Garcia MC (2005) The effect of the mobile phase additives on sensitivity in the analysis of peptides and proteins by high-performance liquid chromatography-electrospray mass spectrometry. J Chromatogr B Analyt Technol Biomed Life Sci 825: 111-123.

107. Jonsson PA, Graffmo KS, Andersen PM, Brannstrom T, Lindberg M, et al. (2006) Disulphide-reduced superoxide dismutase-1 in CNS of transgenic amyotrophic lateral sclerosis models. Brain 129: 451-464.

108. Marshall AG, Hendrickson CL, Shi SD (2002) Scaling MS plateaus with high-resolution FT-ICRMS. Analytical Chemistry 74: 252A-259A.

109. Beavis RC (1993) Chemical Mass of Carbon in Proteins. Analytical Chemistry 65: 496-497.

110. Senko MW, Beu SC, Mclafferty FW (1995) Determination of Monoisotopic Masses and Ion Populations for Large Biomolecules from Resolved Isotopic Distributions. Journal of the American Society for Mass Spectrometry 6: 229-233.

111. He F, Hendrickson CL, Marshall AG (2000) Unequivocal determination of metal atom oxidation state in naked heme proteins: Fe(III)myoglobin, Fe(III)cytochrome c, Fe(III)cytochrome b5, and Fe(III)cytochrome b5 L47R. Journal of the American Society for Mass Spectrometry 11: 120-126.

112. Green MK, Vestling MM, Johnston MV, Larsen BS (1998) Distinguishing small molecular mass differences of proteins by mass spectrometry. Anal Biochem 260: 204-211.

113. Rhoads TW, Lopez NI, Zollinger DR, Morre JT, Arbogast BL, et al. (2011) Measuring copper and zinc superoxide dismutase from spinal cord tissue using electrospray mass spectrometry. Anal Biochem 415: 52-58.

114. Hornberg A, Logan DT, Marklund SL, Oliveberg M (2007) The coupling between disulphide status, metallation and dimer interface strength in Cu/Zn superoxide dismutase. J Mol Biol 365: 333-342.

115. Carroll MC, Outten CE, Proescher JB, Rosenfeld L, Watson WH, et al. (2006) The effects of glutaredoxin and copper activation pathways on the disulfide and stability of Cu,Zn superoxide dismutase. J Biol Chem 281: 28648-28656.

116. Furukawa Y, Fu R, Deng HX, Siddique T, O'Halloran TV (2006) Disulfide cross-linked protein represents a significant fraction of ALS-associated Cu, Zn-superoxide dismutase aggregates in spinal cords of model mice. Proc Natl Acad Sci U S A 103: 7148-7153.

117. Jonsson PA, Ernhill K, Andersen PM, Bergemalm D, Brannstrom T, et al. (2004) Minute quantities of misfolded mutant superoxide dismutase-1 cause amyotrophic lateral sclerosis. Brain 127: 73-88.

118. Kosower NS, Kosower EM, Wertheim B, Correa WS (1969) Diamide, a new reagent for the intracellular oxidation of glutathione to the disulfide. Biochem Biophys Res Commun 37: 593-596.

119. O'Leary MH (1988) Carbon Isotopes in Photosynthesis. BioScience 38: 328-336.

120. Mann M, Meng CK, Fenn JB (1989) Interpreting Mass-Spectra of Multiply Charged Ions. Analytical Chemistry 61: 1702-1708.

121. Wu QY, Vanorden S, Cheng XH, Bakhtiar R, Smith RD (1995) Characterization of Cytochrome-C Variants with High-Resolution Fticr Mass-Spectrometry - Correlation of Fragmentation and Structure. Analytical Chemistry 67: 2498-2509.

122. Ledford EB, Rempel DL, Gross ML (1984) Space-Charge Effects in Fourier-Transform Mass-Spectrometry - Mass Calibration. Analytical Chemistry 56: 2744-2748.

123. Ledford EB, Rempel DL, Gross ML (1984) Space-Charge Effects in Fourier-Transform Mass-Spectrometry .1. Electrons. International Journal of Mass Spectrometry and Ion Processes 55: 143-154.

124. Uechi GT, Dunbar RC (1992) Space-Charge Effects on Relative Peak Heights in Fourier Transform-Ion Cyclotron-Resonance Spectra. Journal of the American Society for Mass Spectrometry 3: 734-741.

125. O'Leary MH, Rife JE, Slater JD (1981) Kinetic and isotope effect studies of maize phosphoenolpyruvate carboxylase. Biochemistry 20: 7308-7314.

126. Farquhar GD, Ehleringer JR, Hubick KT (1989) Carbon Isotope Discrimination and Photosynthesis. Annual Review of Plant Physiology and Plant Molecular Biology 40: 503-537.

127. Deniro MJ, Epstein S (1978) Influence of Diet on Distribution of Carbon Isotopes in Animals. Geochimica Et Cosmochimica Acta 42: 495-506.

128. Karala AR, Ruddock LW (2007) Does s-methyl methanethiosulfonate trap the thiol-disulfide state of proteins? Antioxid Redox Signal 9: 527-531.

129. Borchelt DR, Lee MK, Slunt HS, Guarnieri M, Xu ZS, et al. (1994) Superoxide dismutase 1 with mutations linked to familial amyotrophic lateral sclerosis possesses significant activity. Proc Natl Acad Sci U S A 91: 8292-8296.

130. Wang J, Xu G, Gonzales V, Coonfield M, Fromholt D, et al. (2002) Fibrillar inclusions and motor neuron degeneration in transgenic mice expressing superoxide dismutase 1 with a disrupted copper-binding site. Neurobiol Dis 10: 128-138.

131. Kato S, Sumi-Akamaru H, Fujimura H, Sakoda S, Kato M, et al. (2001) Copper chaperone for superoxide dismutase co-aggregates with superoxide dismutase 1 (SOD1) in neuronal Lewy body-like hyaline inclusions: an immunohistochemical study on familial amyotrophic lateral sclerosis with SOD1 gene mutation. Acta Neuropathol (Berl) 102: 233-238.

132. Stieber A, Gonatas JO, Gonatas NK (2000) Aggregates of mutant protein appear progressively in dendrites, in periaxonal processes of oligodendrocytes, and in neuronal and astrocytic perikarya of mice expressing the SOD1(G93A) mutation of familial amyotrophic lateral sclerosis. J Neurol Sci 177: 114-123.

133. Stieber A, Gonatas JO, Gonatas NK (2000) Aggregation of ubiquitin and a mutant ALS-linked SOD1 protein correlate with disease progression and fragmentation of the Golgi apparatus. J Neurol Sci 173: 53-62.

134. Okado-Matsumoto A, Myint T, Fujii J, Taniguchi N (2000) Gain in functions of mutant Cu,Zn-superoxide dismutases as a causative factor in familial amyotrophic lateral sclerosis: less reactive oxidant formation but high spontaneous aggregation and precipitation. Free Radic Res 33: 65-73.

135. Ince PG, Shaw PJ, Slade JY, Jones C, Hudgson P (1996) Familial amyotrophic lateral sclerosis with a mutation in exon 4 of the Cu/Zn superoxide dismutase gene: pathological and immunocytochemical changes. Acta Neuropathol (Berl) 92: 395-403.

136. Lippard SJ, Burger AR, Ugurbil K, Pantoliano MW, Valentine JS (1977) Nuclear magnetic resonance and chemical modification studies of bovine erythrocyte superoxide dismutase: evidence for zinc-promoted organization of the active site structure. Biochemistry 16: 1136-1141.

137. Pantoliano MW, Valentine JS, Burger AR, Lippard SJ (1982) A pH-dependent superoxide dismutase activity for zinc-free bovine erythrocuprein. Reexamination of the role of zinc in the holoprotein. J Inorg Biochem 17: 325-341.

138. Falconi M, Iovino M, Desideri A (1999) A model for the incorporation of metal from the copper chaperone CCS into Cu,Zn superoxide dismutase. Structure 7: 903-908.

139. Lamb AL, Torres AS, O'Halloran TV, Rosenzweig AC (2001) Heterodimeric structure of superoxide dismutase in complex with its metallochaperone. Nat Struct Biol 8: 751-755.

140. Rumfeldt JA, Lepock JR, Meiering EM (2009) Unfolding and folding kinetics of amyotrophic lateral sclerosis-associated mutant Cu,Zn superoxide dismutases. J Mol Biol 385: 278-298.

141. Vassall KA, Stathopulos PB, Rumfeldt JA, Lepock JR, Meiering EM (2006) Equilibrium thermodynamic analysis of amyotrophic lateral sclerosis-associated mutant apo Cu,Zn superoxide dismutases. Biochemistry 45: 7366-7379.

142. Nordlund A, Oliveberg M (2006) Folding of Cu/Zn superoxide dismutase suggests structural hotspots for gain of neurotoxic function in ALS:

parallels to precursors in amyloid disease. Proc Natl Acad Sci U S A 103: 10218-10223.

143. Banci L, Bertini I, Cramaro F, Del Conte R, Viezzoli MS (2003) Solution structure of Apo Cu,Zn superoxide dismutase: role of metal ions in protein folding. Biochemistry 42: 9543-9553.

144. Assfalg M, Banci L, Bertini I, Turano P, Vasos PR (2003) Superoxide dismutase folding/unfolding pathway: role of the metal ions in modulating structural and dynamical features. J Mol Biol 330: 145-158.

145. Beauchamp C, Fridovich I (1971) Superoxide dismutase: improved assays and an assay applicable to acrylamide gels. Anal Biochem 44: 276-287.

146. Johansson AS, Vestling M, Zetterstrom P, Lang L, Leinartaite L, et al. (2012) Cytotoxicity of superoxide dismutase 1 in cultured cells is linked to zn(2+) chelation. PLoS One 7: e36104.

147. Estevez AG, Spear N, Manuel SM, Radi R, Henderson CE, et al. (1998) Nitric oxide and superoxide contribute to motor neuron apoptosis induced by trophic factor deprivation. J Neurosci 18: 923-931.

148. Lindberg MJ, Normark J, Holmgren A, Oliveberg M (2004) Folding of human superoxide dismutase: disulfide reduction prevents dimerization and produces marginally stable monomers. Proc Natl Acad Sci U S A 101: 15893-15898.

149. Pardo CA, Xu Z, Borchelt DR, Price DL, Sisodia SS, et al. (1995) Superoxide dismutase is an abundant component in cell bodies, dendrites, and axons of motor neurons and in a subset of other neurons. Proc Natl Acad Sci USA 92: 954-958.

150. Guo Y, Duan W, Li Z, Huang J, Yin Y, et al. (2010) Decreased GLT-1 and increased SOD1 and HO-1 expression in astrocytes contribute to lumbar spinal cord vulnerability of SOD1-G93A transgenic mice. FEBS Lett 584: 1615-1622.

151. Sotelo-Silveira JR, Lepanto P, Elizondo V, Horjales S, Palacios F, et al. (2009) Axonal mitochondrial clusters containing mutant SOD1 in transgenic models of ALS. Antioxid Redox Signal 11: 1535-1545.

152. Xu Z, Cork L, Griffin J, Cleveland D (1993) Increased expression of neurofilament subunit NF-L produces morphological alterations that resemble the pathology of human motor neuron disease. Cell 73: 23-33.

153. Levenson CW, Janghorbani M (1994) Long-term measurement of organ copper turnover in rats by continuous feeding of a stable isotope. Anal Biochem 221: 243-249.

154. Choi DW, Koh JY (1998) Zinc and brain injury. Annu Rev Neurosci 21: 347-375.

155. Bush AI, Pettingell WH, Multhaup G, Paradis MD, Vonsattel JP, et al. (1994) Rapid induction of Alzheimer Aß amyloid formation by zinc. Science 265: 1464-1467.

156. Zhang B, Tu P, Abtahian F, Trojanowski JQ, Lee VM (1997) Neurofilaments and orthograde transport are reduced in ventral root axons of transgenic mice that express human SOD1 with a G93A mutation. J Cell Biol 139: 1307-1315.

157. Redler RL, Wilcox KC, Proctor EA, Fee L, Caplow M, et al. (2011) Glutathionylation at Cys-111 induces dissociation of wild type and FALS mutant SOD1 dimers. Biochemistry 50: 7057-7066.

158. Kishigami H, Nagano S, Bush AI, Sakoda S (2010) Monomerized Cu, Zn-superoxide dismutase induces oxidative stress through aberrant Cu binding. Free Radic Biol Med 48: 945-952.

159. de Beus MD, Chung J, Colon W (2004) Modification of cysteine 111 in Cu/Zn superoxide dismutase results in altered spectroscopic and biophysical properties. Protein Sci 13: 1347-1355.

160. Bush AI (2011) A Copper Binding Site within the Pathological Conformer Epitope of Mutant SOD1. Front Neurosci 5: 97.

161. Dringen R (2000) Metabolism and functions of glutathione in brain. Prog Neurobiol 62: 649-671.

162. Ozdinler PH, Benn S, Yamamoto TH, Guzel M, Brown RH, Jr., et al. (2011) Corticospinal motor neurons and related subcerebral projection

neurons undergo early and specific neurodegeneration in hSOD1G(9)(3)A transgenic ALS mice. J Neurosci 31: 4166-4177.

163. Raoul C, Buhler E, Sadeghi C, Jacquier A, Aebischer P, et al. (2006) Chronic activation in presymptomatic amyotrophic lateral sclerosis (ALS) mice of a feedback loop involving Fas, Daxx, and FasL. Proc Natl Acad Sci U S A 103: 6007-6012.

164. Raoul C, Estevez AG, Nishimune H, Cleveland DW, deLapeyriere O, et al. (2002) Motoneuron death triggered by a specific pathway downstream of Fas. potentiation by ALS-linked SOD1 mutations. Neuron 35: 1067-1083.